RV *Poseidon*

Report of

Cruise *POS515*

18.06.2017 – 13.07.2017

Dubrovnik, Croatia to *Catania, Italy*

compiled by

M. Riedel, GEOMAR

J. Bialas, GEOMAR

A. Krabbenhoeft, GEOMAR

V. Bähre, GEOMAR

F. Beeck, GEOMAR

O. Candoni, OGS

M. Kühn, GEOMAR

S. Muff, GEOMAR

J. Rindfleisch, GEOMAR

N. Stange, University of Bremen

Dated: *25.07.2017*

Cruise Report

RV Poseidon **Cruise No.: POS515**
Dates of Cruise: 18.06.2017 – 13.07.2017
Areas of Research: Calabrian Arc, Mediterranean Sea
Port Calls: Dubrovnik, Croatia & Catania, Italy

Institute: GEOMAR Helmholtz Centre for Ocean Research Kiel, Wischhofstrasse 1 – 3, 24148 Kiel, Germany

Department of Geosciences, University of Bremen, Klagenfurter Str. 4, 28359 Bremen, Germany

Istituto Nazionale di Oceanografia e di Geofisica Sperimentale (OGS), Borgo Grotta Gigante 42/c, 34010 Sgonico, Trieste, Italy

Principal Scientist: Michael Riedel

Number of Scientists: 10
Projects: CALVADOS - CALabrian arc mud VolcAnoes: Deep Origin and internal Structure

Cruise Report

This cruise report consists of 73 pages including cover:

1. Scientific crew 3

2. Research programme and objectives 4

3. Narrative of cruise with technical details 10

4. Scientific Results
   4.1 Venere mud volcano 22
   4.2 Poseidon mud volcano 37
   4.3 Sartori mud volcano 45
   4.4 Cetus mud volcano 50

5. Scientific equipment 52
   5.1 Ocean bottom seismometers 52
   5.2 P-Cable 3D imaging system 54
   5.4 Seismic source 56

6. Acknowledgements 57

7. Appendices 58
   A General map of expedition cruise-track 58
   B Station list 59
   Table B.1: OBS deployment at Venere mud volcano. 59
   Table B.2: OBS deployment at Poseidon mud volcano 60
   Figure B.1: Sound speed measured at OBS stations V01 601
   Table B.3: Log of seismic data acquisition at Venere mud volcano 62
   Table B.4: 2D Seismic lines at Poseidon and Sartori mud volcano 66
   Table B.5: 3D Survey lines across Sartotri mud volcano 67
   Table B.6: 2D Survey lines across Cetus mud volcano 70

8. References 71

1. Scientific crew

Name	**Function**	**Institute**
Bialas, Jörg	P-Cable, OBS	GEOMAR
Beeck, Florian	Airgun, P-Cable	GEOMAR
Rindfleisch, Jan	Airgun, P-Cable	GEOMAR
Krabbenhöft, Anne	OBS, P-Cable	GEOMAR
Muff, Sina	P-Cable, OBS	GEOMAR
BähreValentin	P-Cable, OBS	GEOMAR
Kühn, Michel	P-Cable, OBS	GEOMAR
Stange, Nikolas-Ulrich	OBS, P-Cable	University Bremen
Candoni, Oliviero	OBS, P-Cable	OGS
Riedel, Michael	Chief Scientist	GEOMAR
Total 10		

Chief scientist:
Dr. Michael Riedel GEOMAR - Helmholtz Centre for Ocean Research Kiel, Wischhofstrasse 1-3, 24146 Kiel, Germany, +49 341 600 2331

Figure 1 Scientists on board the research vessel POSEIDON during the project CALVADOS: from left to right: Sina Muff, Anne Krabbenhöft, Jan Rindfleisch, Jörg Bialas, Nikolas-Ulrich Stange, Oliviero Candoni (kneeling), Michael Riedel, Michel Kühn, Valentin Bähre, and Florian Beeck.

2. Research programme

Mud volcanoes have been found in various geological settings on passive and active margins but are mostly known from collision zones on Earth. Mud volcanoes are well known to occur on land, where at least 1,000 such structures have been counted. The amount of submarine mud volcanoes is believed to be much larger, and recent improvements in seafloor mapping led to the discovery of many mud volcanoes in all oceans. Specifically in the Eastern Mediterranean Sea more than 500 mud volcanoes are known from several regions like the Mediterranean Ridge, the Anaximander Mountains and Florence Rise, the Nile deep-sea fan area, and the Calabrian arc (Mascle et al., 2014). Within the framework of several European projects, scientists from Italy and other countries collected over the last 10 years numerous multibeam and echo sounder data from the inner and outer Calabrian arc (e.g. Gutscher et al., 2017). By combining multibeam bathymetry and backscatter imagery, integrated with sub-bottom profiles and locally proven from geological sampling, a total of 54 mud volcanoes have been identified in a sector of 35,600 km^2 within the Calabrian Arc (Ceramicola et al., 2014). Sampling has been performed from few mud volcanoes: the Madonna dello Ionio and Pythagoras mud volcano (Praeg et al. 2009), and more recently at Venere and Poseidon mud volcano during expeditionsM112 (Bohrmann et al., 2015) and POS-499 (Bohrmann et al., 2016). The role of the two MVs within the accretionary wedge of the Ionian Sea is rather unclear, although the presence of MVs is well known to be related to the collision zone. In this part the eastern Mediterranean Sea contains the convergent plate boundary where the African plate is being subducted beneath Europe, along which accretionary complexes extend over 1500 km from Calabria to Cyprus (Figure 2).

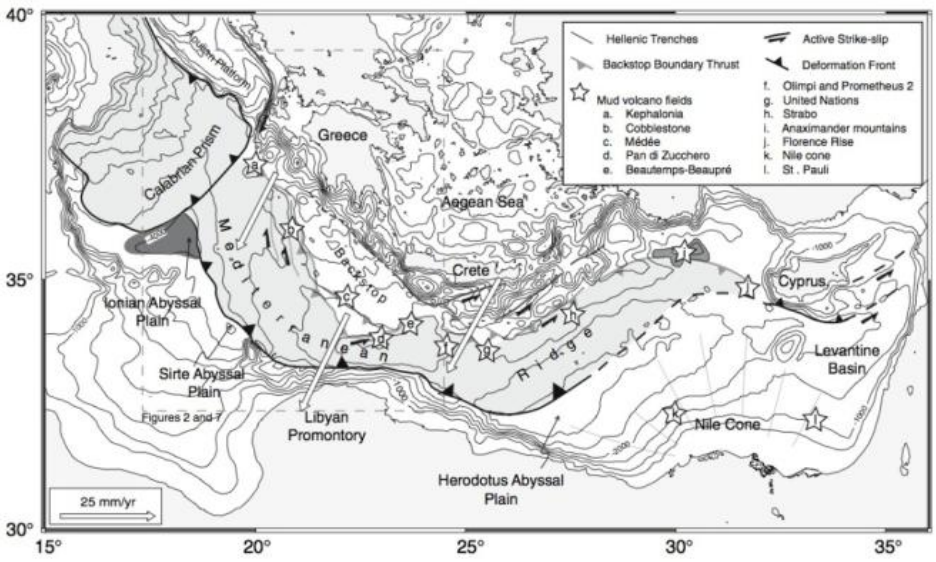

Figure 2. *Geological setting of the eastern Mediterranean (from Rabaute and Chamot-Rooke 2007), showing the Calabrian accretionary prism against the Mediterranean Ridge. White arrows indicate motion of the Aegean backstop with respect to Africa.*

The Calabrian Accretionary Prism (CAP) lies at the SE tip of the arcuate Apennine-Maghrebide subduction system, a product of rapid roll-back of a NW dipping oceanic slab over the last ca. 30 Ma (Neogene) to open back-arc basins in the western Mediterranean Sea (Malinverno and Ryan, 1986).

Since ca. 10 Ma (late Miocene), slab retreat has driven the pulsed opening of back-arc basins in the Tyrrhenian Sea during migration of the accretionary system up to 380 km towards the Ionian domain (Faccenna et al., 2004). Consumption of the slab, and its fragmentation during episodes of tearing beneath bordering continental margins, has narrowed the subduction zone to a tongue of Ionian lithosphere confined between the Maltese and Apulian escarpments (Figure 2), descending NW into the mantle beneath the Aeolian volcanic arc (Faccenna et al., 2004). Roll-back of the subducting slab has slowed or ceased following a regional plate tectonic reorganization at ca. 0.8-0.5 Ma (Goes et al. 2004). Over the same time period, Calabria has undergone a rapid km-scale uplift (Zecchin et al., 2012), argued to be a response to mantle circulation around a slab window beneath the southern Apennines (Faccenna et al., 2011).

Above the subduction zone, the Calabrian accretionary prism is 300 km wide and extends almost 300 km from elevations of up to 1928 m in Calabria, to a frontal thrust in water depths of ca. 4000 m that intersects that of the Mediterranean Ridge (Figure 2; Chamot-Rooke et al., 2005). In the Ionian Sea, Rossi and Sartori (1981) showed the seaward-thinning accretionary prism, referred to as the ‘External Calabrian Arc’, to contain three main morpho-structural zones (Figure 3), recognized in all subsequent work and corresponding to fore-arc basins and pre- and post-Messinian wedges (Praeg et al., 2009; Polonia et al., 2011). The inner fore-arc basins, up to 80 km wide, are underlain by strata up to 2 km thick that is inferred to include thin (<500 m) Messinian evaporites (Minelli and Faccenna, 2010). The pre-Messinian wedge to seaward, up to 100 km wide, is an area of irregular relief that corresponds to thrusts and back-thrusts; it is divided by the up to 750 m high Calabrian Escarpment into an inner plateau and an outer area of higher gradient and relief (Ceramicola et al., 2014). The post-Messinian wedge is up to 100 km wide and includes two main lobes (Figure 3), the western with a décollement at the base of Messinian evaporites and the eastern cutting down into older strata (Polonia et al., 2011). Seismic reflection and refraction data across the outer wedge and its foreland indicate the down-going slab to comprise oceanic or highly-extended crust overlain by up to 4 km of pre-Messinian sedimentary strata, in turn overlain by thick Messinian evaporites (Polonia et al. 2011).

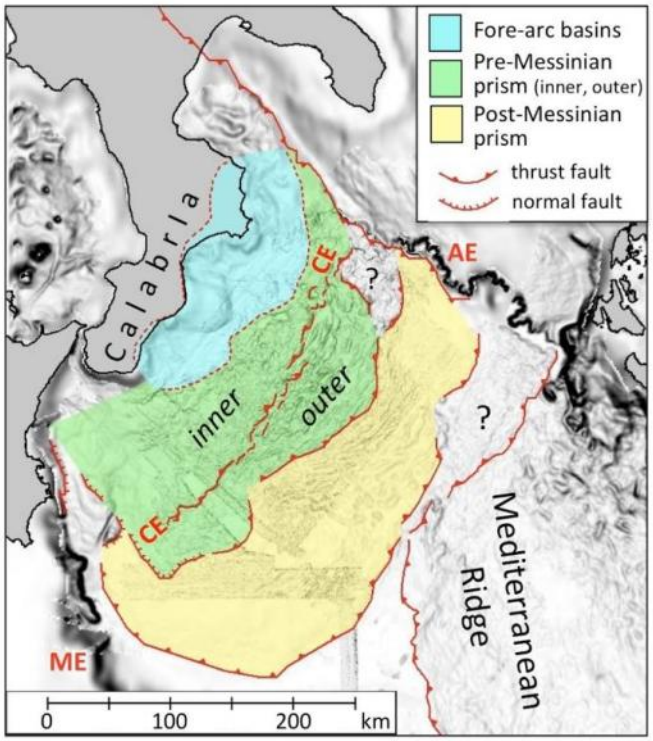

Figure 3. *Main morpho-tectonic zones of the Calabrian accretionary prism (Ceramicola et al. 2014). The inner parts of the fore-arc basins have been raised by on-going uplift of Calabria. The pre-Messinian prism to seaward is divided into inner and outer parts by the Calabrian Escarpment, up to 200 km long and 750 m high. The post-Messinian prism incorporates thick evaporites, also present in the outer Mediterranean Ridge [AE: Apulian Escarpment, CE: Calabrian Escarpment, ME: Malta Escarpment].*

Seismic reflection profiles across the pre-Messinian wedge and fore-arc basins show that many seabed thrust structures record post-Messinian tectonic movements, expressed as offsets of the reflector marking the base of the Plio-Quaternary succession, the largest example being the Calabrian Escarpment (Polonia et al., 2011). With reference to critical wedge theory, the tectonic movements are argued to record a response to the rapid frontal incorporation of Messinian evaporites, resulting in a reduction in taper that was corrected by out-of-sequence thrusting (OOSTs) and sedimentary underplating throughout the Plio-Quaternary advance of the prism (Minelli and Faccenna, 2010). Within the fore-arc basins, seabed thrusts and normal faults could also reflect on-going gravity-driven sliding above thin evaporites (Minelli and Faccenna, 2010). It has subsequently been suggested that the Calabrian Escarpment and other large OOSTs to seaward could have acted as pathways for post-Messinian fluid flow and mud volcanism, although no structurally-controlled pathways were identified (Polonia et al., 2011). Fluid migration within the prism has also been invoked in reference to seismically-imaged diapiric structures within the Plio-Quaternary succession of the fore-arc basins, originally suggested to be of halokinetic origin (Rossi and Sartori, 1981), but recently argued to be shale diapirs recording upward fluid migration from Messinian or older successions (Ceramicola et al. 2014).

Mud volcanoes are abundant within the eastern Mediterranean accretionary systems, and were first identified in the eastern Ionian Sea from cores of mud breccia from a structure on the western Mediterranean Ridge (Cita et al. 1978). The Mediterranean Ridge and its eastern extensions have since become one of the most intensively studied MV populations on Earth, through seabed studies that have identified hundreds of mud volcanoes (Mascle et al. 2014),

and scientific drilling of two examples that has provided evidence of extrusive activity over at least the last 1.2 Ma (Robertson et al. 1996).

In contrast, until recently, little was known about mud volcanism at the Calabrian accretionary prism. In 1981, two cores containing 'pebbly mudstones' were recovered from a seismically unstratified body on the inner prism (subsequently identified as Sartori MV), but mud diapirism as proposed by Cita et al. (1981) was rejected in favour of tectonic chaoticisation along thrusts (Rossi and Sartori 1981; Morlotti et al. 1982). The presence of MVs on the Calabrian accretionary prism was tentatively suggested from a few high backscatter patches observed on partial GLORIA sidescan coverage (Fusi and Kenyon 1996). However, MVs were not proven until 2005, during a campaign of the R/V OGS Explora that acquired the first regional multibeam coverage of Italian waters SE of Calabria, along with cores of mud breccia from two distinctive morphological features (Ceramicola et al. 2006), referred to as the Madonna dello Ionio mud volcanoes in the Spartivento fore-arc basin, and Pythagoras mud volcano on the pre-Messinian wedge to seaward (Praeg et al. 2009). Targeted seismic investigations of these two sites showed both to be the tops of buried extrusive edifices that interfinger with Plio-Quaternary sediments (Figure 4) above a regional unconformity (Praeg et al. 2009), inferred to be of mid-Pliocene age (3-3.5 Ma) by correlation to tectono-stratigraphic records exposed onshore in the Crotone fore-arc basin (Zecchin et al. 2012). These findings supported a model in which mud breccia extrusion was triggered by a tectonic reorganization of the accretionary prism ca. 3 Ma ago and has remained episodically active since, making these among the longest-lived mud volcanoes on record (Praeg et al. 2009; cf. Somoza et al. 2012). Recently, integration of multibeam bathymetry with backscatter data across the Calabrian accretionary prism has revealed at least 54 mud volcanoes across the fore-arc basins and pre-Messinian prism.

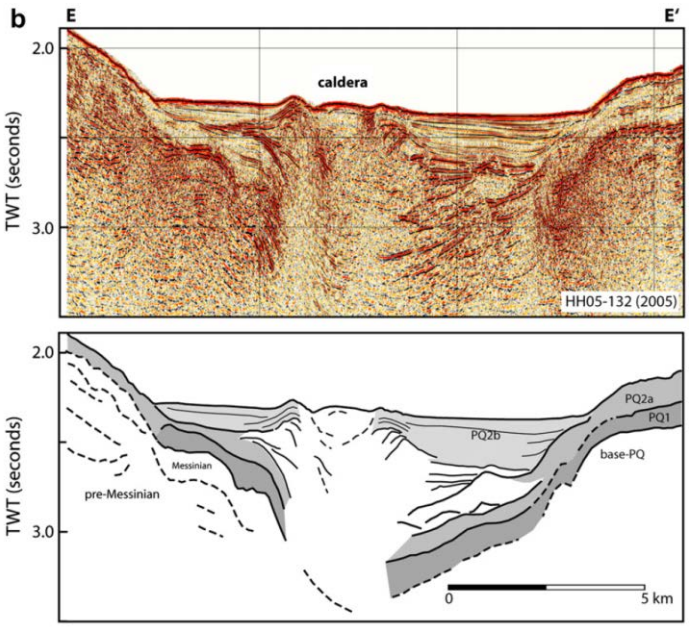

Figure 4. *Seismic image across the Madonna dello Ionio mud volcano and interpretation of stratigraphic units showing interfingering ("Christmas-Tree") of mud sequences of low acoustic impedance and well stratified units of hemipelagic sediments with high acoustic impedance (from Praeg et al., 2009).*

With few possible exceptions most of the mud volcanoes are restricted to the inner plateau of the Calabrian prism, landward of the Calabrian Escarpment (Figure 5). The majority have high backscatter signatures that, based on hemipelagic sedimentation rates and assumed sonar penetration, imply extrusion of mud breccias within the last 56 ka, i.e. during the last glacial-interglacial cycle, consistent with the depths of cored mud breccias at the Madonna dello Ionio, Pythagoras and Sartori mud volcano (Ceramicola et al. 2014). The Madonna dello Ionio and Pythagoras mud volcano were further investigated during two HERMES campaigns equipped with ROVs, which found geological and biological evidence of ongoing mud and/or gas seepage (Praeg et al. 2012).

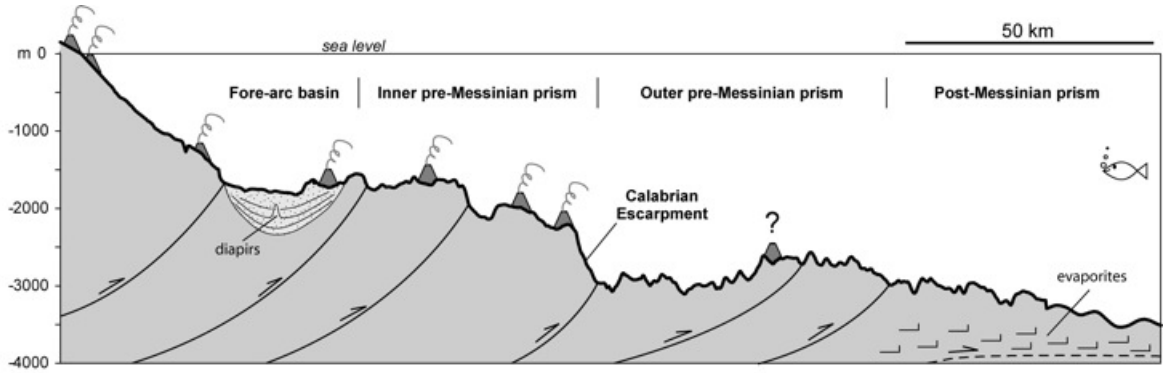

Figure 5. NW-SE bathymetric profile 250 km long across the central part of the Calabrian accretionary prism, schematically summarizing the distribution of mud volcanoes in relation to the main morpho-tectonic zones (from Ceramicola et al. 2014).

The main objectives of our studies are on mud volcanoes and the interactions of geological, physical, and chemical processes shaping these structures. By observing ongoing changes and reconstructing past evolution we will improve estimates of gaseous and dissolved methane emissions over time, as well as better understand the role of mud volcanoes as geohazards. The investigations conducted during this project are based on high-resolution 3D seismic imaging of active MVs in different tectonic zones of the CAP as well as OBS imaging and regional 2D lines to tie the new data to the established stratigraphic framework spanning the past ~6 million years (e.g. Praeg et al., 2009).From these data, we aim to identify changes in mud volcano activity since the late Miocene, as well as to image the deep-rooted feeder system of the mud volcanoes. Our new work builds on findings of R/V Meteor cruise M112 conducted during November/December 2014 as well as new findings made during the Poseidon cruise POS-499.

2.1 Mud volcano evolution

We want to investigate the temporal progression of individual mud flows at different mud volcanoes to constrain a model for the mud volcano genesis. The mud volcanoes

detected on the CAP are characterized by high backscatter areas, which are interpreted to indicate extruded mud breccias. At several mud volcanoes, it is even possible to distinguish the mud flows by outlining areas with different backscatter intensities. This information allows a first interpretation on the succession of the mud flows by assuming that the backscatter intensity is highest when not buried by hemipelagic sediments but decreases with increasing sediment coverage. By acquiring high-resolution 3D seismic data across the mud volcanoes, it will be possible to extend the seafloor maps downwards (and thus backwards in time) and map previous periods of mud volcano activity. The seismic signature of extruded mud bodies (low acoustic impedance, chaotic reflectivity) is distinctly different from that of regular hemipelagic sediments (layered sequences of higher impedance reflectivity). The complex nature of inter-fingering of mud bodies and hemipelagic sediments (referred to as "Christmas-Tree" signature) is best imaged using 3D seismic data; and only 3D seismic data allow a volumetric assessment of the mud extruded. Using regional 2D lines we will be able to tie the newly acquired 3D data into the existing regional stratigraphic framework defined by Praeg et al. (2009).

2.2 Mud volcano morphologies

Surface expressions of mud volcanoes are highly variable and depend primarily on the fluid content of the extruded mud. Muds with low porosities form mud domes or ridges, more cohesive muds with intermediate fluid content can build large structures with high elevations, whereas high-porosity muds create mud pies on the seafloor. On the CAP various types of mud volcano morphologies could be recognized and the more detailed we can image these structures the more information about the mud flow characteristics can be drawn. Imaging especially the morphologies e.g. of individual flows or the edifices gives new insights into mud volcano processes, which are only possible by high-resolution mapping. The 3D seismic data acquired with the P-cable system will allow us to develop maps of buried (past) mud flows and by using seismic advanced attributes (such as amplitude-draped coherency) we will be able to define internal properties of these older flows allowing identifications of potential changes in the extruded mud-properties over time or their changes post-extrusion, such as consolidation and porosity reduction.

2.3 Deep roots of the mud volcanoes

By selecting different mud volcanoes across the CAP, we are able to characterize different tectonic regimes and their internal structures controlling the location and evolution

of these mud volcanoes. Venere mud volcano is located at the southern rim of the fore-arc basin, but Poseidon mud volcano is within the inner pre-Messinian prism. OBS and regional 2D seismic lines will be used to image the deeper structure of the mud volcanoes. Integration with existing seismic lines previously acquired (including those from cruise M111, Kopp et al., 2015) will provide further structural control on MV location and evolution.

3. Narrative of cruise with technical details

All times and dates listed in this section are local time (UTC + 2).

June16, 2017, Friday

Arrival and loading of compressor container onboard research Vessel POSEIDON.
Arrival of scientific crew (Beeck, Rindfleisch) in Dubrovnik, Croatia

June 18, 2017, Sunday

Arrival of scientific crew (Riedel, Bialas, Krabbenhöft, Muff, Bähre, Kühn, Stange) in Dubrovnik, Croatia. All personal embark on vessel.

June 19, 2017, Monday

Scientific equipment arrived and was loaded onboard.
Departure Dubrovnik at 16:00 and transit to first study site at Venere mud volcano.
Scientific crew begins installing all scientific gear in laboratories and on deck.
15:30 Safety briefing for all scientific crew

June 20, 2017, Tuesday

Continue transit to first study site at Venere mud volcano. All day continue to install scientific gear. Preparation for OBS deployment included building anchors, programming releasers and pressure cases with recorders, testing radio antennae and flash lights.
10:20 Safety drill for all crew and scientists

June 21, 2017, Wednesday

08:00 Arrival at first OBS drop position at Venere mud volcano. We start with a test of all 13 releasers. The releasers were mounted onto the frame of the CTD unit and lowered using the CTD winch wire to 1500 m water depth. We also run the CTD to measure seawater properties in order to calculate sound speed for the ocean column. These velocities are later useful for OBS re-localization as well as for navigational purposes (e.g. determining distance of receivers from airgun based on observed travel times of the direct wave) and migration of the reflection data.

08:30 CTD frame lowered to1500m

09:15 All releasers responded and were disabled

09:50 CTD frame back on deck

10:30 OBS V01 deployed

10:49 OBS V02 deployed

11:05 OBS V03 deployed

11:20 OBS V04 deployed

11:32 OBS V05 deployed

11:45 OBS V06 deployed

12:04 OBS V07 deployed

12:24 OBS V08 deployed

12:43 OBS V09 deployed

12:56 OBS V10 deployed

13:08 OBS V11 deployed

13:19 OBS V12 deployed

During Afternoon, we continue to prepare the Trawl-Doors of the P-Cable system; which are stored attached to the outside of the stern during non-P-cable data acquisition.

We decided to being surveying in 2D mode due to limited time available preparing the entire 3D system. A set of 12 lines from the main P-Cable survey were selected, crossing the OBS grid. These lines are a test for our acquisition software, GPS navigation routines, as well as airgun and compressor operations.

17:00 Streamer with 4 active sections (blue oil-filled streamers) and airgun deployed

18:20 Compressor on full service load with gun pressure at 165 bar

However, we encounter issues with the trigger box and the GI gun is misfiring, in part due to the wrong trigger;

To overcome the trigger problem, the geometrics computer provides an internal trigger and the computer is synced with the GPS so that navigation can be accurately defined;

We further encountered serious problems with all lithium batteries used with the streamer birds. The batteries are all non-functional.

The two birds attached to the streamer do not respond: one bird has a motor-problem and is fixed to a depth of 8 m. The other bird is at 0.5 m depth and its position can also not be changed.

19:45 We decide to pull in streamer and remove the birds.

19:55 Streamer re-deployed without birds

20:00 Compressor ground-cable needs to be repaired. Stopping compressor and halt airgun firing.

20:08 Compressor functional again.

20:11 Speed of vessel to 4kn and start survey lines

June 22, 2017, Thursday

01:30 Geometrics computer malfunctions; restart of recording software

08:00 Finishing lines before starting P-cable preparations

08:30 Pulling in gear and prepare P-Cable

High leakage problems (> 300)

We also detected problems with GPS on airgun-float: most likely it took on water from high humidity, i.e. no seawater), but unit is fried and non-functional for the remainder of the entire cruise.

17:15 Cross-cable on deck for testing

We require a string of Serial-numbers (SN) of each “T-box” and we are awaiting this list from Gero Wetzel, who was asked to help from shore (table received at 20:00)

No operations overnight: ship keeps station.

June 23, 2017, Friday

08:00 Continue testing P-Cable system.

14:00 Decision to test system in water

15:20 Start deploying P-Cable

15:43 First three streamer sections deployed (current at 1.3 amp; leakage at 43).

Test shows that streamer section #3 can no longer be seen: pull back on deck
Streamer #4 attached but leakage > 1000
System is brought back on deck and we see that T-box #4 took in seawater due to a screw not fully tightened. The box (original SN-6119) replaced by new box with SN-6117.

18:15 10 sections deployed and check, but box #6 not detected

18:22 Using 2nd Geometrics box, but same problems: decide to abandon 3D deployment and go for 2D streamer instead;

19:30 All P-cable gear on deck
Prepared 2D streamer with 3 sections (solid state)
Overnight we though to run long refraction lines

20:00 Encounter issues with GI gun: injector not firing

22:40 GI gun repaired and back in water

22:56 GI gun hydrophone already broken and generator not firing
All gear back in and no further activity over night; require creating new airgun strings, which need to dry and harden over 10 hours

June 24, 2017, Saturday

08:00 begin preparing for P-Cable deployment
The system is put into the water one streamer at a time and testing the unit immediately; progress slow, but testing seems successful to see immediate issues on all parts; we switched box #6, which appears to be broken;

16:30 Testing of all P-Cable sections in water, but communication failed and cross-cable is seen only until box #9

16.45 New airgun strings are not ready yet and no additional options exist, so we decide to halt all operations and keep ship stationary again.

June 25, 2017, Sunday

08:00 Begin of preparations for new P-cable deployment
14 boxes, 16 streamers; box 1 and box 14 have solid state with 2 sections each.

13:45 P-cable completely deployed; setting 2nd trawl-door

14:10 We no longer receive GPS signal from starboard trawl-door

14:15 Recording unit started
Record length: 4.5 s

Delay 0ms
Sample rate 0.5 ms
128 channels in total (16×8)

14:25 Airgun deployed and firing, 170 bar

14:30 Lost box 14 with streamer 15 and 16; only 112 channels recorded

15:45 Leakage is increasing from ~80 at beginning of survey to now ~120

16:20 Leakage at 290 and increasing fast

16:27 Leakage > 500: abort survey!
No recovery of system possible any more (overtime regulations)
We instead run 3 refraction lines (NW-SE orientation) with P-cable deployed; for these long offsets lines, we reduce airgun firing rate to 10 seconds

June 26, 2017, Monday

06:00 Recover all gear and start testing
While recovering backboard trawl-door and P-cable, the starboard trawl-door moves across the data cable! We recover all streamers to prevent any damage to system.

With all gear on deck, we require more time for repair the P-cable system and re-deploy than initially thought, with high uncertainties if it will be functional; potential weather issues forecasted for the middle of the week and battery-limitations on OBS force us to go for a 2D survey across Venere.
This way, we will be able to acquire a useable pseudo-3D reflection grid as well as a full coverage for 3D OBS mirror imaging;
We remove cross-cable from drum and lay it out on backboard working deck for testing. All blue streamers are connected for a 2D streamer and together with stretch-section and deck cable, the 2D streamer is put onto the drum for ease of deployment and recovery.

11:30 2D streamer and airgun deployed; start surveying using the same 84 parallel survey lines originally intended for P-Cable acquisition.

Survey parameters: 0.5 ms sample rate; 4.5 seconds record length
No deep-water delay; injector fires 55 ms after generator

Streamer is 150 m long (active section) and made up from 12 blue-colored oil-filled streamers; 96 channels in total

25 m stretch and 25 m extra deck-cable; airgun is 20m behind vessel

Two channels are dead:

#49 (1st channel in section 5) and #65 (channel 5 in section 6)

After line #2, the navigation-depth sounder switched back on at bridge

15:30 – 16:30 Discussion about state of compressor container

June 27, 2017, Tuesday

04:00 Working/Supply compressor from ship turned off; we lost ~120 shots; survey gap is right across central portion of Venere mud volcano (Murphy!). We re-fill this gap later during the survey.

08:00 Finished 12 survey lines

17:30 Finished 18 survey lines

Gun pressure varies between 165 bar and 175 bar.

21:00 – 22:30

Changing order of survey lines; original sequence was optimized for P-cable system; with a 2D streamer, we can make tighter turns; thus, a new sequence of lines was designed by J. Bialas and M. Riedel; this may provide additional time for completing yet missing refraction lines or any additional gaps that may happen in the survey;

Also, we plan to recover all OBS on Sunday, July 2nd, and move to the next survey region at Poseidon mud volcano, starting re-deployment on Monday, July 3rd, followed by 1 day of refraction survey lines. In this plan, the P-cable will hopefully be deployed by Tuesday, July 4th.

June 28, 2017, Wednesday

08:00 Sequence of new lines with tighter turns seems to be working

All gear functions well

P-cable cross-cable on backboard deck was tested: we encountered a problem in the lead-in cable to box #13; since this lead-in cable is no longer functional, we are unable to use these 2 solid-state streamers.

The smaller (shorter) cross-cable now is consisting of 13 boxes. We replace 10m long section-cables with 15 m long segments to increase overall spread.

New survey will be defined, once time-line is more predictable.

June 29, 2017, Thursday

All day: continue acquiring 2D lines

June 30, 2017, Friday

All day: continue acquiring 2D lines

July 1, 2017, Saturday

10:30 End of acquiring parallel lines across Venere mud volcano

11:36 Start 2D refraction survey; airgun at 10 second firing interval

July 2, 2017, Sunday

06:00 End of survey at Venere mud volcano

Recover streamer and airgun

During the night, wind was high with up to 18 m/s, high seas developed;

06:45 Start OBS recovery sequence

We start at OBS V03, then move along the long-edge of the OBS grid due to strong winds and surface currents.

OBS	Time released	Time on surface	Time on deck
V01	10:50	11:14	11:22
V02	10:24	10:47	10:57
V03	07:05	07:32	07:40
V04	07:46	08:12	08:26
V05	09:58	10:20	10:32
V06	11:15	11:32	11:49
V07	11:41	12:02	12:12
V08	09:28	09:54	10:07
V09	08:13	08:37	08:46
V10	08:37	09:03	09:16
V11	09:06	09:28	09:34
V12	12:05	12:27	12:31

High winds and swell prevent additional acquisition of data between Venere and Poseidon mud volcano. We finish the transit and wait on station at Poseidon mud volcano until Monday morning.

July 3, 2017, Monday

Weather is steady with slightly lower wind and swell, allowing us to deploy the OBS.

05:58 OBS P01 deployed
06:13 OBS P02 deployed
06:27 OBS P03 deployed
06:39 OBS P04 deployed
06:51 OBS P05 deployed
07:05 OBS P06 deployed
07:20 OBS P07 deployed
07:52 OBS P08 deployed
08:08 OBS P09 deployed
08:27 OBS P10 deployed
08:42 OBS P11 deployed
08:54 OBS P12 deployed

Weather is still steady and has improved for 2D seismic data acquisition.

09:20 Deploy 2D streamer
09:40 Deploy Airgun

Data acquisition across the two refraction lines at 10 second shot interval and 8 seconds recording time. Sample rate: 0.5 seconds.

After the 2 refraction lines, we acquire a few lines towards and across Sartori mud volcano, lying about 10km further SW.

Winds increase continuously and forecast predicts wind force 7 – 8 over night. We therefore stop data acquisition and recover all gear.

19:30 All gear on deck

Waiting on weather until Tuesday

Preliminary data quality assessment shows low internal reflectivity beneath and around Poseidon mud volcano. In contrast, the lines acquired at Sartori show distinct mud-flow layers onlapping on surrounding sedimentary layers. Below the central portion of Sartori, deeper reflections are identified.

We therefore decided to try the next P-Cable acquisition at Sartori and if possible acquire 2D lines across the Poseidon mud volcano chain.

July 4, 2017, Tuesday

08:00 Winds and seas still high; no new data acquisition until late in afternoon

16:00 Start deploy streamer and airgun

16:45 Start data acquisition with lines in region of Poseidon mud volcano chain

July 5, 2017, Wednesday

06:00 End 2D survey

06:30 Start recover OBS

OBS	Time Released	Time on surface	Time on deck
P01	12:27	12:59	13:07
P02	11:55	12:26	12:35
P03	11:22	11:52	12:05
P04	07:35	08:04	08:16
P05	10:47	11:21	11:31
P06	10:15	10:45	10:56
P07	09:41	10:10	10:23
P08	06:24	06:52	07:10
P09	07:03	07:33	07:42
P10	08:06	08:34	08:44
P11	08:37	09:05	09:18
P12	09:08	09:38	09:48

06:30 Start reconfiguring the P-Cable system

14:00 Deploy P-Cable system

15:15 Port-side trawl-door deployed

15:45 Start surveying; make turn to Sartori

Survey P7000: 7 seconds shot interval, 6.5 seconds recording

18:40 All communication to P-Cable lost

Bringing in starboard trawl-door first: upon close inspection we recognized a problem with the strength-member of the cross-cable: at T-box #1, the strength-member was cut and all weight of towing the system (including trawl-doors) was on the data-cable. This has caused failure of the communication, despite that we were still able to measure current and had no leakage problem.

We brought in the first two T-boxes, exchange cables, strength-members and removed streamer #1 (two solid state sections). The active length of the cross-cable is now 60m, with the paravanes towed at a cross-distance of 120 m.
The cause of the issue was a broken shackle, most likely due to ware and tare.

21:00 All gear back out, and all is functional.
Start profile of Sartori 3D cube at 22:05

July 6, 2017, Thursday

08:00 no further problems recognized during the night:
We acquired 9 lines in ~14 hours, averaging 1.5 hour per line and turn. This is within the predicted frame of total survey time of 5 days for 81 lines.

July 7, 2017, Friday

3D P-cable survey continues without interruption

July 8, 2017, Saturday

3D P-cable survey continues without interruption

July 9, 2017, Sunday

17:15 Geometrics software stopped updating the window-display of several channels, and we lost connection to a few of the streamers. Reboot of the PC running the system created additional communication problems. We then switched off the power unit, rebooted and finally regained full access to the P-Cable.

18:00 Compressor off, as air filter top has blown off. We temporarily fixed the filter, which will suffice until the end of our expedition. A complete repair will be done back at Sauer&Sohn in Kiel.

18:36 All streamers connected and recognized and data acquisition back to normal.

July 10, 2017, Monday

08:00 Survey continues without interruptions.

09:30 We started to define fill-in profiles to increase coverage of the 3D cube.
Our current fold map as of this morning is shown below in Figure 6.

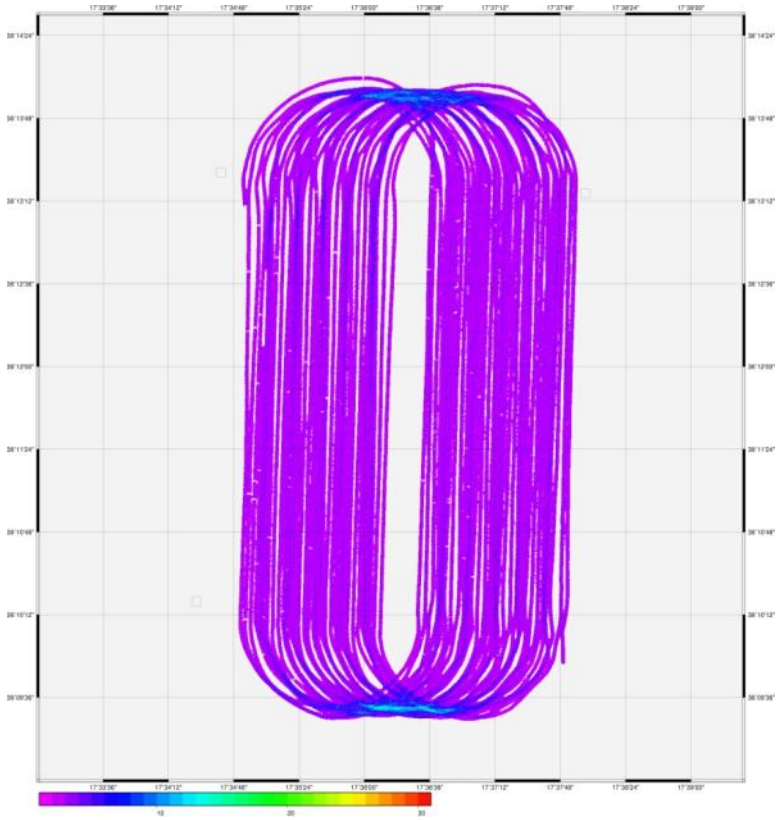

Figure 6. Preliminary fold map of the Sartori 3D P-Cable cube as of July 10, 2017.

July 11, 2017, Tuesday

08:00 Further evaluation of fold-map and in-fill procedures

16:00 End of 3D survey

17:00 All gear on deck

17:05 Start steaming to next study site: CETUS mud volcano

20:30 Start deploy airgun and streamer, made of 4 oil-filled sections

21:00 Start shooting profiles

Airgun on deck, leakage problems

Airgun Re-deployed

July 12, 2017, Wednesday

06:00 End of profiles; recover all gear

Trawl-doors recovered and secured on deck

Dismounting and packing up

07:30 Start steaming towards Geodesy Stations

20:00 Arrival at geodesy stations

23:00 All completed at geodesy stations

July 13, 2017, Thursday

10:00 In Port of Catania

12:00 Start offloading all gear

15:00 Trucks won't arrive until Friday morning due to delays at ferry terminal;
A security firm is hired to dispose guards protecting gear sitting on pier over night;

July 14, 2017, Friday

09:00 Start of truck loading, Compressor-container removal, and custom procedures

14:00 All gear loaded onto trucks, paperwork for customs completed;
Remaining scientists disembark vessel;

4. Scientific Results

4.1 Venere mud volcano

Venere is a double-cone mud volcano situated within a larger canyon system (Figure 7). Regional bathymetry from M112 (Bohrmann et al., 2015) and high-resolution AUV bathymetry (Bohrmann et al., 2016) define the distinct morphology. Short-distance mud flows are seen, mostly on the SW flank of the cones. Several gas flares were previously mapped (Bohrmann et al., 2016), but we did not collect any new multibeam water-column data to verify the occurrences. Ring-faults are seen at the seafloor defining a circular caldera of the entire mud volcano feature. Seafloor backscatter shows high seafloor reflectivity around the two cones, whereas the surrounding area is characterized by low to medium backscatter strength (Figure 8).

We acquired data on 12 OBS and along 84 parallel 2D lines (Figure 9). For refraction velocity analyses, an additional set of 7 lines were acquired with longer offsets to the OBS (Figure 10).

Using the 84 parallel lines, a pseudo 3D analysis can be performed. On board, we did analysis time-slices through the 3D volume for first quality data analyses (Figure 11, 12).

A cross-line acquired in perpendicular direction to the main 84 parallel lines highlights the still present static offsets between individual lines (Figure 13). A post-expedition processing will remove these static shifts by using the multibeam data as absolute depth-datum.

A first check on the OBS recording data showed high-quality OBS records on all channels (Figure 14). Refracted arrivals were identified on most OBS.

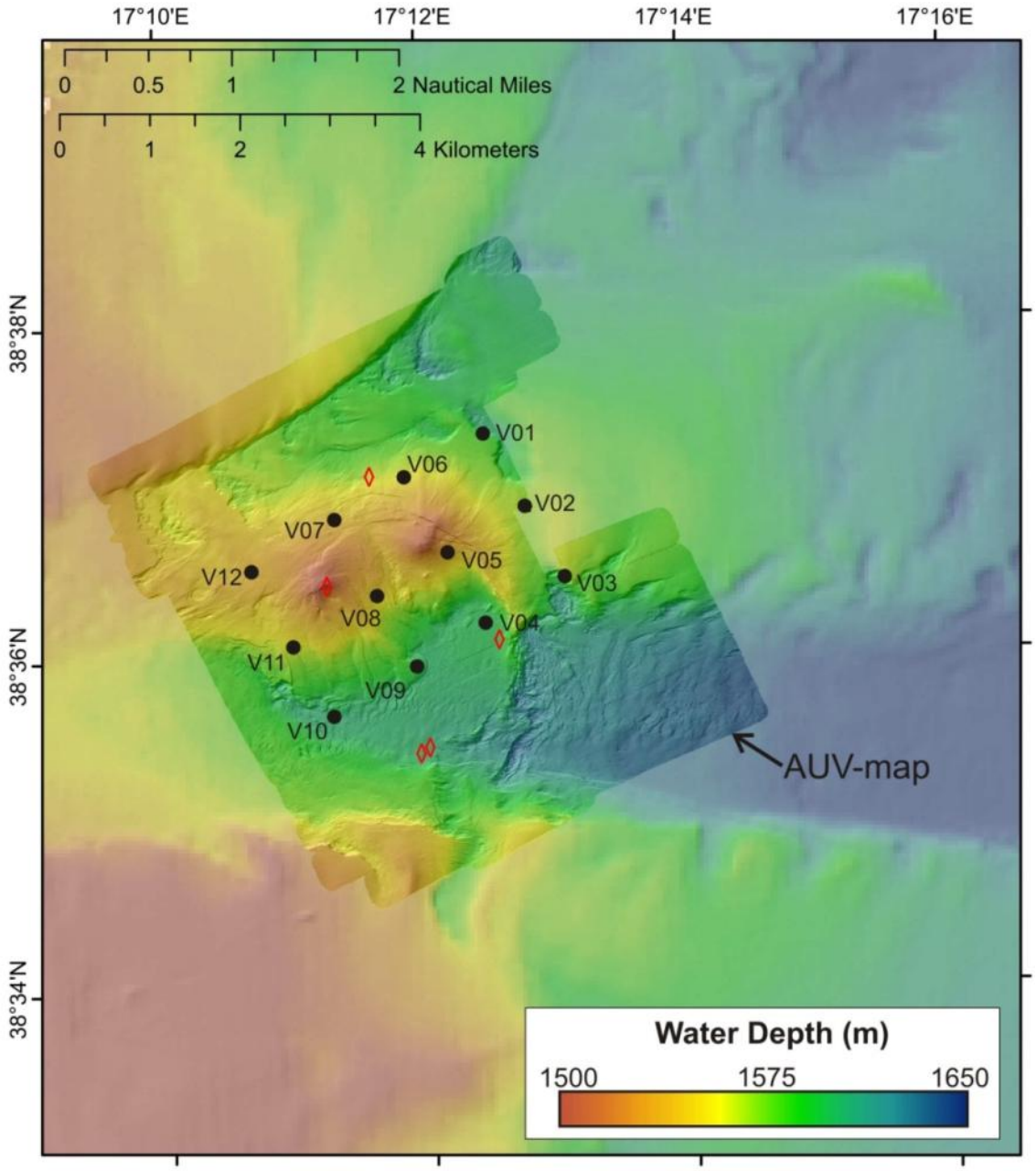

Figure 7. Image showing morphology of the Venere mud volcano from regional and high-resolution AUV bathymetry. Location of gas flares are shown with red symbols (from Bohrmann et al., 2016). OBS deployed during POS515 are shown with black dots. Regional data are from cruise M112 (Bohrmann et al., 2015) and AUV data are from cruise P499 (Bohrmann et al., 2016).

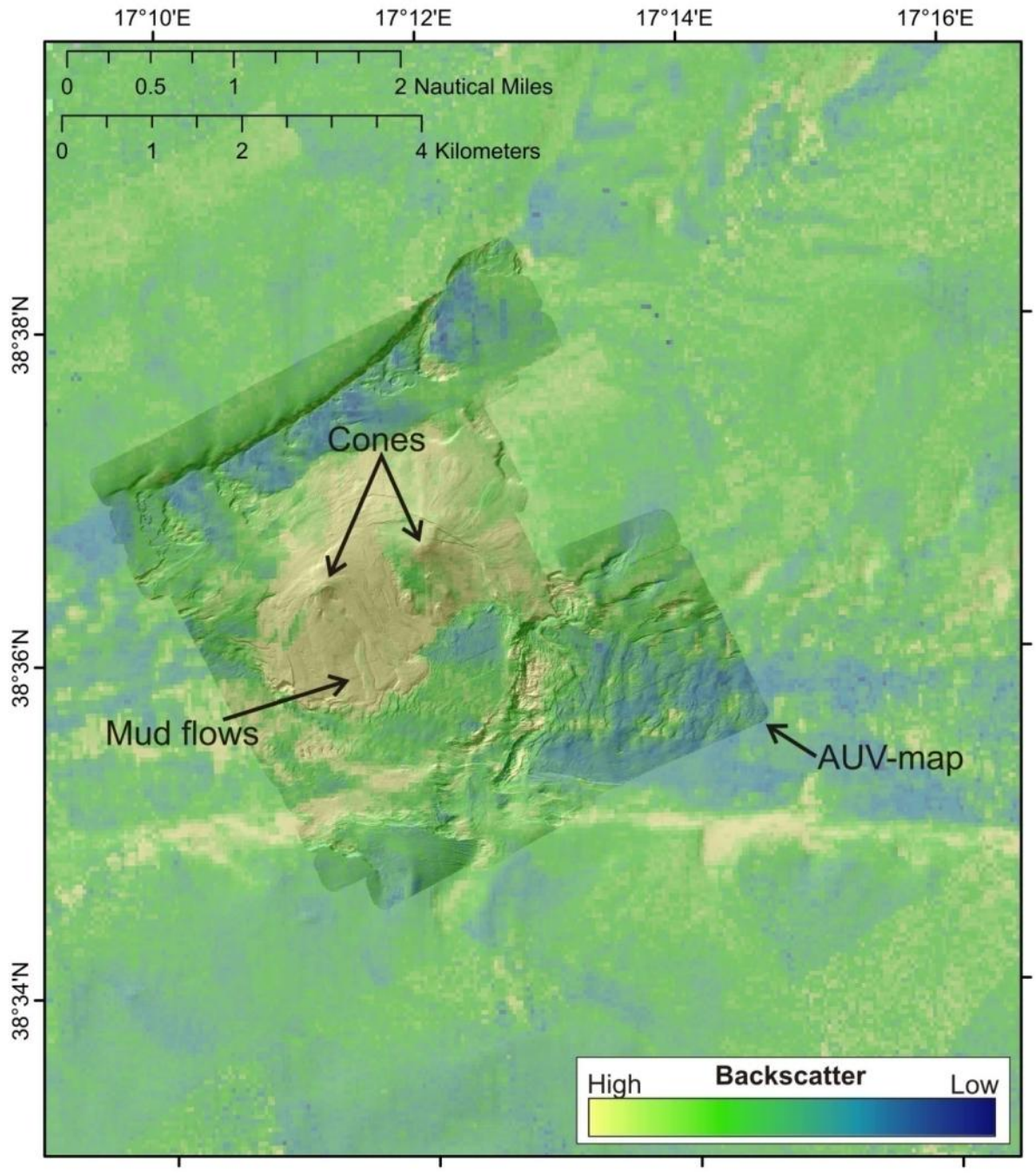

Figure 8. Morphology of the Venere mud volcano using backscatter. Recent mud flows emanating from the two cones show high backscatter, whereas the surrounding regions show mostly low seafloor backscatter values. Regional data are from cruise M112 (Bohrmann et al., 2015) and AUV data are from cruise P499 (Bohrmann et al., 2016).

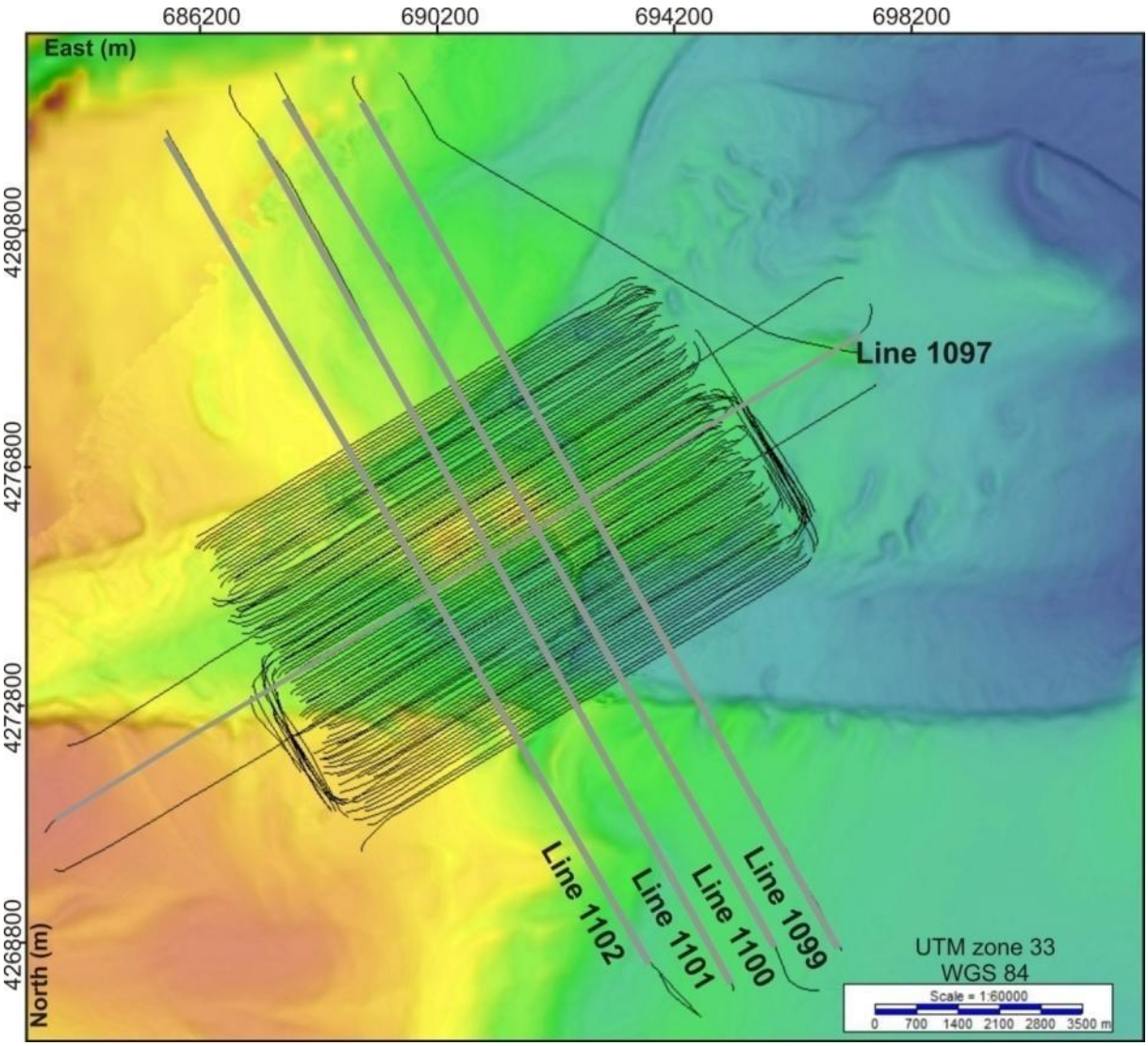

Figure 9. Map of 2D seismic data acquired across Venere mud volcano with bathymetry grid as background. Five examples of survey lines acquired across the OBS grid for refraction velocity analyses are highlighted with thick grey lines.

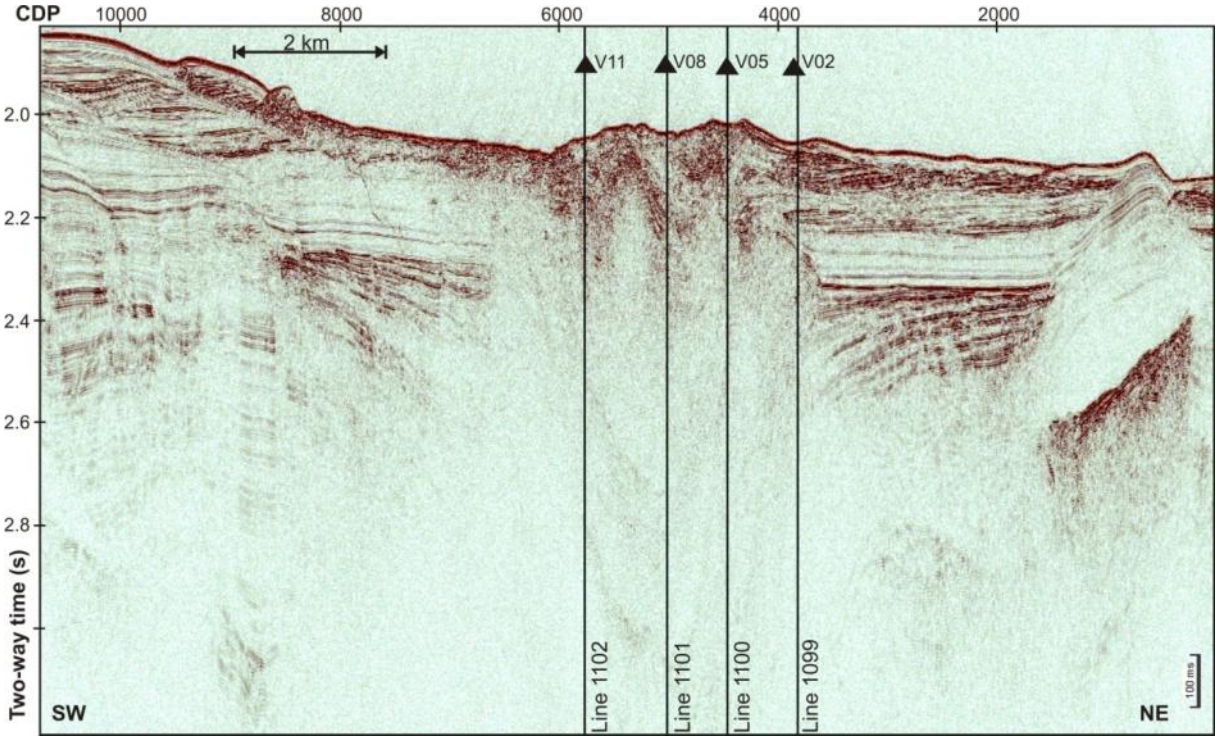

Figure 10a. Seismic Line 1097, shot in SW-NE direction across Venere mud volcano. OBS positions crossed are shown by black triangles.

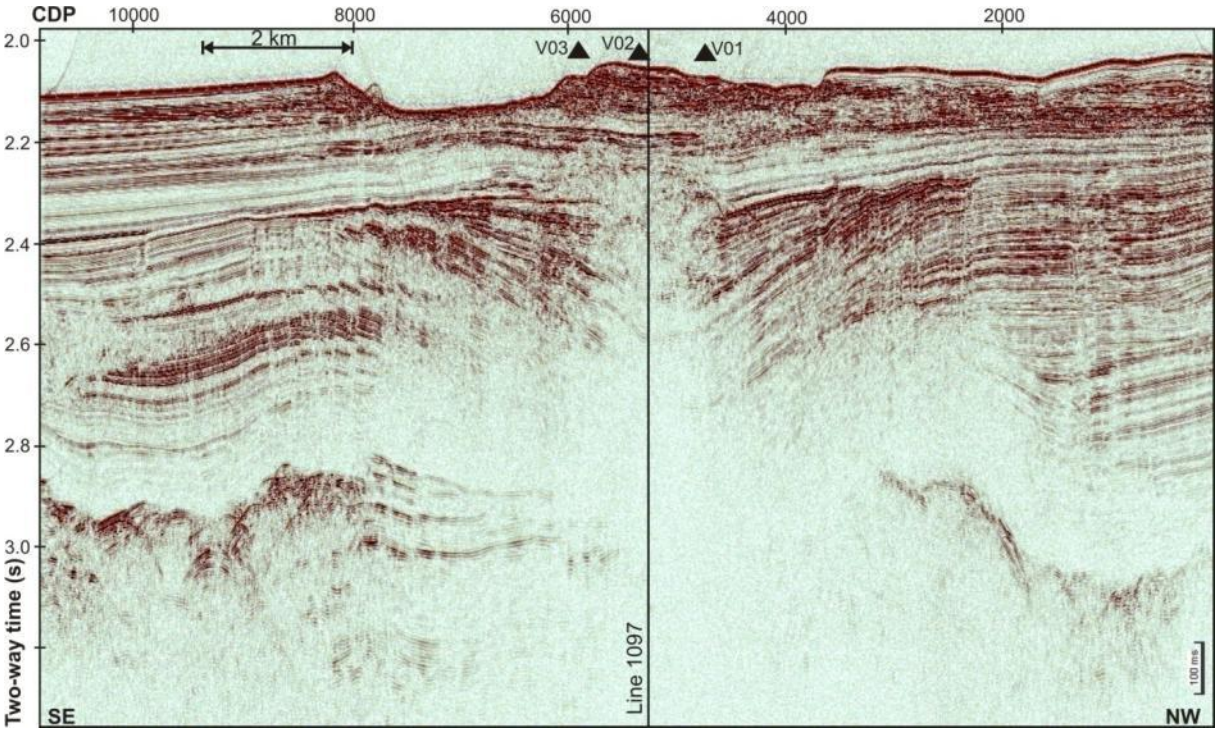

Figure 10b. Seismic Line 1099, shot in SE-NW direction across Venere mud volcano. Note the prominent down-dipping reflections beneath the centre of the mud volcano, small-offset faulting within the sediment sequence below the regional unconformity (at ~2.4 s two-way time), and deep higher reflectivity acoustic basement.

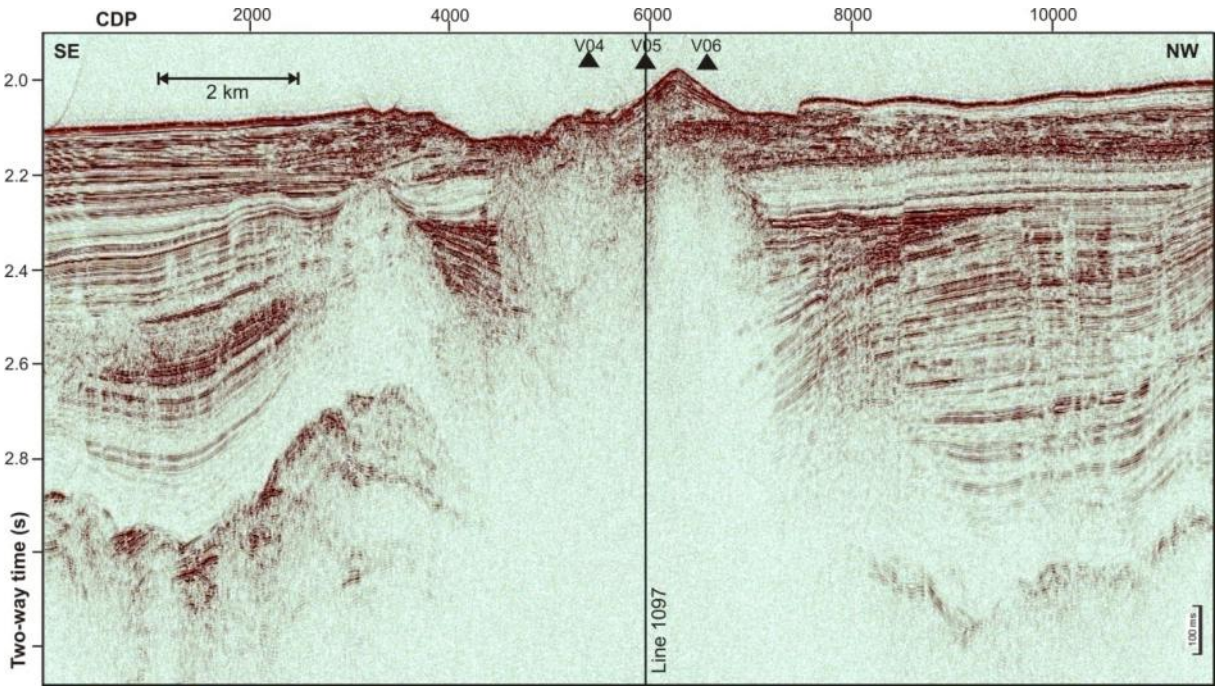

Figure 10c. Seismic Line 1100, shot in SW-NE direction across Venere mud volcano. Beneath the central portion of the mud volcano, seismic blanking is caused by the mud-breccia ascending from greater depth, forming the seafloor cone-like expressions.

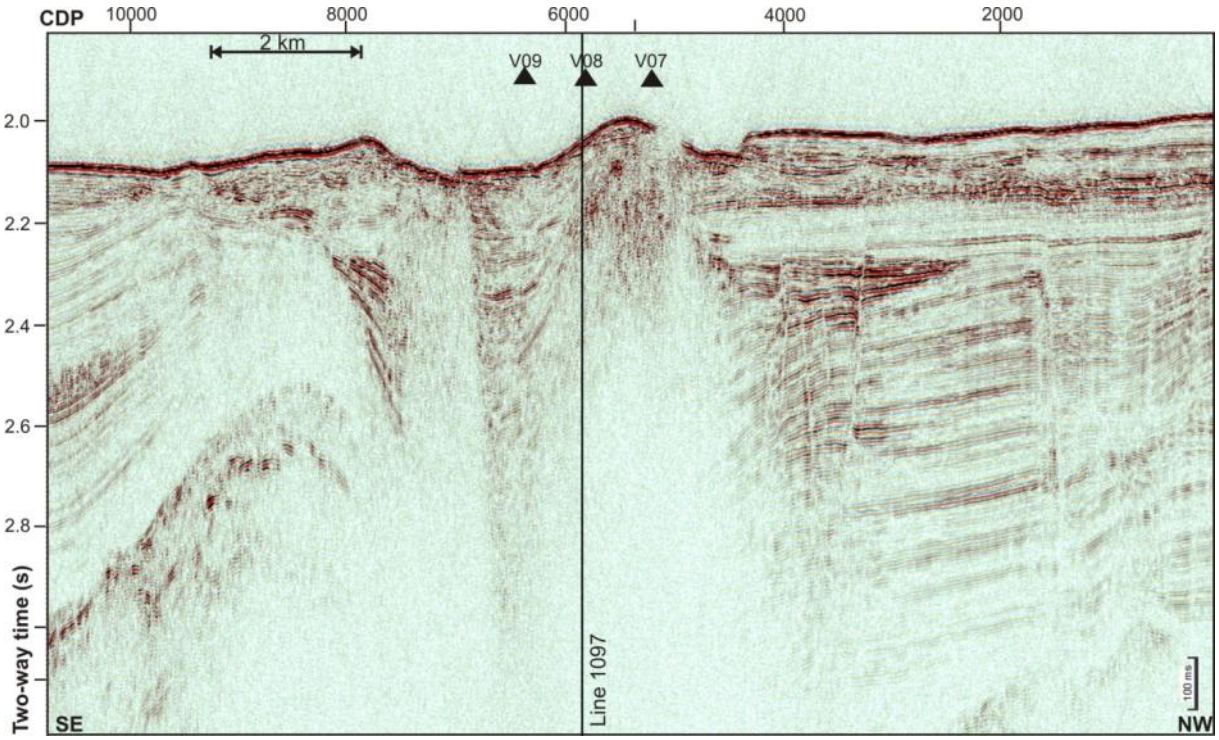

Figure 10d. Seismic Line 1101, shot in SE-NW direction across Venere mud volcano.

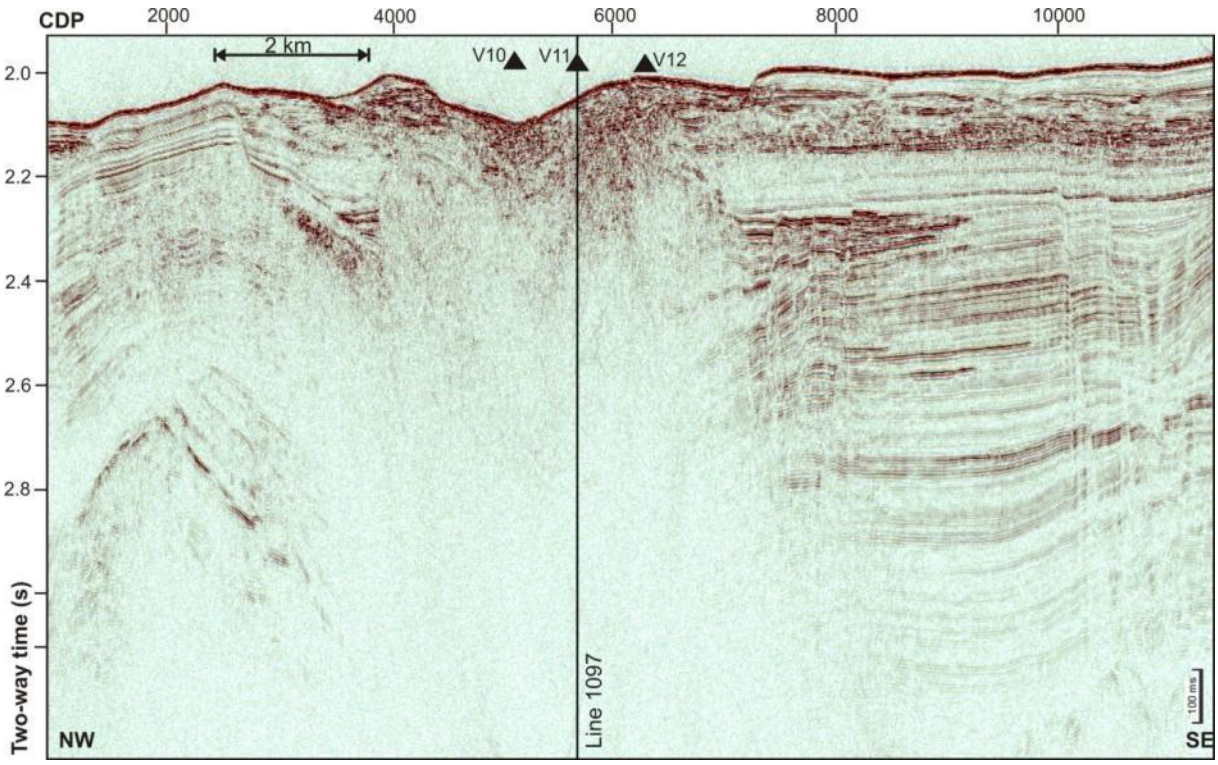

Figure 10e. Seismic Line 1102, shot in SW-NE direction across Venere mud volcano.

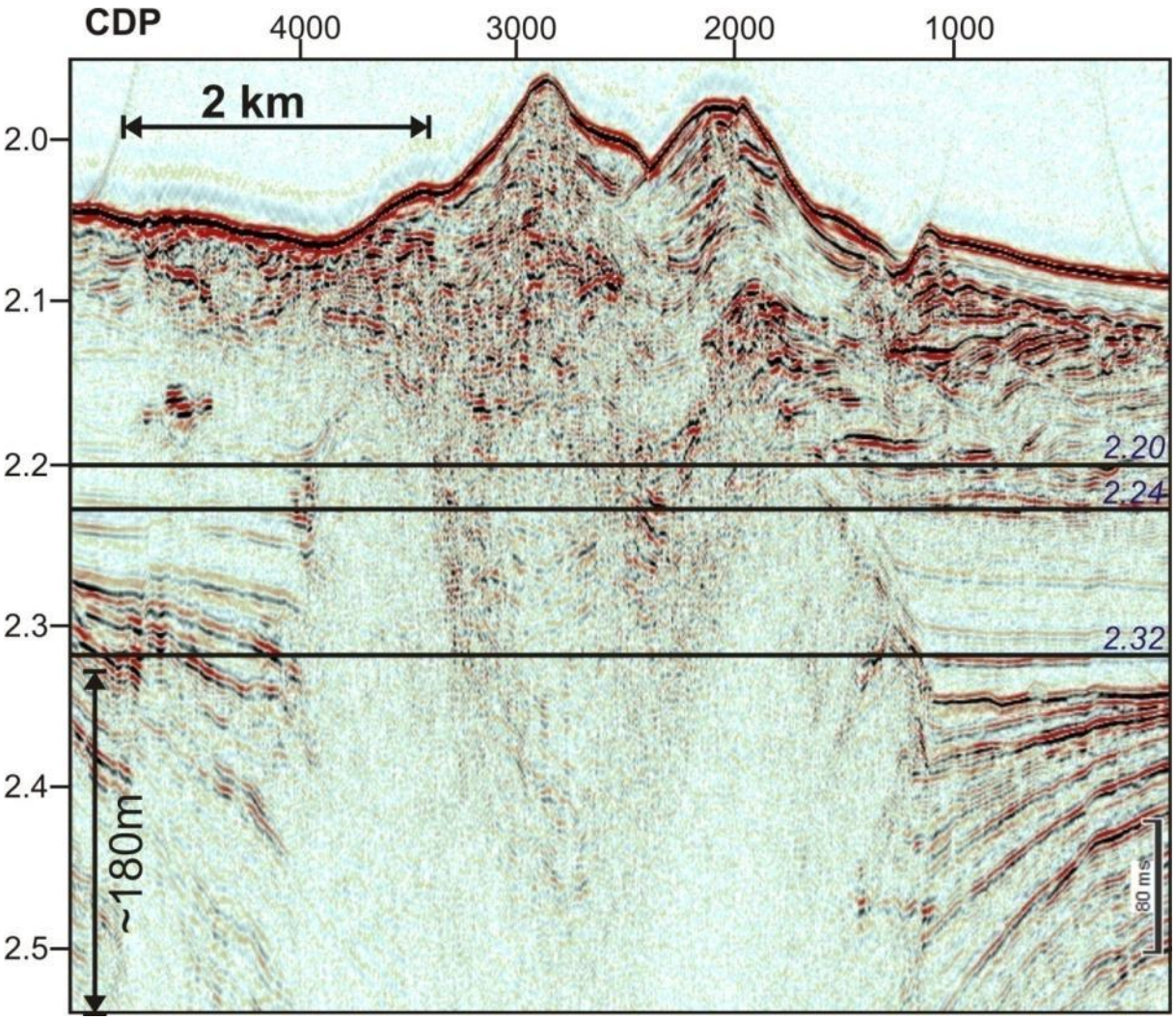

Figure 11. Line 1027 from the set of 84 parallel lines across the double cone structure of Venere mud volcano. Indicated are the three depths of time slices shown below.

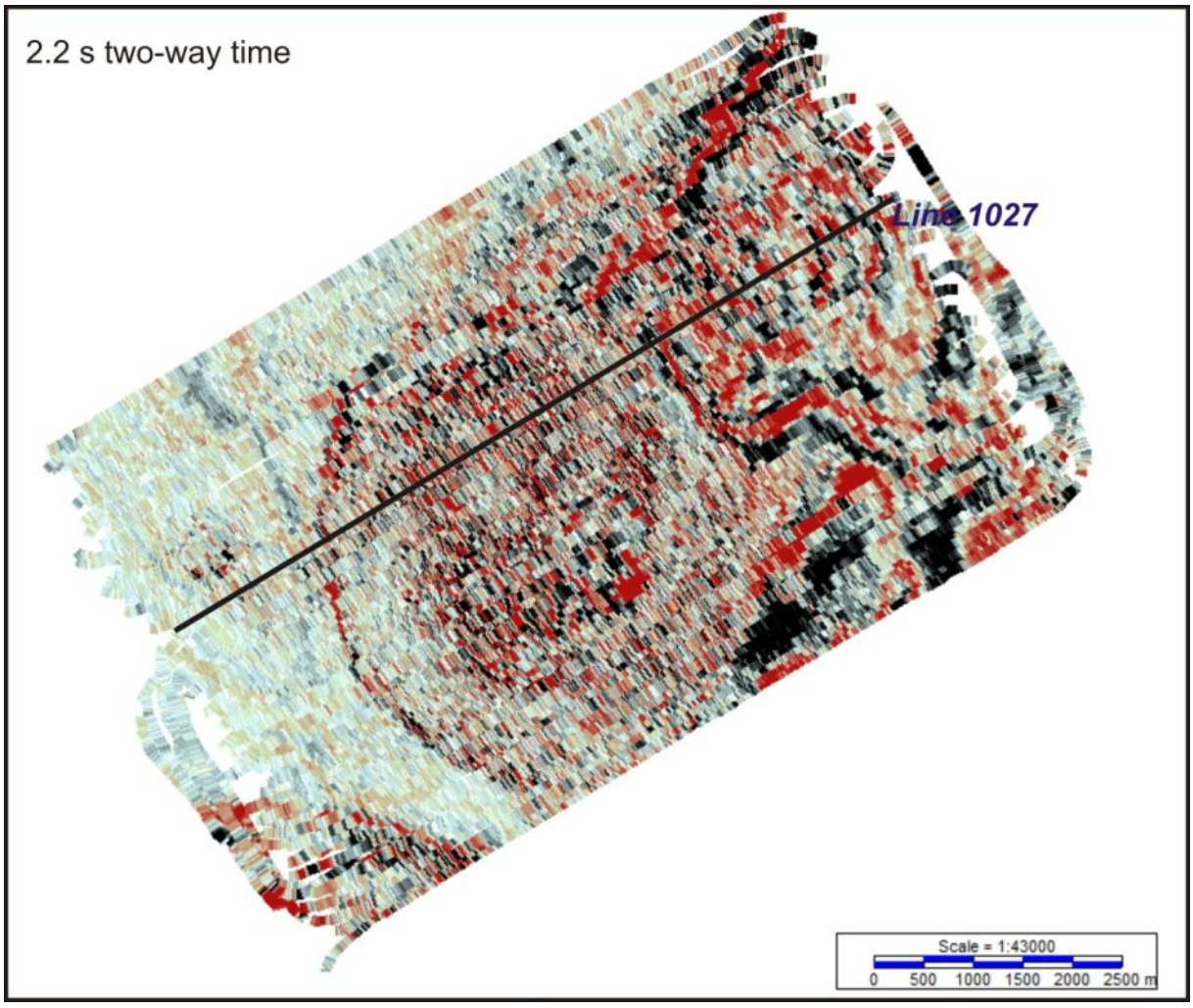

Figure 12a. Time slice of reflection amplitude at 2.2 seconds two way travel time using all 84 parallel lines. A circular shaped feature marks the extent of the Venere mud volcano composed of mud breccias and mud flows and is sharply truncated relative to the surrounding layered sediments.

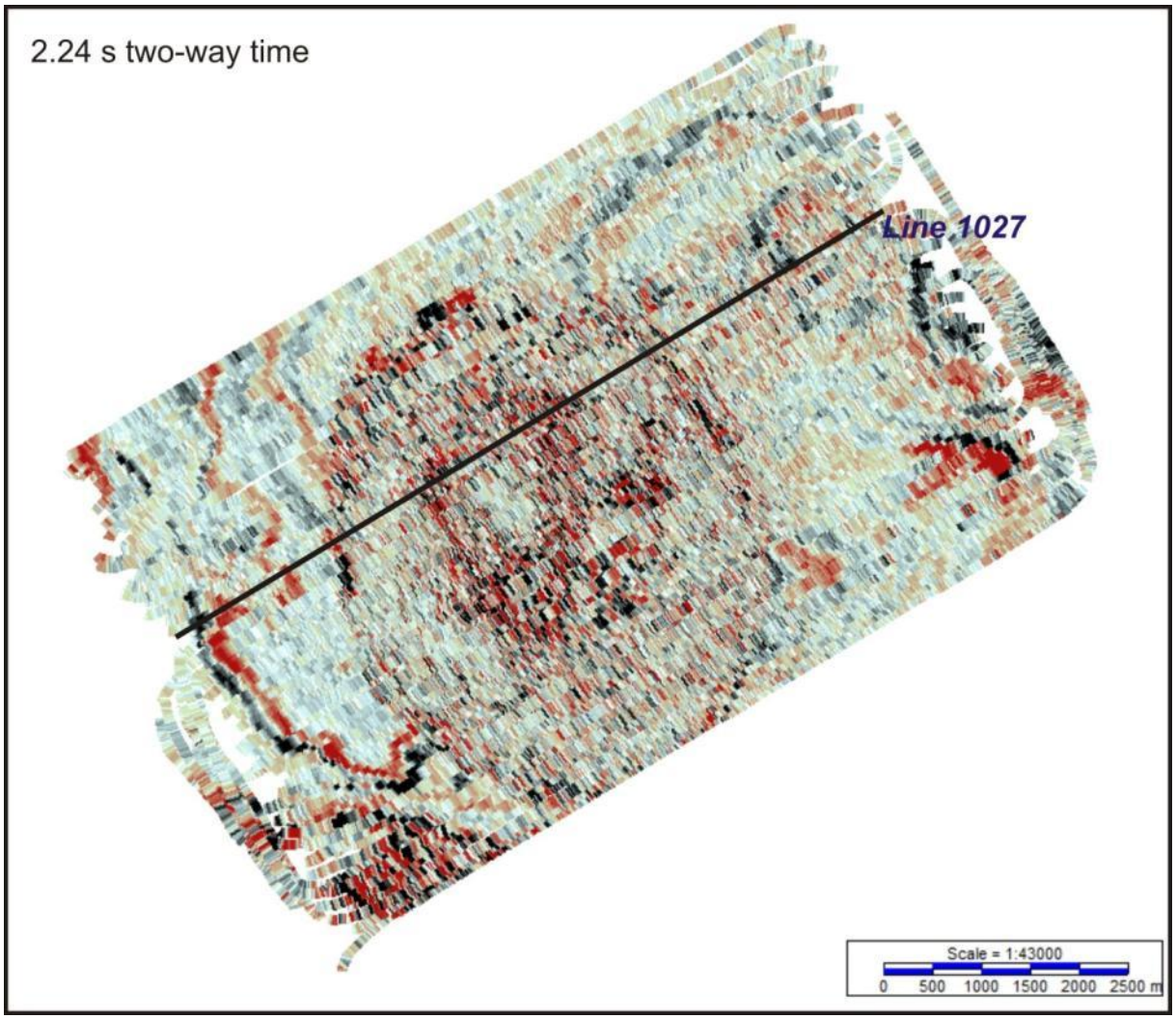

Figure 12b. Time slice of reflection amplitude at 2.24 seconds two way travel time using all 84 parallel lines.

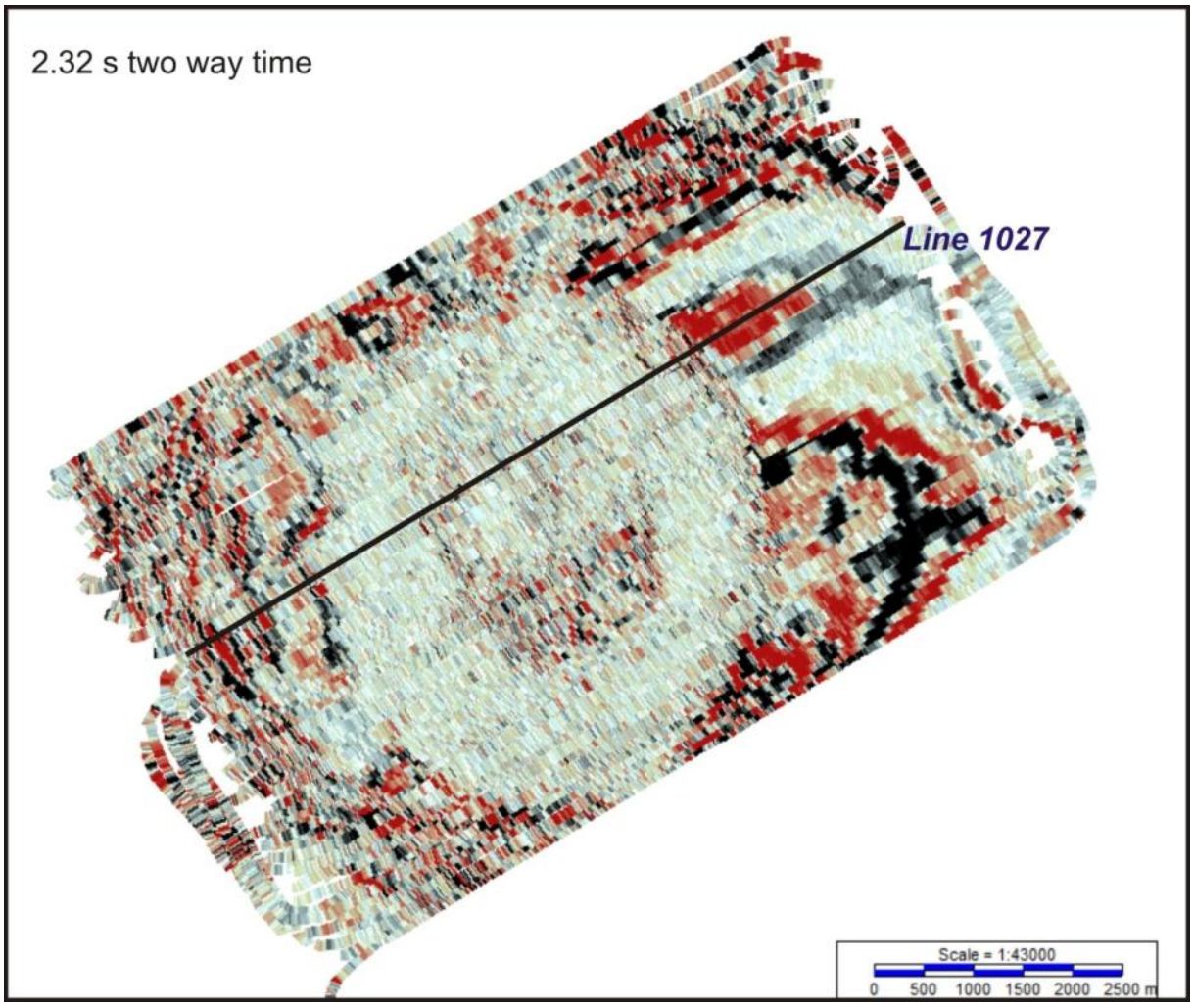

Figure 12c. Time slice of reflection amplitude at 2.2 seconds two way travel time using all 84 parallel lines. A donut-shaped structure of the Venere mud volcano is evident. The low-amplitude circular zone is made from mud-breccia. An inner ring of higher reflection amplitude is made from individual sheeted mud flows. This ring is sharply truncated relative to the surrounding sedimentary layers.

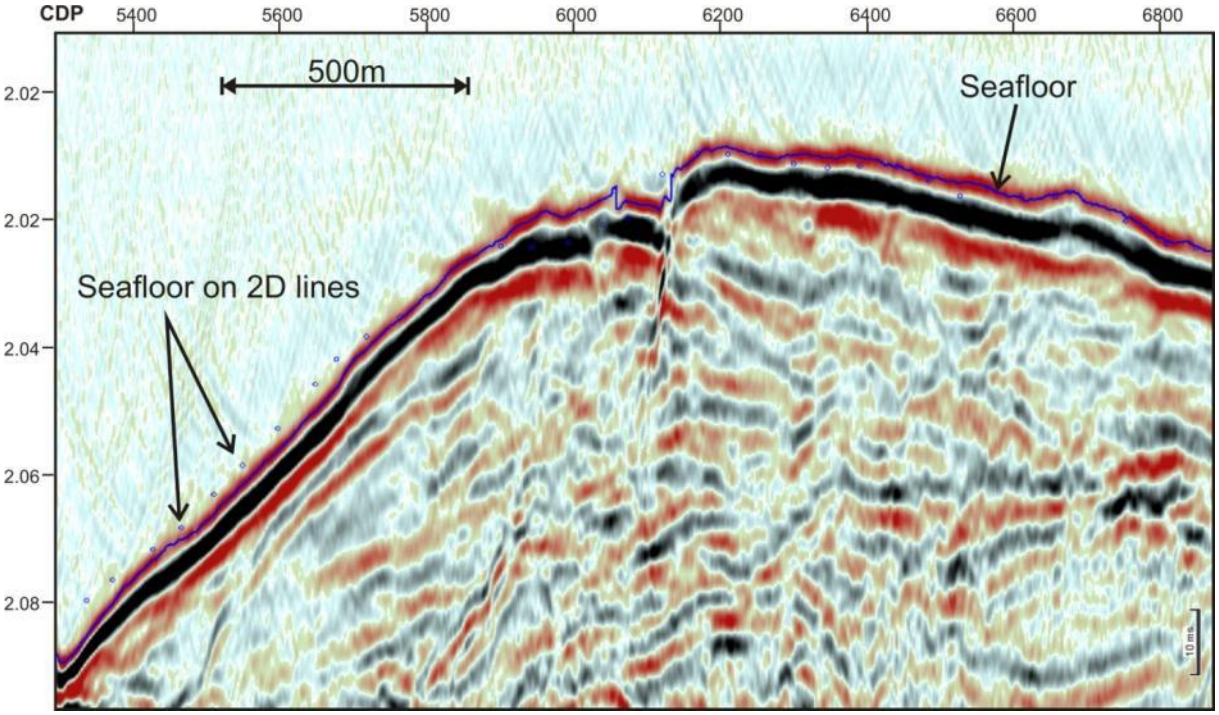

Figure 13. Zoom of reflection line 1100 (show perpendicular to the 84 parallel lines) with the continuously picked seafloor shown as solid blue line. Seafloor picks from the crossing lines are shown as blue circles. The seafloor travel-time picks of the 84 survey lines do vary relative to the crossing line in a non-systematic way. This residual static problem will be adjusted post-cruise using the multibeam bathymetry data as absolute datum. This will also increase the sharpness and accuracy of the time slices seen above.

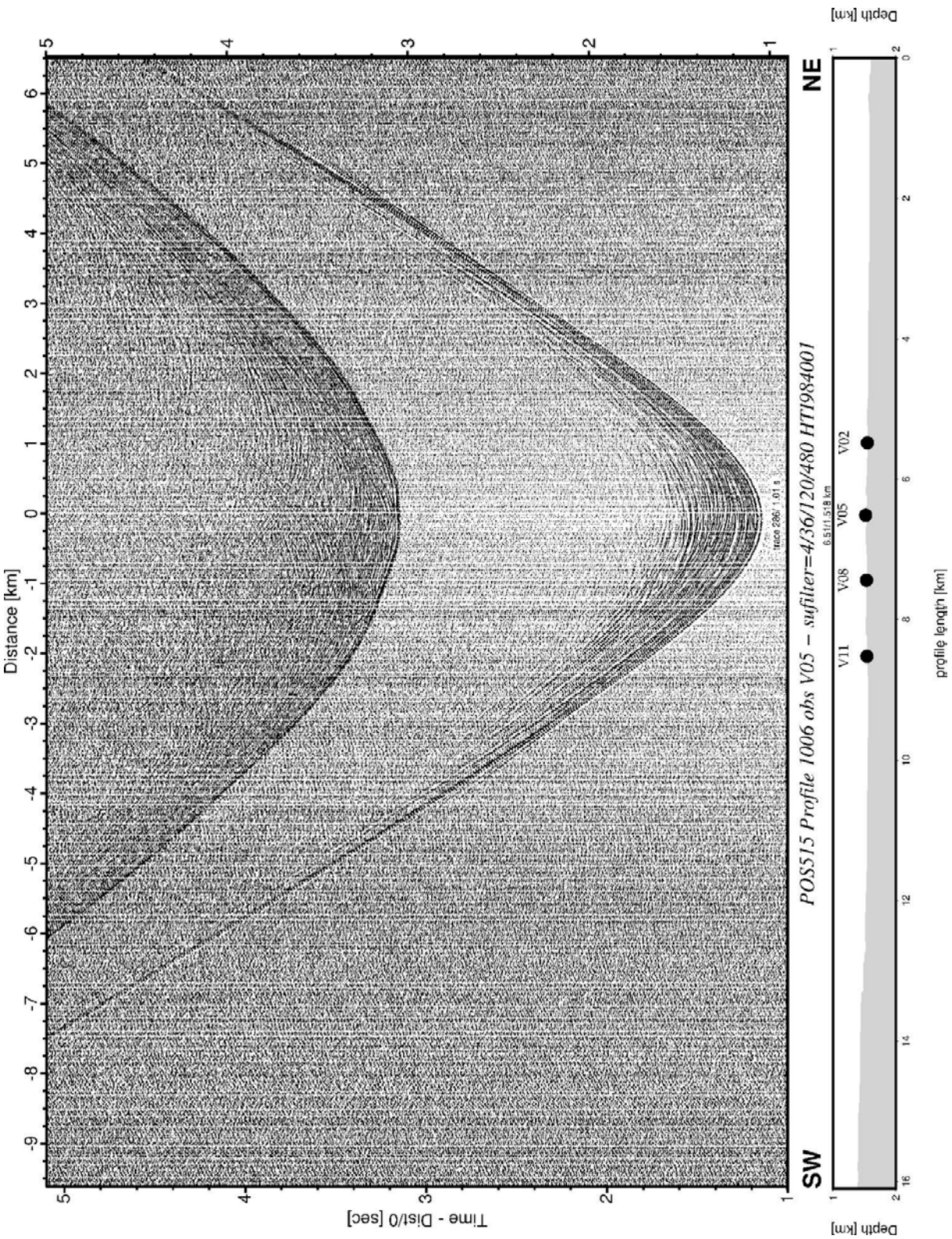

Figure 14a. OBS Record for Station OBS V05 (hydrophone data) showing late refracted arrivals (starting at 3 seconds).

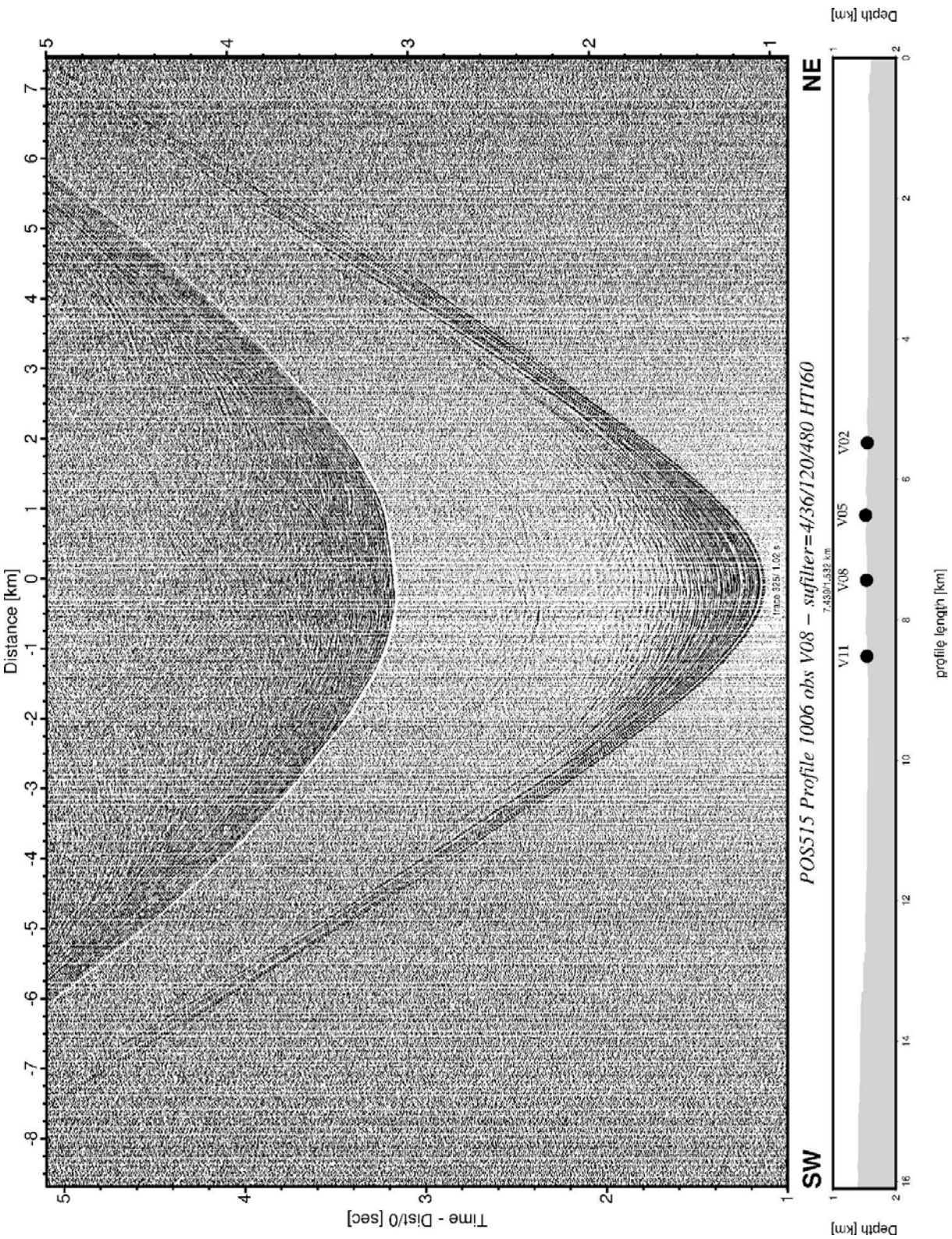

Figure 14b. OBS Record for Station OBS V08 (hydrophone data) showing refracted arrivals (starting at ~2.8 seconds) with an apparent low velocity.

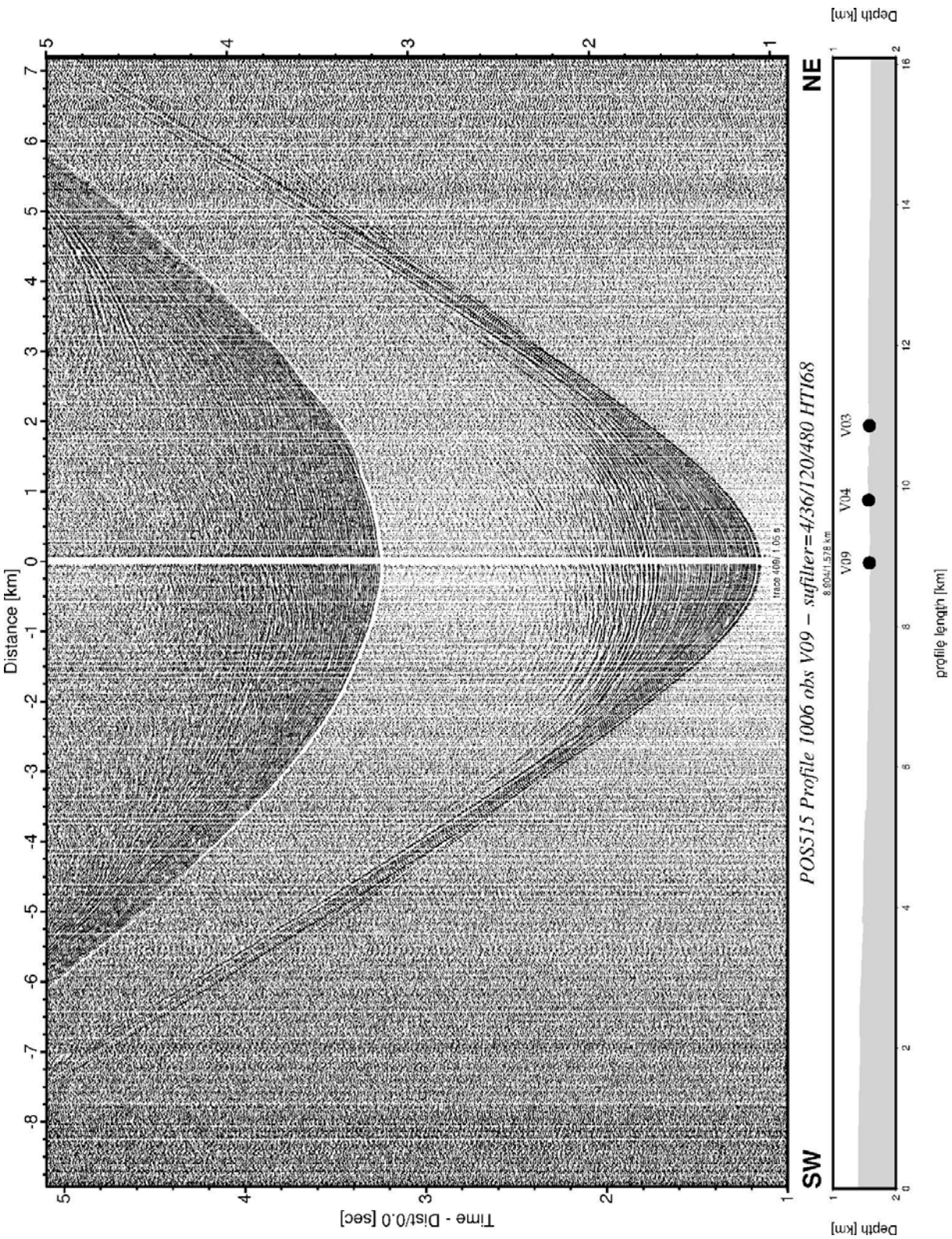

Figure 14c. OBS Record for Station OBS V09 (hydrophone data) showing late refracted arrivals (starting at 3 seconds) with faster velocities than seen on OBS V08 and V05.

4.2 Poseidon mud volcano

This region is characterized by a chain of several mud volcanoes, all showing flat-topped morphology (Figure 15) with high backscatter (Figure 16), in contrast to Venere (cone-type volcano). Here we acquired first 2D seismic data for refraction velocity analyses and a set of regional 2D lines (Figure 17). The 2D data shot after OBS deployment showed very low reflectivity (Figure 18, 19) and only shallow depth penetration of the airgun signals. We therefore abbreviated the survey here and focused on Sartori, which had shown a better seismic sub-surface structure. The OBS, however, did record high quality data with many refracted arrivals (Figure 20).

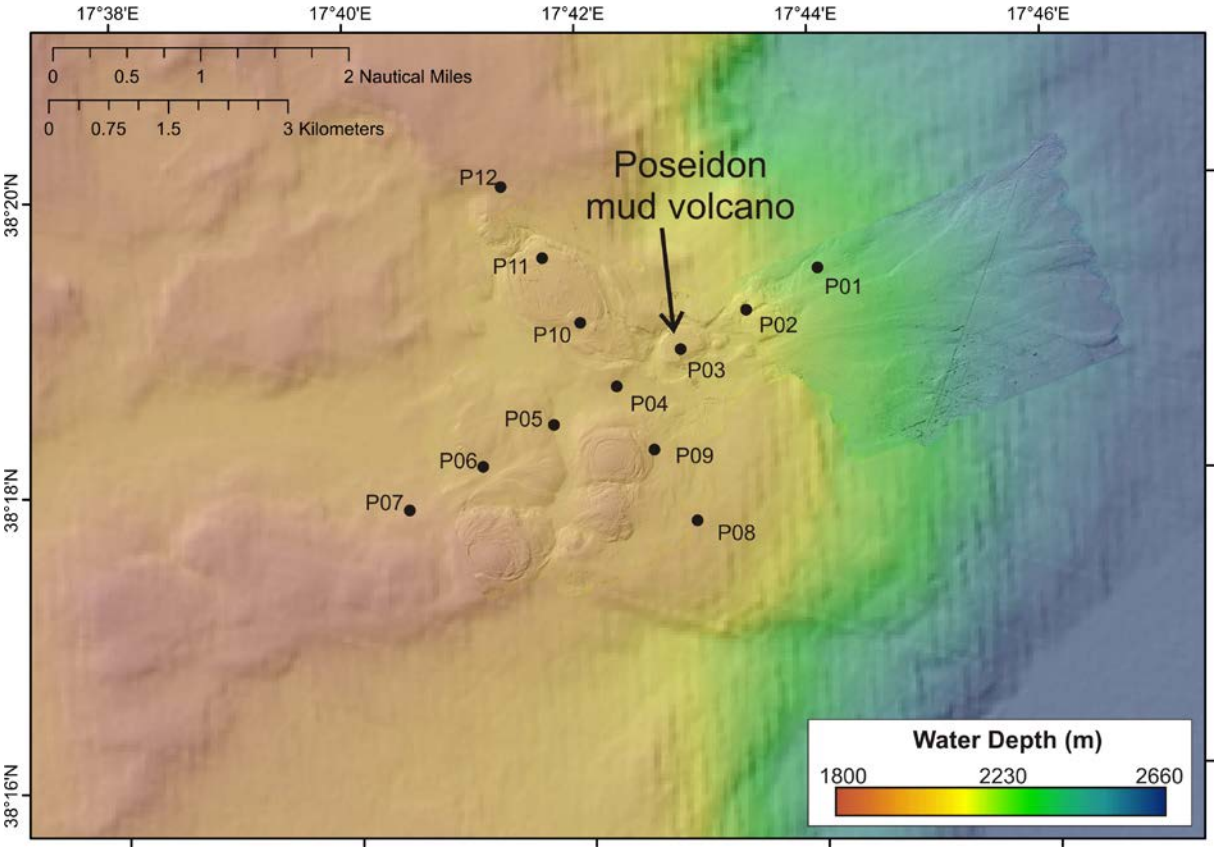

Figure 15. Map of OBS (black triangles) deployed across the Poseidon mud volcano chain. Also shown is the seafloor bathymetry from regional (M112, Bohrmann et al., 2015) and high resolution AUV mapping (P499, Bohrmann et al., 2016).

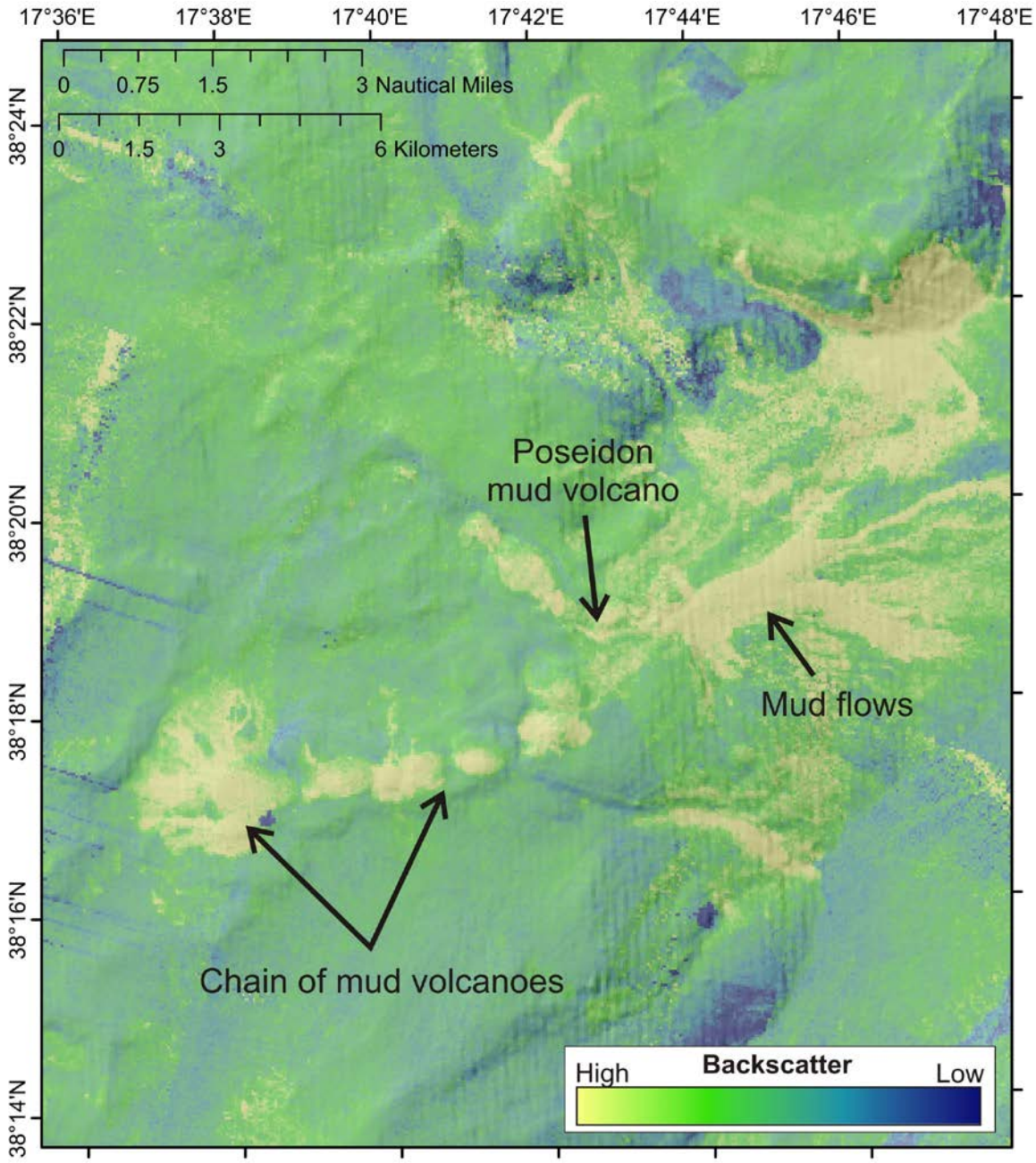

Figure 16. Map of seafloor backscatter across the Poseidon mud volcano chain. Regional data are from cruise M112 (Bohrmann et al., 2015) and high resolution AUV data are from cruise P499 (Bohrmann et al., 2016).

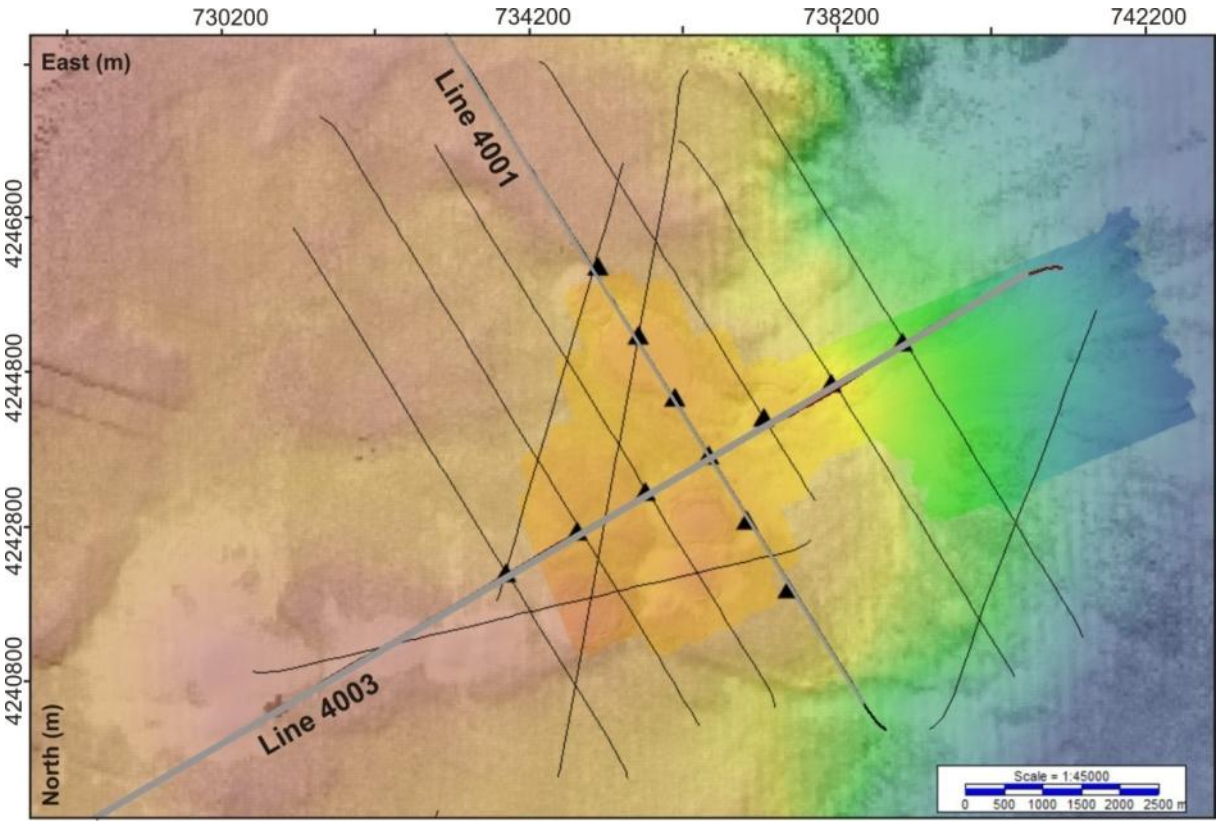

Figure 17. Map of combined bathymetry and backscatter data with OBS position and location of all seismic profiles acquired across the Poseidon mud volcano chain. Two examples of the long-offset refractions lines are highlighted with grey color and shown below.

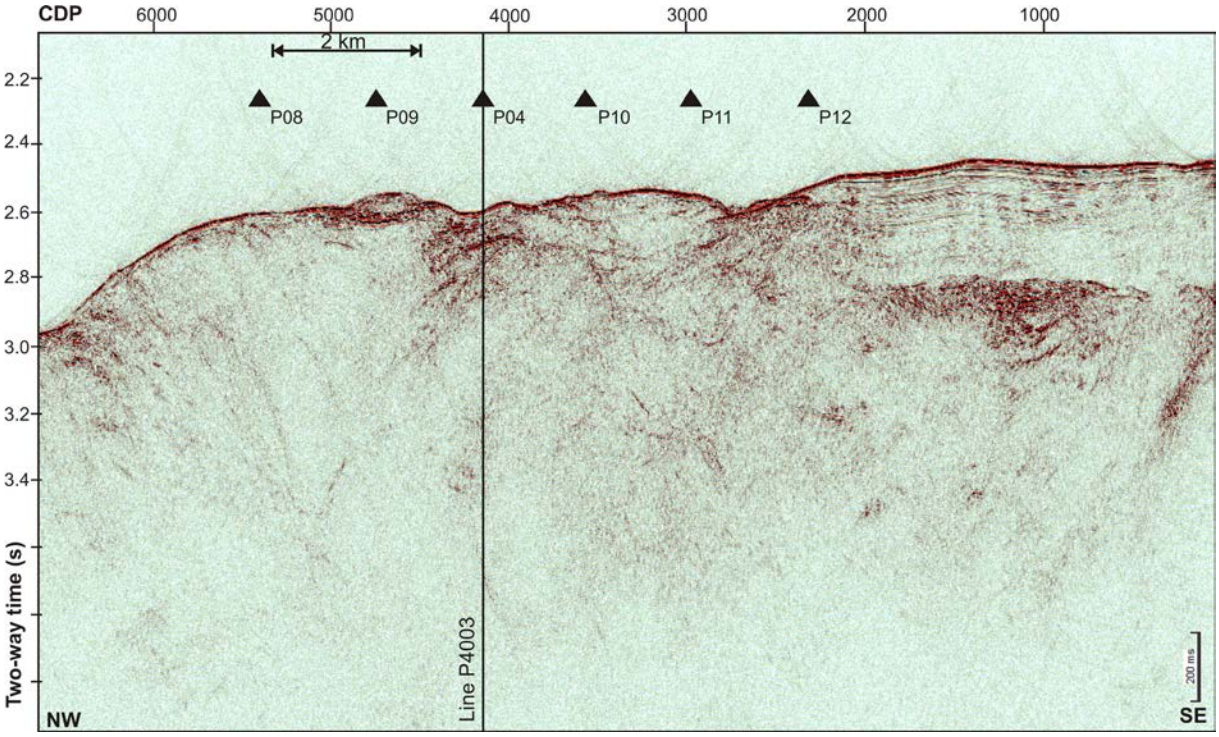

Figure 18. Image of line P4001 across NW-SE line of OBS at Poseidon mud volcano. Note the absence of deep reflectivity as well as distinct zonation or reflection events around the mud volcano. Locations of OBS are indicated by black triangles.

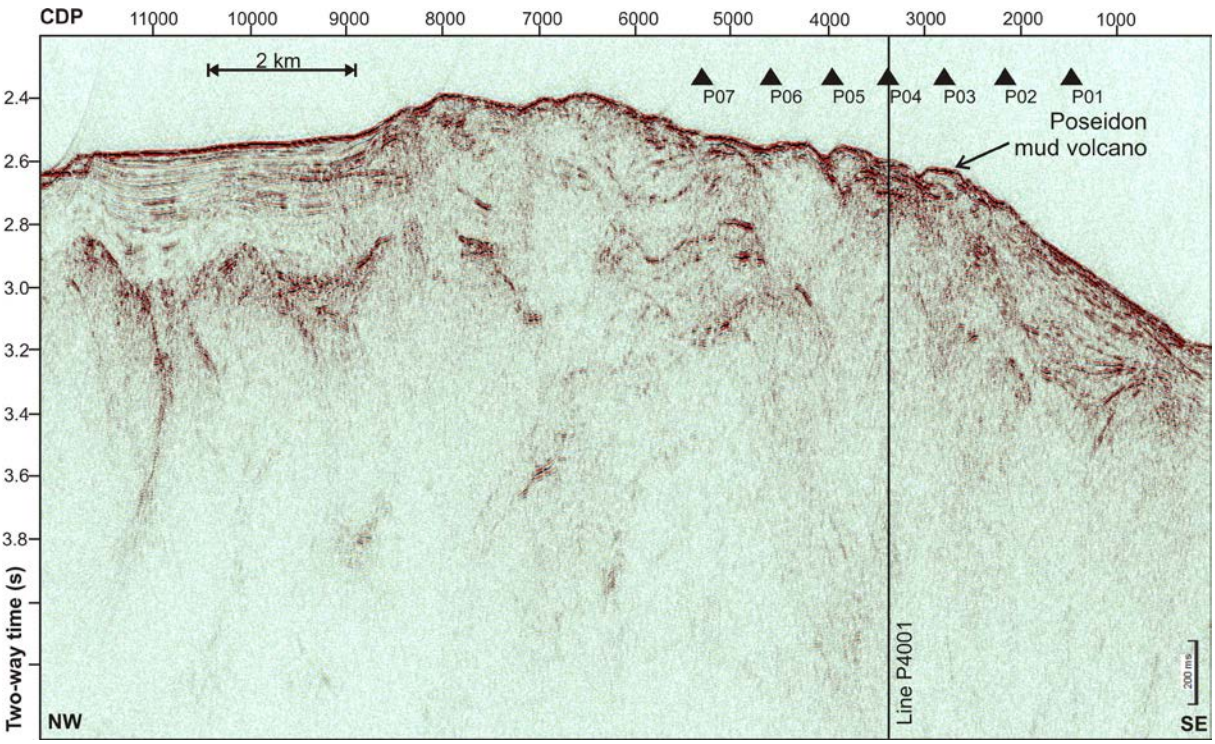

Figure 19. Image of line P4003 across SW-NE line of OBS at Poseidon mud volcano chain. Note the absence of deep reflectivity as well as distinct mud flows or reflection events around the mud volcano itself. Locations of OBS are indicated by black triangles.

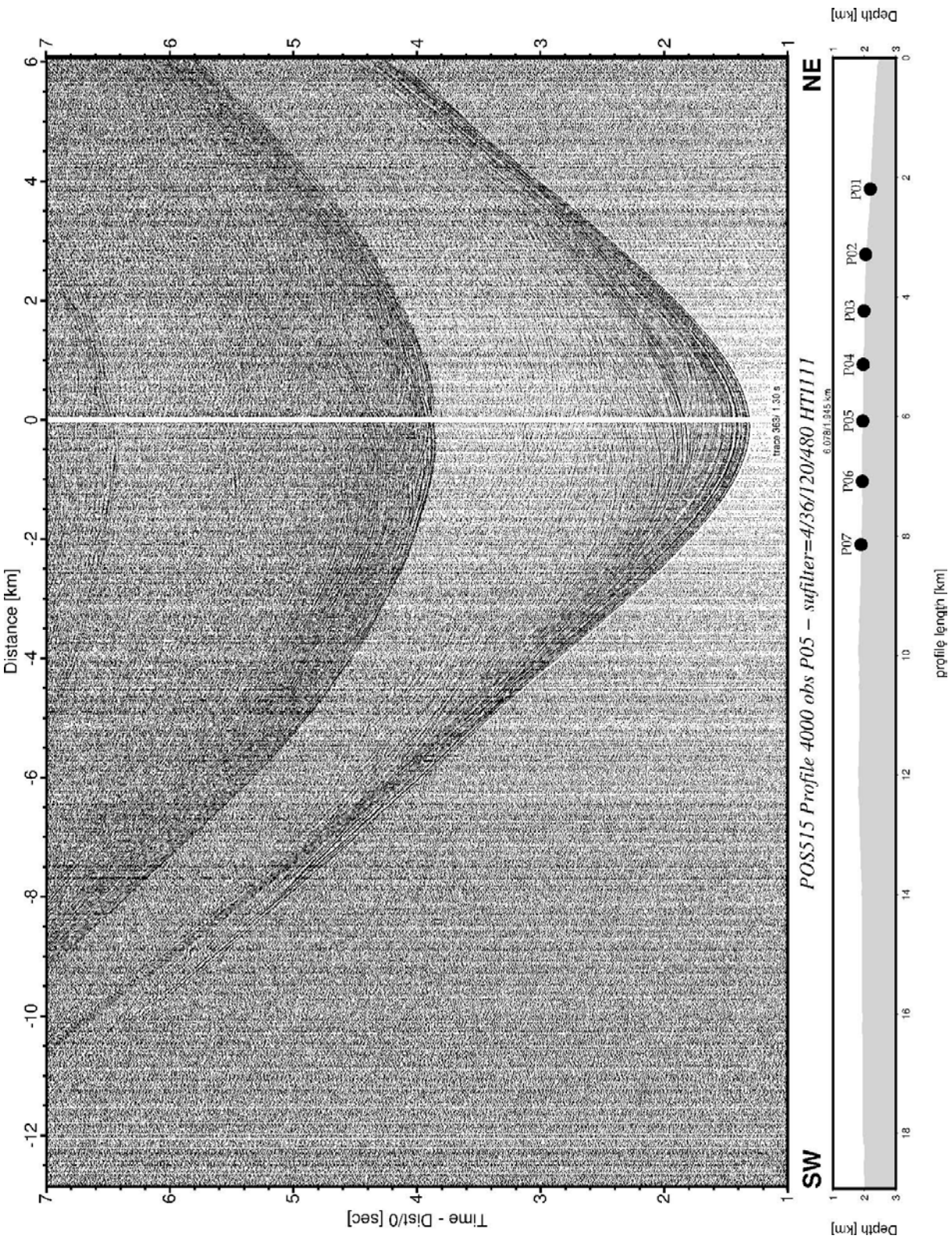

Figure 20a. OBS Record for Station OBS P05 (hydrophone data) showing refracted arrivals starting at 3 seconds.

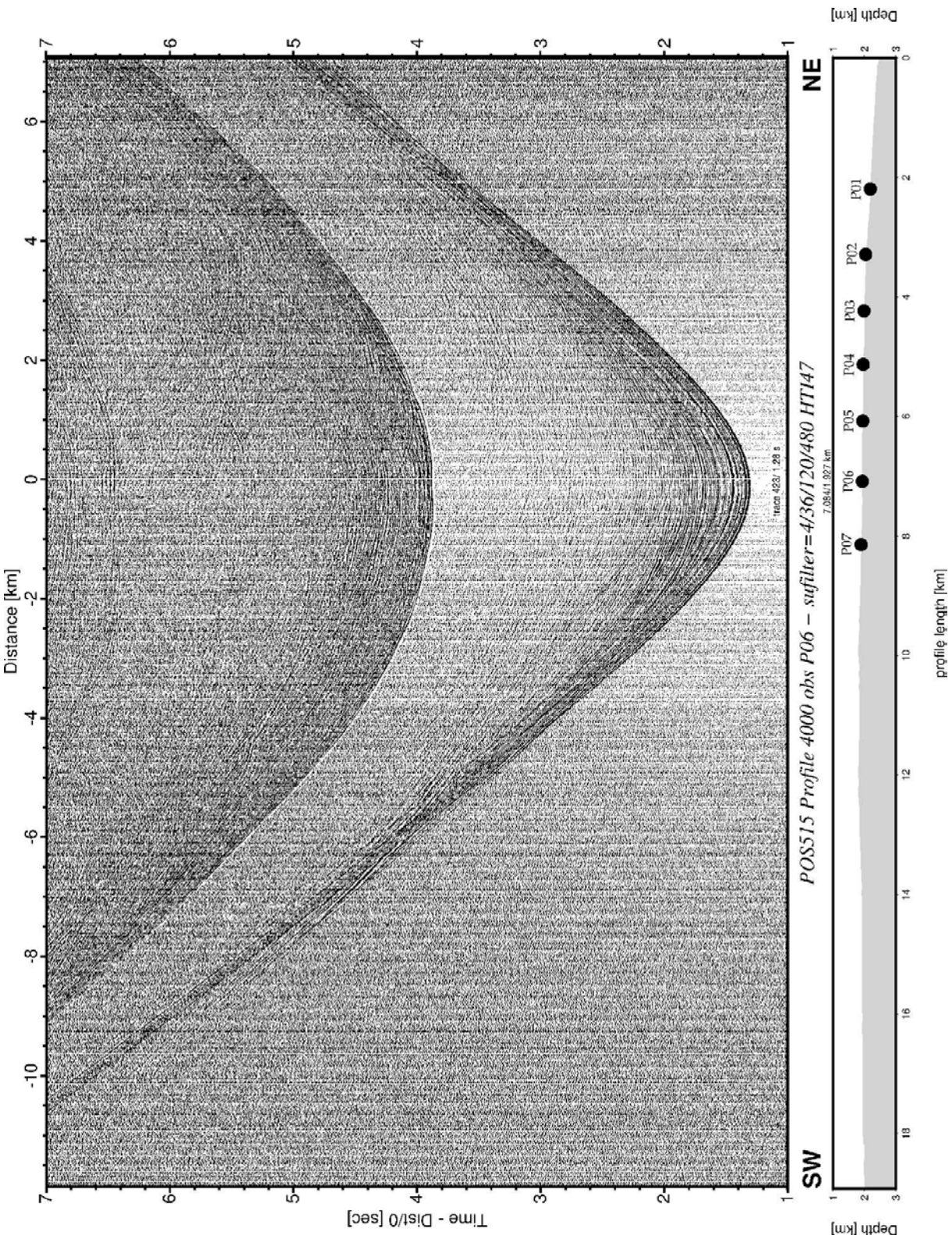

Figure 20b. OBS Record for Station OBS P06 (hydrophone data) showing refracted arrivals starting at 3 seconds.

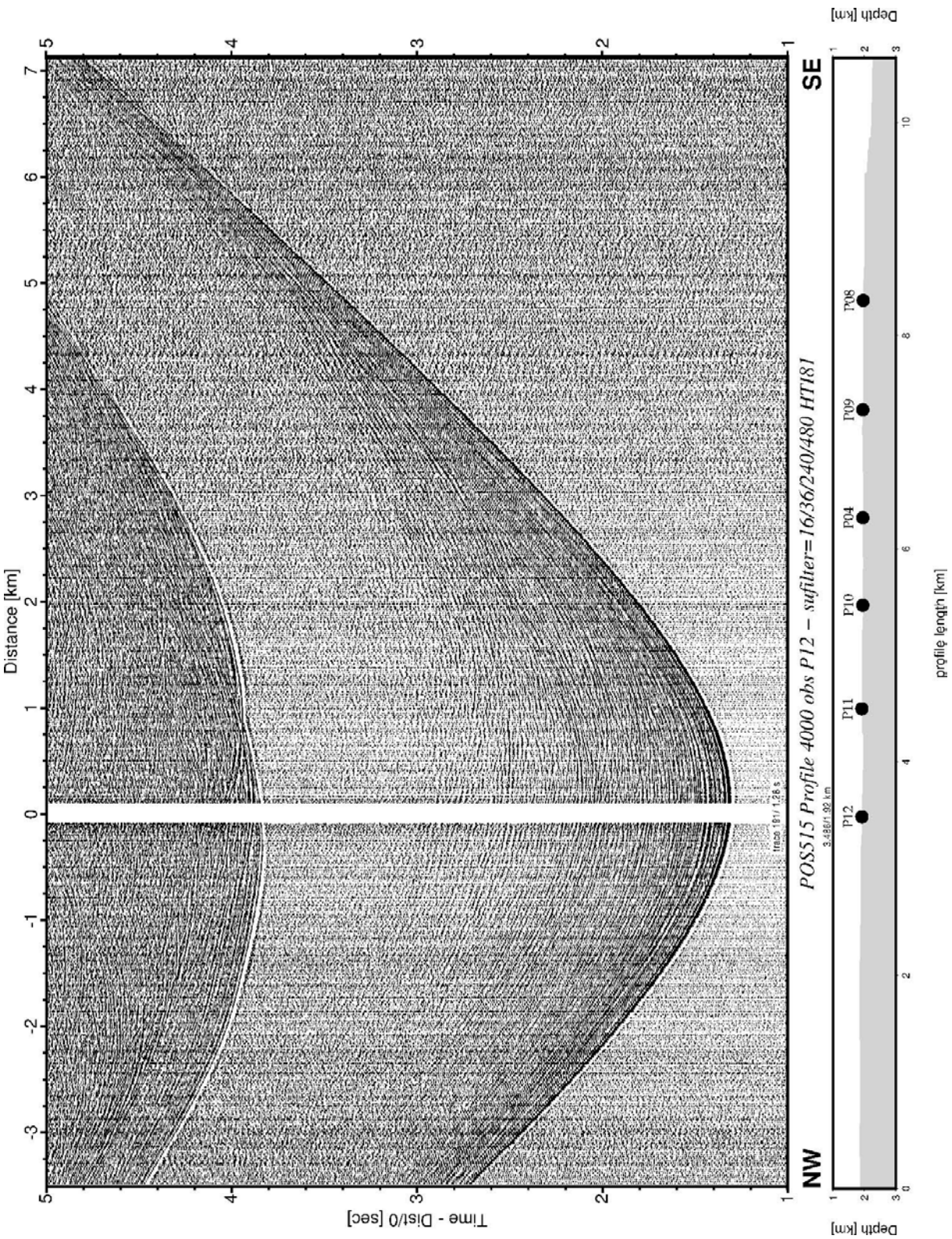

Figure 20c. OBS Record for Station OBS P12 (hydrophone data) showing refracted arrivals starting at 4 seconds at the farthest offset to the SE.

4.3 Sartori mud volcano

Sartori mud volcano is a flat-top structure with several distinct mud flows emanating from the western edge of the volcano (Figure 21, 22). Although not the initial target for 3D P-Cable surveying, reconnaissance data acquisition (Figure 23) showed well-layered mud flows, deep stratigraphy, as well as a root of the mud volcano (Figure 24), ideal for 3D seismic imaging, which is in stark contrast to the region around the Poseidon mud volcano. We do lack OBS velocity information for time-migration, but the data acquired only a few kilometers north at Poseidon mud volcano can be extrapolated to Sartori mud volcano.

After acquisition of additional 2D sections across Poseidon MV and the recovery of all twelve OBS, we acquired a P-Cable 3D survey of 4.8 km × 5.8 km grid of 82 N-S oriented survey lines at 60 m spacing (Figure 25). After 5 days of continuous data acquisition with 67 parallel lines, we filled several holes in the 3D coverage by surveying an additional 22 lines.

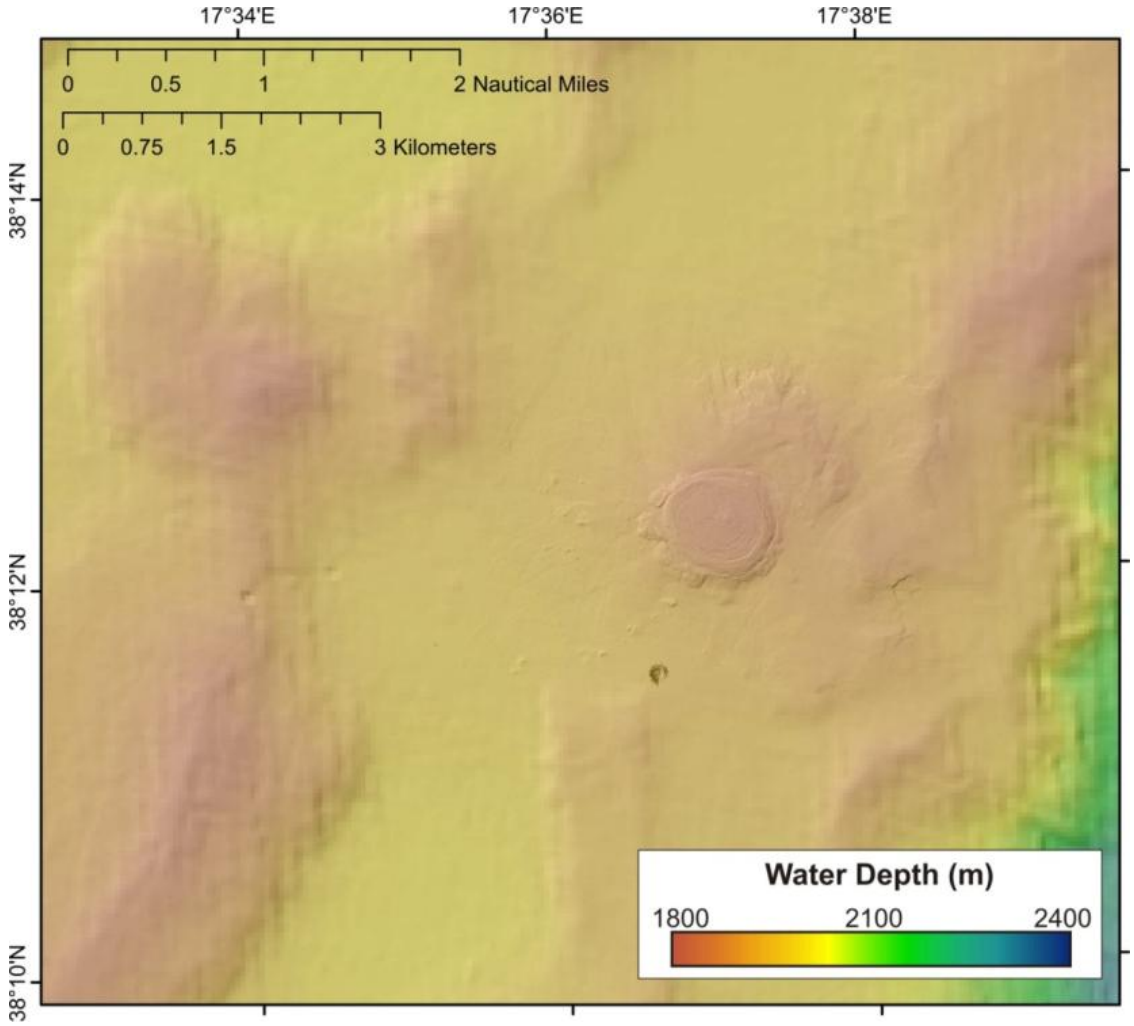

Figure 21. Seafloor bathymetry around Sartori mud volcano. Regional data are from cruise M112 (Bohrmann et al., 2015) and high resolution AUV data are from cruise P499 (Bohrmann et al., 2016).

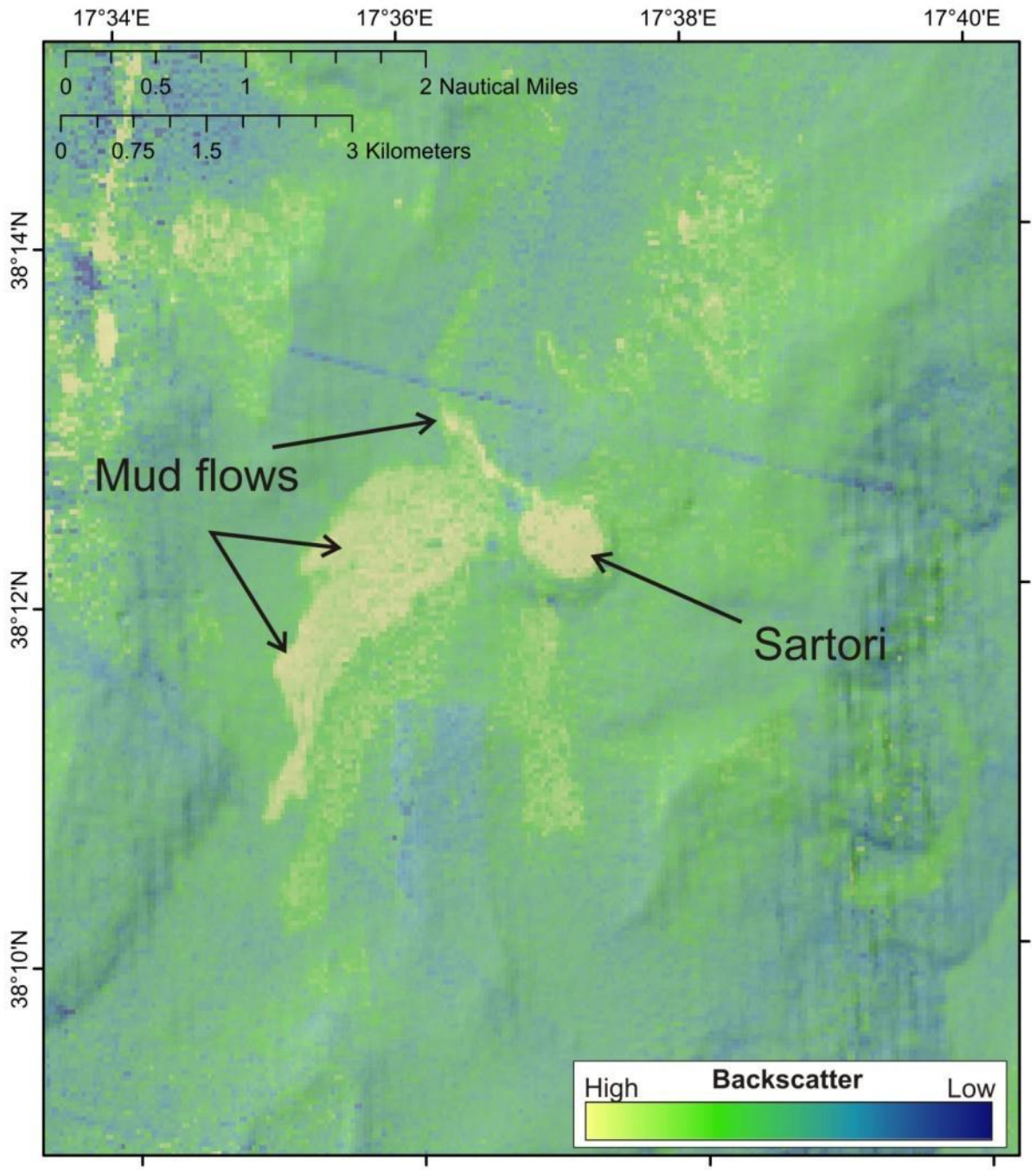

Figure 22. Image showing seafloor backscatter around the Sartori mud volcano. Regional data are from cruise M112 (Bohrmann et al., 2015) and high resolution AUV data are from cruise P499 (Bohrmann et al., 2016). Several distinct high-backscatter mud flows that are partially overlapping are seen west and south of the flat-top mud mound. One smaller mud flow appears to have transported mud to the north.

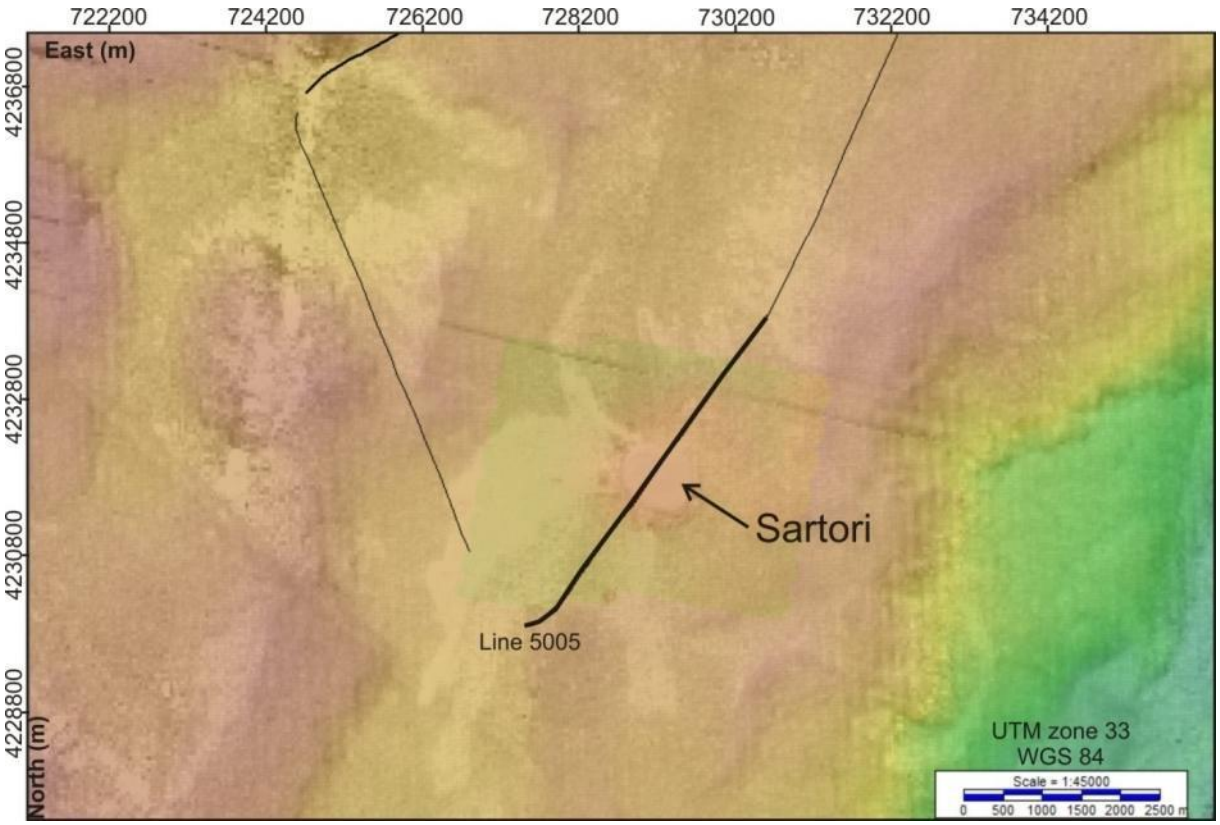

Figure 23. Map of the region around Sartori mud volcano combining backscatter and bathymetry, showing high backscatter regions of mud flows to the west of the almost circular and flat-top mud mound itself. Seismic line 5005 is highlighted by a thick black line and shown below.

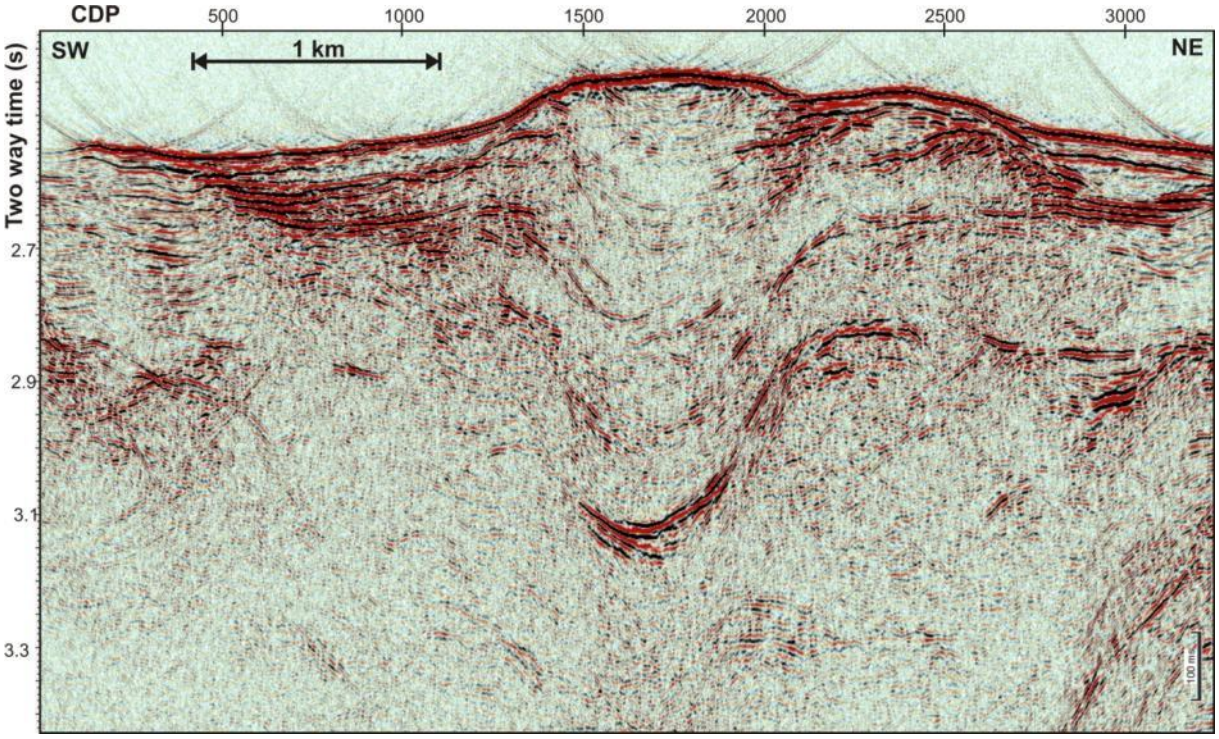

Figure 24. Seismic line 5005 across Sartori mud volcano. A thick sequence of stacked mud flows forming onlaps on regular sedimentary layers is seen in the SW portion of the line. Beneath the central portion of the volcano deep reflectivity appears to form a bowl-shape structure.

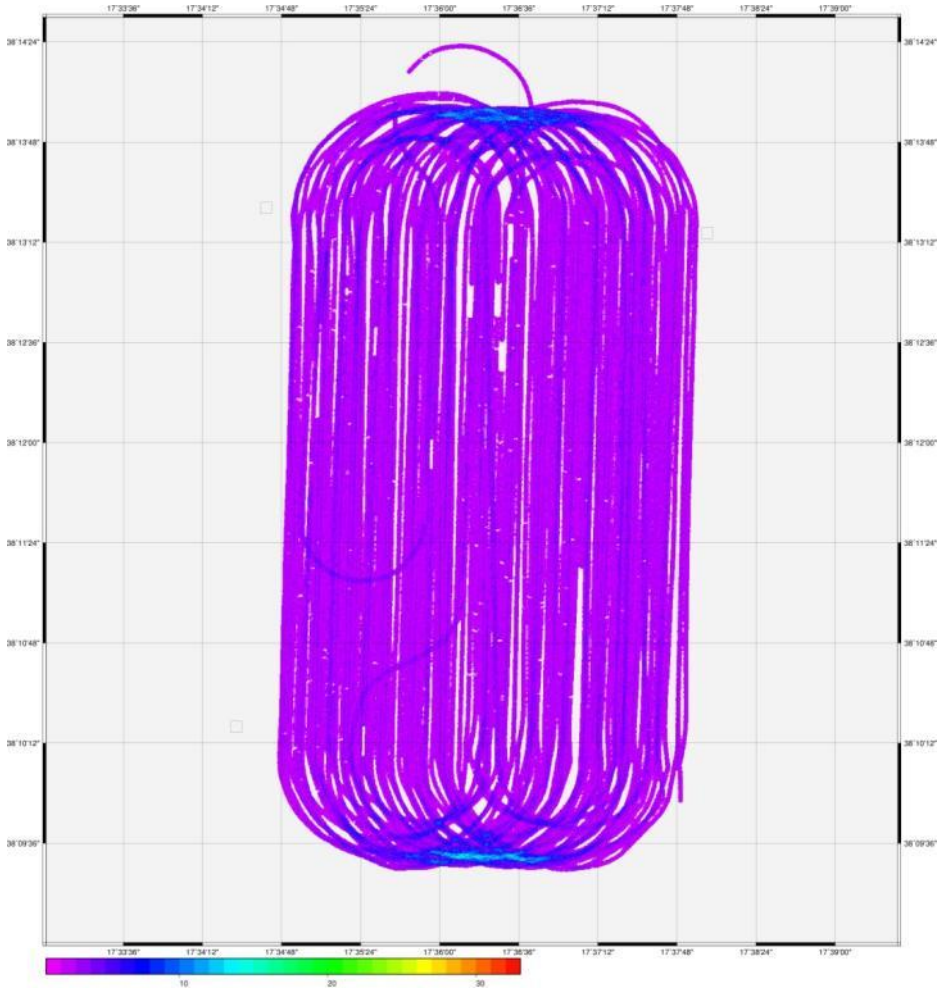

Figure 25. Final fold map for the Sartori 3D P-cable survey by incorporating all data with navigation strings recorded. Several shots with the GPS string missing will be added post-expedition.

4.4 Cetus mud volcano

Our last target of the expedition is the Cetus mud volcano. It is the furthest South-located feature visited. The E-W elongated structure shows high backscatter rims (Figure 26). Seismic data across the structure show outstanding rim-like structures and a central zone of the mud volcano made from a stack of mud flows (Figure 27, 28).

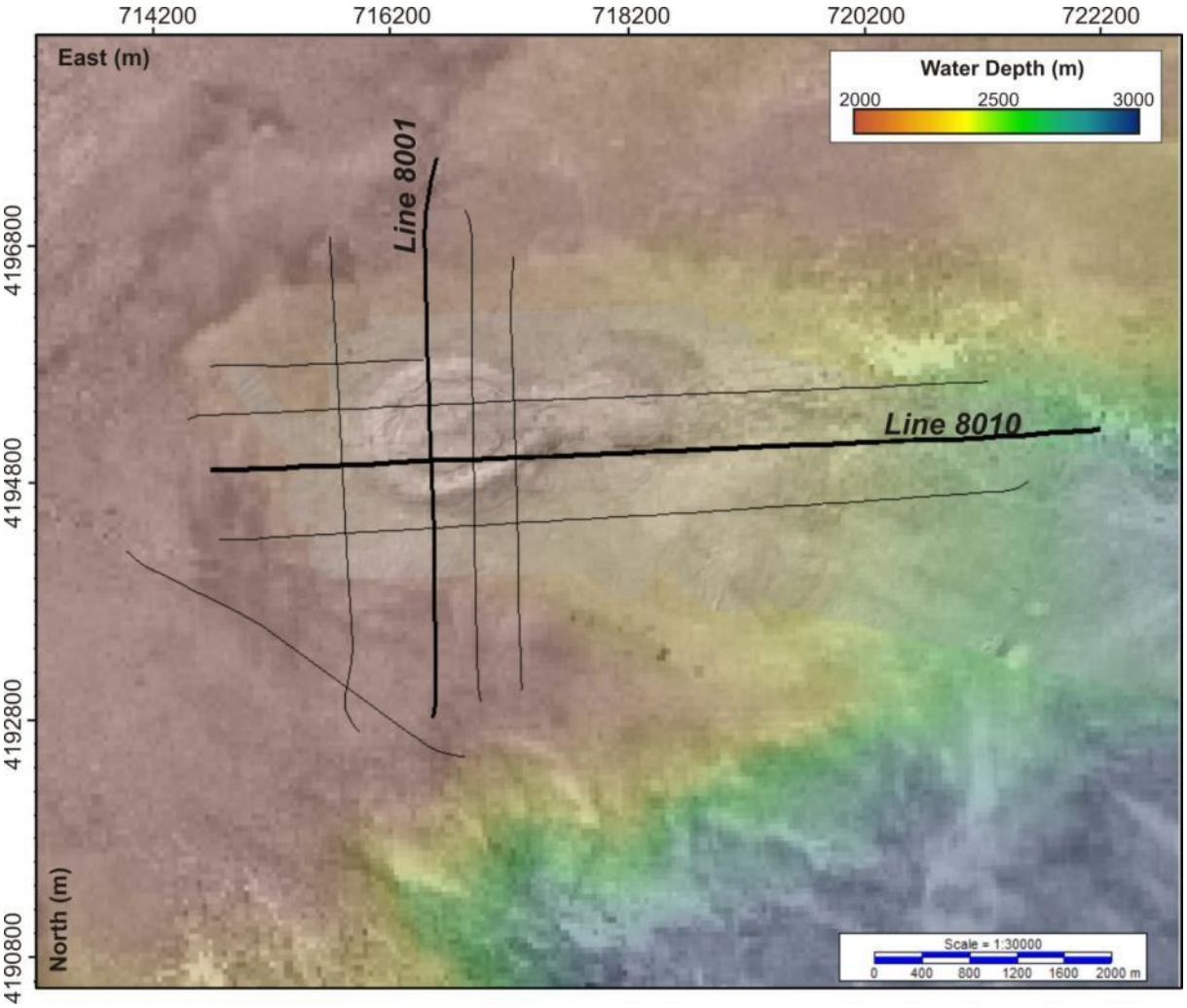

Figure 26. Location of seismic lines acquired at Cetus mud volcano (two examples shown below are highlighted in thick black lines). The bathymetry and backscatter is combined.

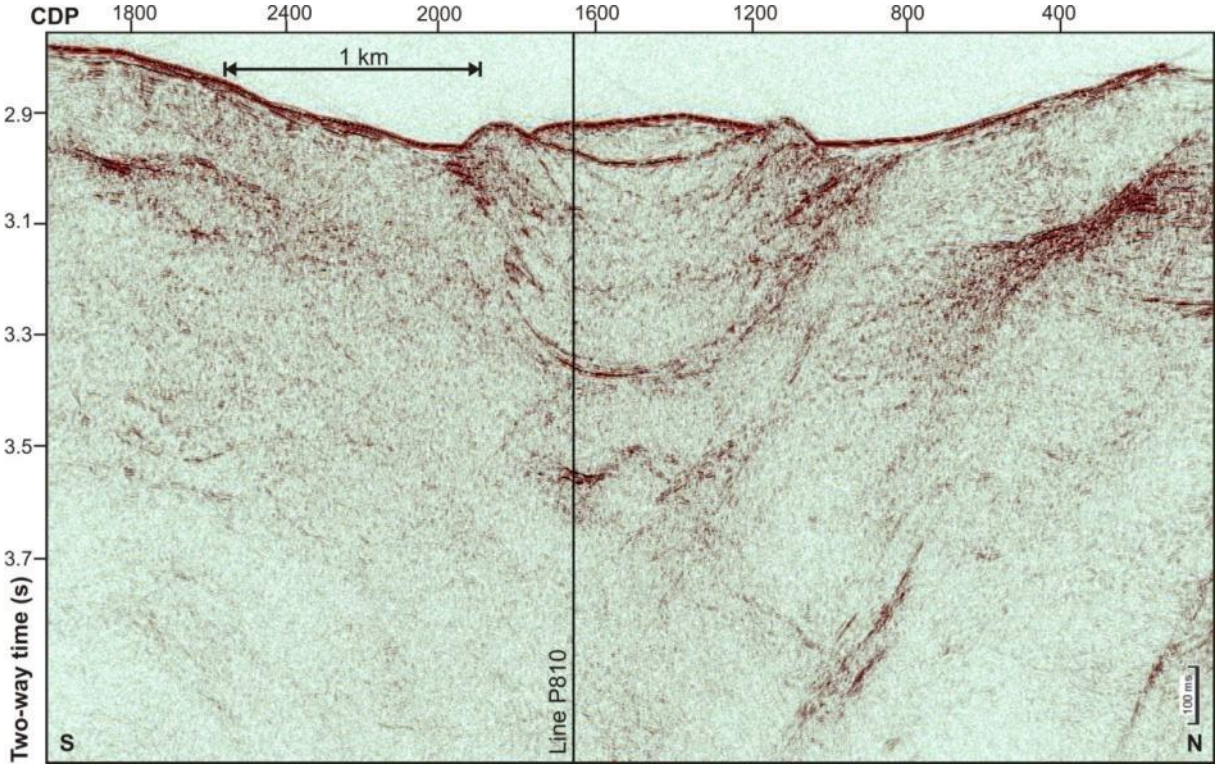

Figure 27. Seismic line 8001 across Cetus mud volcano.

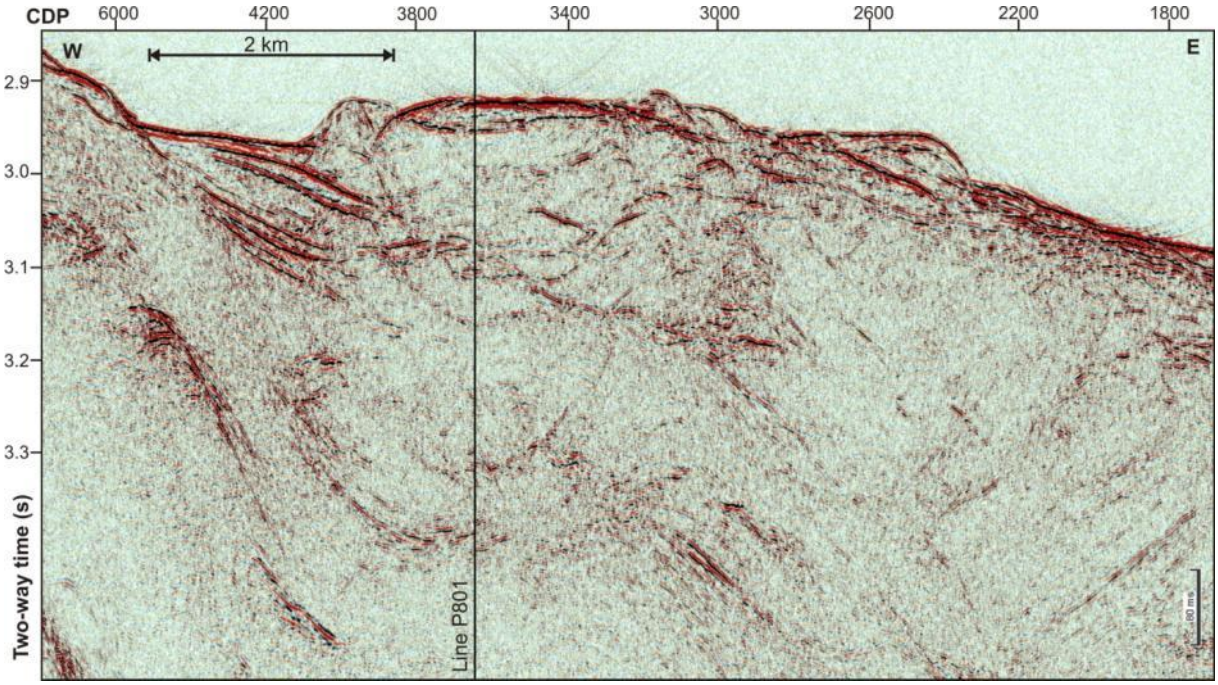

Figure 28. Seismic line 8010 across Cetus mud volcano.

5. Scientific equipment

5.1 Ocean bottom seismometers

A total of 12 Ocean bottom seismometer (OBS) instruments were provided by GEOMAR and were successfully deployed at the Venere and Poseidon mud volcanoes. The GEOMAR Ocean Bottom Seismometer 2002 (OBS-2002) is a design based on experience gained with the GEOMAR Ocean Bottom Hydrophone (Flueh and Bialas, 1996) and the GEOMAR OBS (Bialas and Flueh, 1999). The basic system (Figure 29) is constructed to carry a hydrophone and a seismometer for active-source seismic profiling. However, due to the modular design of the front end of the system carrier it can be adapted to different seismometers and hydrophones or pressure sensors. The sensors are *HTI-04_PCA_ULF* hydrophones from High Tech Inc. The seismometer is deployed between the anchor and the OBS frame, which allows for optimal coupling to the seafloor. The three-component seismometer K/MT-210 manufactured by KUM GmbH is housed in a titanium pressure tube. Short-period geophones with a 4.5 Hz natural frequency were used during POS515. The recording device is an *MBS* recorder of *SEND GmbH*, which is contained in its own pressure tube and mounted next to the flotation opposite of the release transponder (Figure 29). The floatation is made of syntactic foam and is rated, as are all other components of the system, for a water depth of 6000 m.

While deployed to the seafloor the entire system rests horizontally on the anchor frame. The instrument is attached to the anchor with a release transponder. The release transponder is the *K/MT562* made by KUM GmbH. Communication with the instrument located on the seafloor for release and range estimation is possible through a transducer hydrophone, which is lowered from the vessel by ~20 m into the water. Over ranges of 4 to 5 miles release and range commands are successful. After releasing its anchor weight (~60 kg), the OBS instrument turns 90° into the vertical position and ascends to the sea surface. This ensures a maximally reduced system height and water current sensibility at the ground (during measurement). Additionally, the sensors are well protected against damage during recovery and the transponder is kept underwater, allowing for continuous acoustic communication between vessel and the OBS, while the instrument floats to and at the surface.

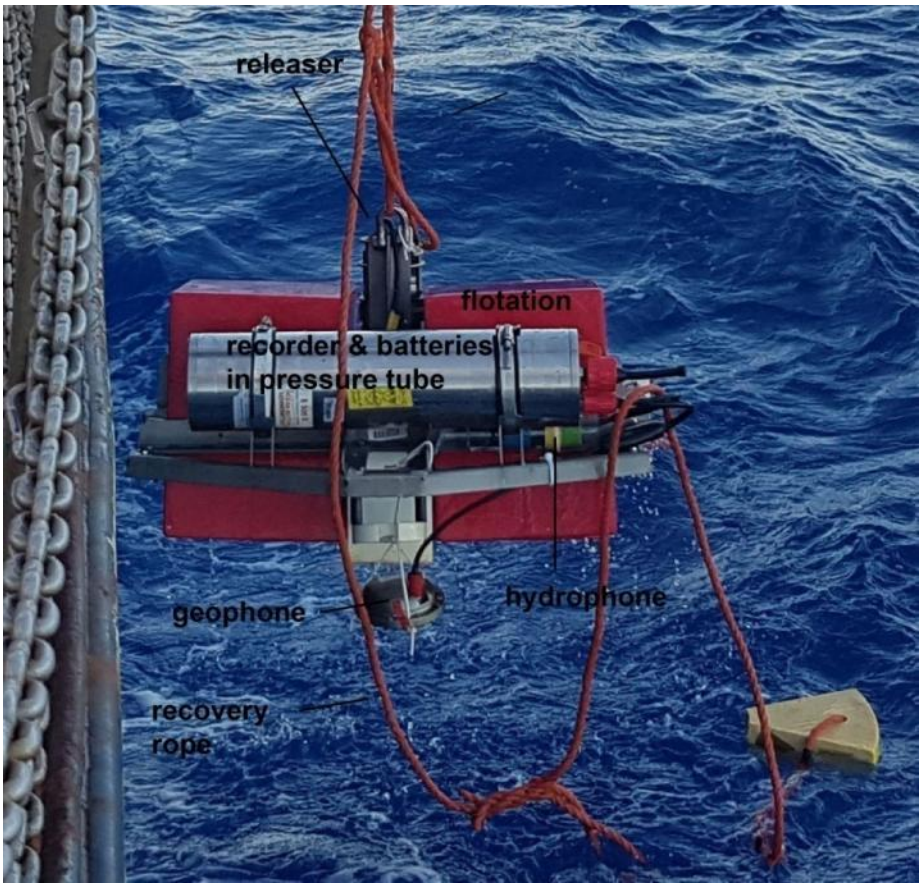

Figure 29. Ocean Bottom seismometer (OBS), recovered at portside of R/V POSEIDON during research expedition POS515; all system components are labeled. Details see text.

5.2 P-Cable 3D imaging system

The P-cable system (Figure 30) allows towing multiple short streamers across a cable for wider swath-imaging and reducing line-spacing for more surveying (compared to towing a single streamer). We have attempted deploying the system numerous times at Venere mud volcano, but failed repeatedly due to a number of technical problems, including current leakage, failure of lead-in cables, and streamer-issues.

At Sartori mud volcano we deployed a P-Cable system made from 12 parallel streamers (oil-filled and solid-state streamers). The sequence of deploying the system is depicted in Figure 31.

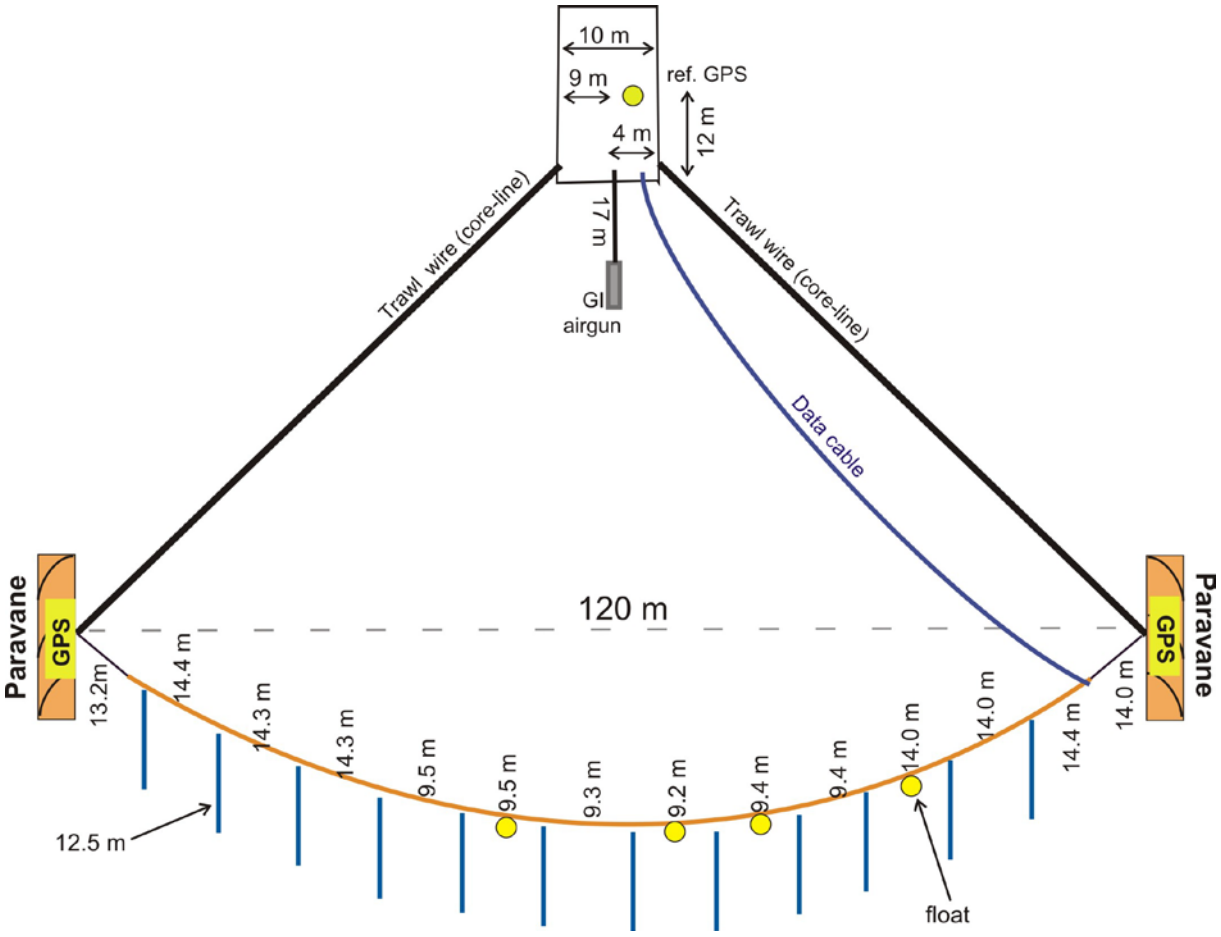

Figure 30. Schematic drawing of the P-Cable used at the Sartori mud volcano. Two paravanes (also referred to as trawl-doors) are towed with the core-lines using the two main winches on board R/V POSEIDON. Between the trawl-doors, a cross-cable is towed, to which twelve short 12.5 m long streamer-sections are connected with T-boxes and lead-in cables. Lengths between streamers along the cross-cable, as well as offset of the GI airgun behind stern are also shown. The entire system is towed at a speed of ~3.5 kn, so that the horizontal distance between the paravanes is ~120m, which corresponds to a 60 m effective spread in common mid-point coverage.

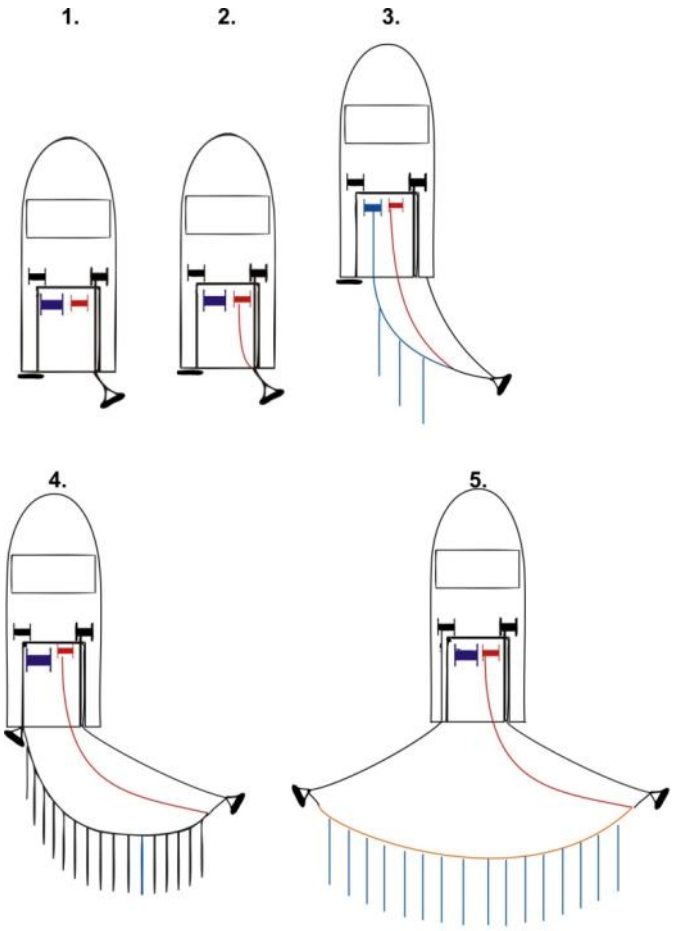

Figure 31. Sequence of P-cable deployment: 1. Starboard paravane is released from vessel, 2. Data cable (red drum) is added, 3. Cross-cable with streamers (blue) is added while additional length of wire is given on paravane and data cable, 4. Completely deployed cross cable with all streamers, 5. Release of port-side paravane and final stretching of cross cable.

5.3 2D multichannel streamer

The individual streamer sections can be combined into a single 2D streamer. The individual streamers are combined with their digitizer ("bottle") to a stretch-section (25 m) and a tow cable (80 m). We add a repeater to the data cable, connecting the streamer to the recording unit inside the laboratory. We have used different types of 2D streamers during CALVADOS. The first 10 lines acquired at Venere mud volcano were made from three solid-state streamer sections. The bulk of the remaining 2D lines are acquired with a 150 m long streamer, made from12 oil-filled sections (details see Table 1 and geometry in Figure 32).

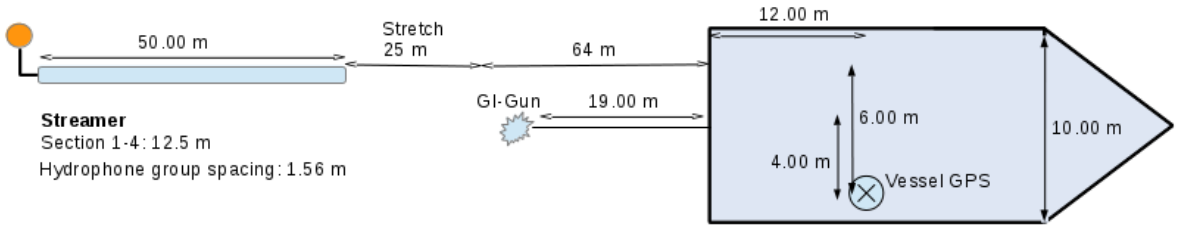

Figure 32. Geometry for all 2D seismic data collection. Length of streamer varies between surveys, but gun position and GPS position on board remain identical.

5.4 Seismic source

The seismic source used during the project was a single 210 in^3 (~3.4 L) GI gun. The injector is fired with a delay of 50 ms after the generator. For the most part of the survey, the gun was towed ~2 m below sea surface. However, for the long refraction lines at Poseidon mud volcano, we added an extra 2 m rope to lower the gun to greater depth. This was done mainly for safety reasons due to higher seas than usually seen during the previous survey lines. This may also help generating deeper frequencies, for further offset detection of the arrivals on the OBS.

6. Acknowledgements

We would like to thank the master Matthias Günther and the ship's crew of R/V POSEIDON for their relentless support and making our research possible. This cruise was funded through the GEOMAR ship budget and the RD4 "Marine Geodynamic" internal budget. We would like to thank Prof. Dr. Herzig and the management team at GEOMAR for providing the substantial financial support to carry out this expedition. Additional thanks go to our RD4 team assistants Jasmin Mögeltönder and Anne Völsch, as well as Klas Lakschewitz for logistical support.

7. Appendices

A General Map of cruise-track from Dubrovnik to Catania, and location of mud volcanoes visited.

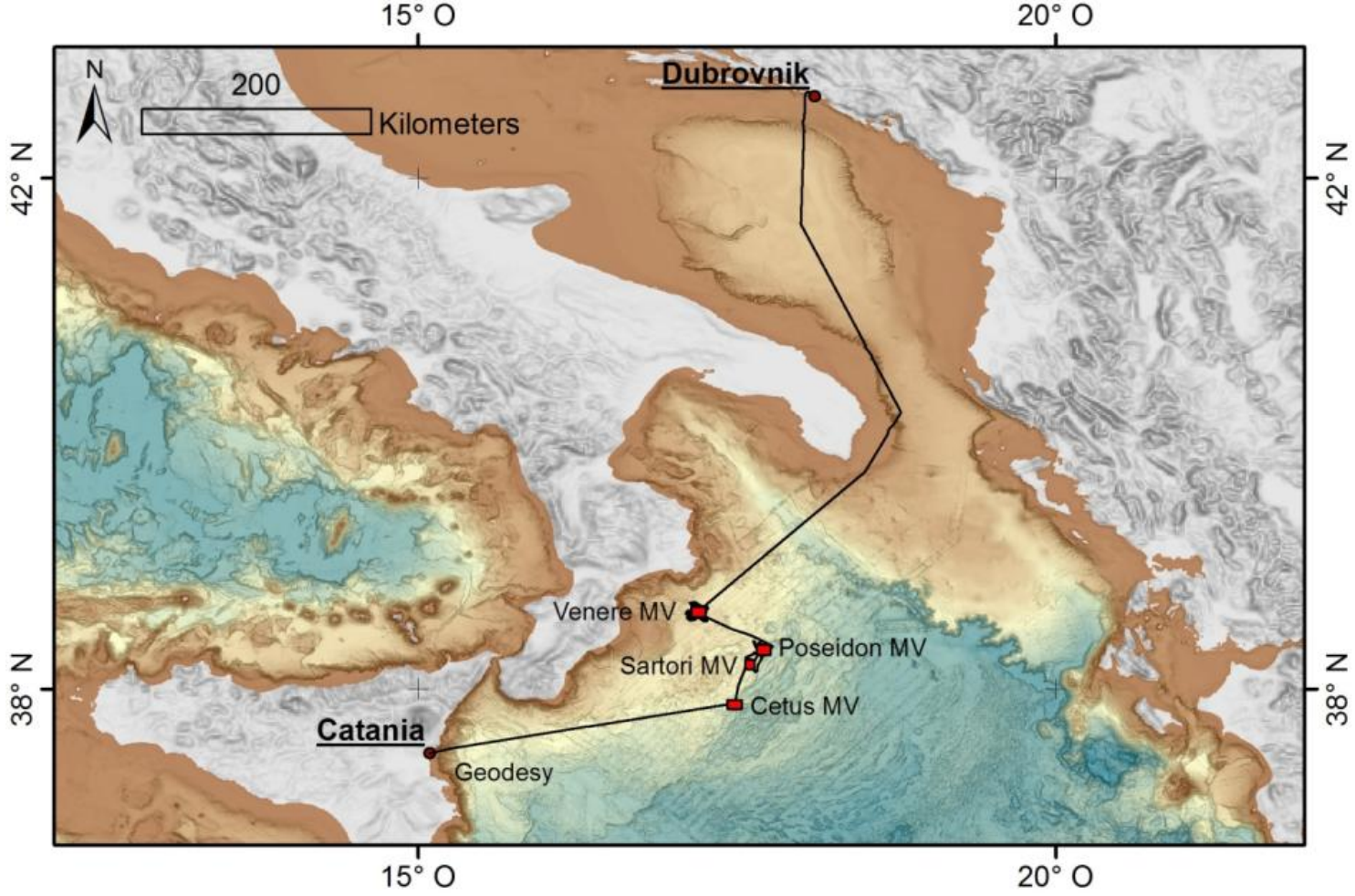

B Station list

Table B.1: OBS deployment at Venere with all instrument specifications.

Instrument	Release	Recorder MBS	Cylinder	Radio Beacon	Radio Freq.	Flash Light	Hydrophone HTI	Geophone Owen	Deployment				Rise Time (min)
									Date / UTC Time (dd.mm.yy / hh:mm)	LAT (N) D:M	LON (E) D:M	DEPTH (m)	
OBS V01	134071	020504	12	Y02-026	C	R07-016	81	24	21.06.17 / 08:31	38°37.290	17°12.490	1560	26
OBS V02	250177	000611	24	W01-041	B	U02-066	7		21.06.17 / 08:49	38°36.841	17°12.837	1540	26
OBS V03	447756	010708	52	RF-700A1	B	W01-061	111		21.06.17 / 09:05	38°36.414	17°13.132	1558	26
OBS V04	451146	971201	43	A08-041	A	U02-093	46	1205-130	21.06.17 / 09:20	38°36.133	17°12.493	1568	26
OBS V05	442205	020509	11	A08-046	B	N11-069	984001	0104-008	21.06.17 / 09:32	38°36.581	17°12.211	1511	25
OBS V06	450403	001006	4	Y10-052	C	S01-737	31203403	1205-128	21.06.17 / 09:45	38°37.046	17°11.892	1517	25
OBS V07	450656	989903	76	A08-037	A	M03-015	40	1001-116	21.06.17 / 10:04	38°36.773	17°11.364	1507	25
OBS V08	447417	000616	5	Y10-058	D	U11-032	60	1205-134	21.06.17 / 10:24	38°36.321	17°11.664	1527	25
OBS V09	451207	980907	53	Y10-056	D	T07-084	68		21.06.17 / 10:43	38°35.878	17°11.972	1578	26
OBS V10	450215	990712	84	U09-053	A	T08-066	302		21.06.17 / 10:56	38°35.590	17°11.370	1575	26
OBS V11	450445	980403	42	Y10-054	D	B01-065	483041	0205-029	21.06.17 / 11:08	38°36.006	17°11.037	1541	26
OBS V12	430326	020507	30	V08-067	B	S01-735	102	1609-131	21.06.17 / 11:19	38°36.460	17°10.702	1508	25

Table B.2: OBS deployment at Poseidon mud volcano with all instrument specifications.

Instrument	Release	Recorder MBS	Cylinder	Radio Beacon	Radio Freq.	Flash Light	Hydrophone HTI	Geophone Owen	Deployment				Rise Time (min)
									Date / UTC Time	LAT (N)	LON (E)	DEPTH	
									(dd.mm.yy / hh:mm)	D:M	D:M	(m)	
OBS P01	430326	020504	12	A08-037	A	M03-015	102	1609-131	03.07.17 / 03:58	38°19.375	17°44.075	2169	36
OBS P02	450656	000611	24	Y10-52	C	S01-737	40	1001-116	03.07.17 / 04:13	38°19.107	17°43.406	2049	34
OBS P03	450215	010708	52	W01-041	B	U02-066	302	-099	03.07.17 / 04:27	38°18.886	17°42.823	1971	33
OBS P04	451146	971201	43	V08-067	B	S01-735	46	1205-130	03.07.17 / 04:39	38°18.640	17°42.293	1942	32
OBS P05	447756	020509	11	A08-046	B	N11-069	111		03.07.17 / 04:51	38°18.385	17°41.729	1935	32
OBS P06	450403	001006	4	Y10-054	D	W01-065	47	1205-128	03.07.17 / 05:05	38°18.118	17°41.128	1919	32
OBS P07	450445	980903	76	Y02-026	C	R07-016	116	0205-029	03.07.17 / 05:20	38°17.837	17°40.495	1905	32
OBS P08	451207	000616	5	A08-041	A	U02-093	68		03.07.17 / 05:51	38°17.694	17°43.004	1963	33
OBS P09	134071	980907	53	U09-053	A	T08-066	81	0309-045	03.07.17 / 06:08	38°18.180	17°42.668	1941	32
OBS P10	250177	001005	84	Y10-058	D	U11-032	7		03.07.17 / 06:27	38°19.046	17°42.061	1920	32
OBS P11	442205	980403	42	A08-041	B	W01-061	984001	0104-008	03.07.17 / 06:41	38°19.504	17°41.736	1914	32
OBS P12	447417	020507	30	Y10-056	D	T07-084	60	1205-134	03.07.17 / 06:54	38°19.977	17°41.385	1893	32

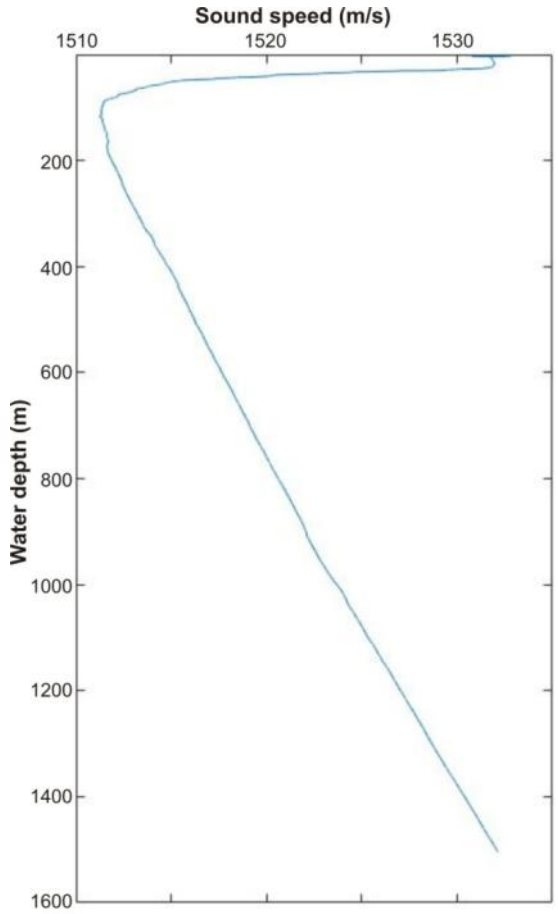

Figure B.1: Sound speed defined from CTD data at Venere mud volcano acquired during releaser test.

Table B.3: Log of seismic data acquisition at Venere mud volcano

Profile No.	Date	Time Start	Time End	Latitude Start	Longitude Start	Latitude End	Longitude End	Shot-No. Start	Shot-No. End
2D seismic lines Survey P1000 - Test Survey									
1001	21.06.2017	03:53	19:10	not recorded		38°38.463	17°13.764	140	1856
1002	21.06.2017	19:33	20:37	38°36.404	17°14.164	38°35.270	17°09.340	2181	2958
1003	21.06.2017	20:58	22:03	38°35.980	17°09.000	38°38.130	17°13.798	3204	3988
1004	21.06.2017	22:29	23:35	38°37.190	17°14.350	38°35.015	17°09.390	4293	200
1005	21.06.2017	23:54	00:57	38°35.790	17°09.280	38°37.980	17°14.030	not recorded	5500
1006	22.06.2017	01:19	02:23	38°36.930	17°14.410	38°34.850	17°09.640	5786	6560
1007	22.06.2017	02:45	03:45	38°35.550	17°09.230	38°37.730	17°14.100	6820	7590
1008	22.06.2017	04:10	05:15	38°36.770	17°14.700	38°34.620	17°09.800	7900	8677
1009	22.06.2017	05:36	06:40	38°35.480	17°09.290	38°37.660	17°14.210	8935	9686
1010	22.06.2017	07:12	08:15	38°36.410	17°14.780	38°34.310	17°10.000	10060	10826
3D seismic lines									
1	25.06.2017	14:16	14:27	38°34.160	17°10.890	38°34.492	17°11.630	13335	13458
OBS shooting lines, no streamer									
1	25.06.2017	16:17	19:35	38°32.750	17°15.610	38°40.631	17°10.219	not applicable	
2	25.06.2017	20:05	22:31	38°40.562	17°09.454	38°32.660	17°14.910		
3	25.06.2017	23:20	03:44	38°32.580	17°14.290	38°40.590	17°08.770		
2D seismic lines Survey P1005									
1012	26.06.2017	10:15	11:20	38°33.990	17°10.490	38.36.147	17°15.306	18060	18830
1013	26.06.2017	11:54	13:12	38°37.400	17°15.040	38°35.310	17°09.340	19251	20186
1014	26.06.2017	13:44	14:48	38°34.030	17°10.480	38°36.240	17°15.200	20569	21551
1015	26.06.2017	15:24	16:47	38°37.500	17°14.150	38°35.360	17°09.350	21786	22774
1016	26.06.2017	17:17	18:21	38°34.030	17°10.350	38°36.183	17°15.171	22145	23890
1017	26.06.2017	18:57	20:09	38°37.503	17°14.108	38°35.387	17°09.313	24321	25185
1018	26.06.2017	20:39	21:41	38°34.077	17°10.386	38°36.216	17°15.214	25544	26269
1019	26.06.2017	22:14	23:22	38°37.530	17°14.030	38°35.400	17°09.240	26682	27504

1020	26.06.2017	23:49	00:56	38°34.080	17°10.330	38°36.308	17°15.256	27835	28628
1021	27.06.2017	01:33	02:47	38°37.530	17°13.902	38°35.450	17°09.280	29065	29977
1022	27.06.2017	03:18	04:21	38°34.122	17°10.320	38°36.290	17°15.120	30337	31096
1023	27.06.2017	04:54	06:08	38°37.630	17°14.050	38°35.485	17°09.242	31500	32375
1024	27.06.2017	06:40	07:42	38°34.164	17°10.288	38°36.311	17°15.088	32763	33509
1025	27.06.2017	08:16	09:20	38°37.664	17°14.012	38°35.585	17°09.362	33911	34680
1026	27.06.2017	09:49	10:52	38°34.194	17°10.258	38°36.360	17°15.090	35027	35791
1027	27.06.2017	11:26	12:32	38°37.660	17°13.920	38°35.540	17°09.160	36190	36988
1028	27.06.2017	13:00	14:10	38°34.240	17°10.270	38°36.370	17°14.500	37328	38162
1029	27.06.2017	14:45	15:54	38°37.720	17°13.990	38°35.580	17°09.170	38589	39404
1030	27.06.2017	16:24	17:30	38°34.230	17°10.180	38°36.390	17°14.990	not recorded	40260
1031	27.06.2017	18:06	19:11	38°37.761	17°13.919	38°35.616	17°09.147	40988	41805
1032	27.06.2017	19:43	20:49	38°34.296	17°10.198	38°36.443	17°14.976	42160	42944
1033	27.06.2017	21:06	22:11	38°36.970	17°14.505	38°34.810	17°09.650	43149	43934
1034	27.06.2017	22:32	23:40	38°35.230	17°11.530	38°36.740	17°15.110	44175	44988
1035	28.06.2017	23:53	00:56	38°37.010	17°14.480	38°34.850	17°09.630	45175	45916
1036	28.06.2017	not recorded	02:23	not recorded		38°36.510	17°14.930	46145	46965
1037	28.06.2017	02:34	03:47	38°37.020	17°14.440	38°34.910	17°09.670	46213	47979
1038	28.06.2017	04:07	05:20	38°34.400	17°10.120	38°36.550	17°14.930	48207	49085
1039	28.06.2017	05:37	06:44	38°37.070	17°14.450	38°34.943	17°09.640	49300	50089
1040	28.06.2017	06:59	08:03	38°34.435	17°10.087	38°36.576	17°14.890	50275	51040
1041	28.06.2017	08:21	09:28	38°37.107	17°14.414	38°34.970	17°09.604	51254	52052
1042	28.06.2017	09:43	10:49	38°34.466	17°10.100	38°36.620	17°14.900	52238	53038
1043	28.06.2017	11:06	12:13	38°37.130	17°14.360	38°34.990	17°09.560	53232	54041
1044	28.06.2017	12:28	13:33	38°34.500	17°10.100	38°36.650	17°14.870	54216	55002
1045	28.06.2017	13:52	14:55	38°37.160	17°14.320	38°35.035	17°09.590	55230	55980
1046	28.06.2017	15:12	16:26	38°34.530	17°09.990	38°36.670	17°14.820	56197	57076
1047	28.06.2017	16:45	17:50	38°37.200	17°14.630	38°35.060	17°09.520	57304	58080
1048	28.06.2017	18:05	19:10	38°34.559	17°10.028	38°36.705	17°14.792	58260	59043

1049	28.06.2017	19:27	20:24	38°37.236	17°14.316	38°35.098	17°09.512	59239	59931
1050	28.06.2017	20:39	21:42	38°34.602	17°10.008	38°36.733	17°14.778	60104	60865
1051	28.06.2017	21:59	22:58	38°37.252	17°14.288	38°35.100	17°09.400	61047	61784
1052	28.06.2017	23:09	00:11	38°34.840	17°10.450	38°36.780	17°14.780	61920	62670
1053	29.06.2017	00:28	01:30	38°37.280	17°14.290	38°34.708	17°09.357	62858	63500
1054	29.06.2017	01:40	02:45	38°34.650	17°09.860	38°36.810	17°14.740	63730	64511
1055	29.06.2017	03:04	04:04	38°37.310	17°14.240	38°35.220	17°09.480	64737	65454
1056	29.06.2017	04:20	05:25	38°34.690	17°09.890	38°36.380	17°14.690	65646	66436
1057	29.06.2017	05:43	06:42	38°37.390	17°14.270	38°35.229	17°09.241	66641	67339
1058	29.06.2017	06:56	07:59	38°34.724	17°09.885	38°36.871	17°14.667	67508	68273
1059	29.06.2017	08:17	09:16	38°37.407	17°14.170	38°35.261	17°09.381	68484	69189
1060	29.06.2017	09:31	10:33	38°34.772	17°09.888	38°36.930	17°14.730	69369	70122
1061	29.06.2017	10:58	11:51	38°37.181	17°13.677	38°35.268	17°09.312	70361	71064
1062	29.06.2017	12:03	13:13	38°34.830	17°09.880	38°36.966	17°14.688	71198	71932
1063	29.06.2017	13:22	14:23	38°37.580	17°13.980	38°35.450	17°09.260	72146	72882
1064	29.06.2017	14:38	15:24	38°34.830	17°09.790	38°37.040	17°14.760	73071	73830
1065	29.06.2017	16:17	17:18	38°38.230	17°13.470	38°36.130	17°08.750	74250	74984
1066	29.06.2017	17:31	18:33	38°35.660	17°09.200	38°37.814	17°14.001	75135	75878
1067	29.06.2017	18:51	19:51	38°38.309	17°13.537	38°36.181	17°08.743	76086	76812
1068	29.06.2017	20:04	21:04	38°35.702	17°09.173	38°37.843	17°13.962	76970	77685
1069	29.06.2017	21:20	22:24	38°38.329	17°13.477	38°36.160	17°08.610	77886	78653
1070	29.06.2017	22:38	23:35	38°35.770	17°09.220	38°37.890	17°13.970	78815	79502
1071	29.06.2017	23:56	00:56	38°38.239	17°13.247	38°36.193	17°08.596	79736	80488
1072	30.06.2017	01:09	02:07	38°35.815	17°09.239	38°37.910	17°13.920	80612	81326
1073	30.06.2017	02:24	03:26	38°38.430	17°13.470	38°36.280	17°08.570	81538	82280
1074	30.06.2017	03:42	04:46	38°35.810	17°09.130	38°37.950	17°13.900	82470	83246
1075	30.06.2017	05:04	06:05	38°38.460	17°13.430	38°36.307	17°08.647	83457	84179
1076	30.06.2017	06:19	07:20	38°35.842	17°09.089	38°37.980	17°13.882	84344	85074
1077	30.06.2017	07:36	08:37	38°38.468	17°13.406	38°36.336	17°08.619	85269	85999

1078	30.06.2017	08:51	09:58	38°35.874	17°09.063	38°38.197	17°14.068	86174	86955
1079	30.06.2017	10:10	11:14	38°38.490	17°13.400	38°36.360	17°08.570	87126	87888
1080	30.06.2017	11:30	12:24	38°35.956	17°09.138	38°38.400	17°13.840	87888	88746
1081	30.06.2017	12:41	13:42	38°38.500	17°13.290	38°36.403	17°08.551	88936	89670
1082	30.06.2017	13:54	14:51	38°35.960	17°09.030	38°38.080	17°13.800	89815	90503
1083	30.06.2017	15:09	16:18	38°38.600	17°13.340	38°36.440	17°08.530	90720	91550
1084	30.06.2017	16:31	17:30	38°35.960	17°08.970	38°38.110	17°13.770	91703	92409
1085	30.06.2017	17:49	18:57	38°38.611	17°13.333	38°36.473	17°08.520	92634	93446
1086	30.06.2017	19:11	20:12	38°35.966	17°08.990	38°38.144	17°13.742	93614	94341
1087	30.06.2017	20:29	21:39	38°38.363	17°13.927	38°36.510	17°08.501	94541	95390
1088	30.06.2017	21:53	22:53	38°36.025	17°08.975	38°38.175	17°13.726	95555	96280
1089	01.07.2017	23:14	00:14	38°38.588	17°13.200	38°36.530	17°08.440	96489	97244
1090	01.07.2017	00:27	01:28	38°36.120	17°09.109	38°38.278	17°13.812	97410	981160
1091	01.07.2017	01:44	02:50	38°38.690	17°13.220	38°36.570	17°08.449	98327	99125
1092	01.07.2017	03:06	04:05	38°36.080	17°08.900	38°38.280	17°13.820	99305	100032
1093	01.07.2017	04:23	05:26	38°38.730	17°13.220	38°36.590	17°08.400	100238	101007
1094	01.07.2017	05:42	06:49	38°36.118	17°08.850	38°38.276	17°13.650	101187	101986
1095	01.07.2017	07:08	08:08	38°38.768	17°13.176	38°36.630	17°08.379	102212	102934
1095t	01.07.2017	8:08	08:37	38°36.630	17°08.379	38°38.157	17°06.919	102934	103274
2D seismic lines P1006									
1096	01.07.2017	08:51	10:54	38°34.743	17°08.896	38°38.770	17°15.720	103362	104090
1097	01.07.2017	11:06	12:54	38°38.240	17°15.940	38°34.208	17°06.958	104176	104829
1098	01.07.2017	13:10	15:04	38°33.630	17°06.850	38°37.670	17°16.120	104912	105607
1098t	01.07.2017	15:04	16:43	38°37.670	17°16.120	38°40.610	17°10.240	105607	106198
1099	01.07.2017	16:43	18:48	38°40.610	17°10.240	38°32.680	17°15.642	106198	106942
1100	01.07.2017	19:05	21:59	38°32.713	17°14.875	38°40.671	17°09.390	107048	108083
1101	01.07.2017	22:17	not recorded	38°40.460	17°08.844	38°32.510	17°14.312	108192	108830
1102	02.07.2017	00:35	03:58	38°32.483	17°13.547	38°40.390	17°07.970	108855	110239

Table B.4: 2D Seismic lines at Poseidon and Sartori mud volcano

Profile No.	Date	Time Start	Time End	Latitude Start	Longitude Start	Latitude End	Longitude End	Shot-No. Start	Shot-No. End
2D seismic lines Survey P4000									
5001	03.07.2017	08:22	09:57	38°21.579	17°40.117	38°17.041	17°34.000	110444	111015
5002	03.07.2017	10:20	11:24	38°18.000	17°45.501	38°19.160	17°45.090	111270	111520
5003	03.07.2017	11:30	14:18	38°19.810	17°45.600	not recorded		111559	112575
5004	03.07.2017	14:21	15:03	38°14.665	17°34.020	38°11.940	17°35.340	112590	112862
5005	03.07.2017	15:21	16:13	38°11.420	17°36.140	38°13.430	17°38.090	112996	113435
5006	03.07.2017	16:13	17:23	38°13.430	17°38.090	38°16.332	17°39.880	113435	114039
2D seismic lines P6000									
6001	04.07.2017	14:54	15:48	38°17.860	17°40.470	38°20.690	17°41.630	115124	115581
6002	04.07.2017	18:00	17:12	not recorded		38°17.080	17°44.920	115600	116300
6003	04.07.2017	17:30	18:36	38°17.410	17°45.510	38°21.203	17°42.750	116444	117018
6004	04.07.2017	18:46	20:01	38°21.209	17°42.137	38°16.467	17°40.909	117105	117744
6005	04.07.2017	21:18	21:25	38°16.535	17°41.425	38°20.487	17°38.532	117890	118465
6006	04.07.2017	21:42	22:50	38°20.934	17°39.121	38°16.730	17°42.150	118610	119199
6007	04.07.2017	23:02	23:15	38°16.890	17°42.810	38°20.830	17°39.963	119308	119921
6008	05.07.2017	00:34	01:20	38°21.308	17°41.022	38°18.288	17°43.244	120085	120502
6009	05.07.2017	01:28	02:24	38°17.955	17°43.072	38°17.210	17°38.495	120547	121035
6010	05.07.2017	02:53	03:58	38°17.030	17°38.670	38°18.960	17°43.120	121282	121838

Table B.5: 3D Survey lines across Sartori mud volcano

Profile No.	Date	Time Start	Time End	Latitude Start	Longitude Start	Latitude End	Longitude End	Shot-No. Start	Shot-No. End
3D P-Cable Survey P7000									
7001	05.07.2017	20:00	20:58:00	38°10.147	17°37.385	38°13.287	17°37.940	124037	124543
7002	05.07.2017	21:39	22:31	38°13.278	17°36.260	38°10.110	17°36.150	124893	124543
7003	06.07.2017	23:07	00:17	38°10.100	17°37.790	38°13.399	17°37.895	125654	126251
7004	06.07.2017	00:55	01:47	38°12.842	17°36.188	38°10.120	17°36.090	126400	127023
7005	06.07.2017	02:29	03:35	38°10.130	17°37.730	38°13.270	17°37.860	127373	127950
7006	06.07.2017	04:15	05:11	38°13.290	17°36.140	38°10.130	17°36.060	128182	128770
7007	06.07.2017	05:54	06:49	38°10.147	17°37.674	38°13.293	17°37.820	129136	129603
7008	06.07.2017	07:24	08:29	38°13.280	17°36.124	38°10.150	17°36.023	129908	130460
7009	06.07.2017	09:10	10:00	38°10.167	17°37.656	38°13.171	17°37.778	130979	131241
7010	06.07.2017	10:38	11:42	38°13.200	17°36.087	38°10.150	17°35.980	131577	132128
7011	06.07.2017	12:19	13:13	38°10.200	17°37.630	38°13.308	17°37.741	132454	132901
7012	06.07.2017	13:50	14:49	38°13.340	17°36.050	38°10.150	17°35.940	133220	133720
7013	06.07.2017	15:25	16:28	38°10.140	17°37.580	38°13.280	17°37.680	134034	134573
7014	06.07.2017	17:05	17:56	38°13.290	17°36.000	38°15.148	17°35.892	134892	135322
7015	06.07.2017	18:34	19:42	38°10.147	17°37.525	38°13.296	17°37.657	135652	136229
7016	06.07.2017	20:21	21:12	38°13.273	17°35.959	38°10.147	17°35.847	136562	137001
7017	06.07.2017	21:53	22:57	38°10.170	17°37.483	38°13.360	17°37.600	137356	137911
7018	06.07.2017	23:33	00:25	38°13.300	17°35.890	38°09.911	17°35.855	138217	137600
7019	07.07.2017	01:05	02:00	38°10.150	17°37.440	38°13.290	17°37.560	139013	139473
7020	07.07.2017	02:36	03:35	38°13.290	17°35.870	38°10.150	17°35.770	139780	140288
7021	07.07.2017	04:12	05:05	38°10.150	17°37.420	38°13.290	17°37.530	140608	141064
7022	07.07.2017	05:44	06:24	38°13 266	17°35 841	38°10.154	17°35.731	141384	141889
7023	07.07.2017	07:20	08:19	38°10.174	17°37.381	38°13.301	17°37.485	142214	142720
7024	07.07.2017	09:03	10:00	38°13.281	17°35.803	38°10.060	17°35.690	143093	143594
7025	07.07.2017	10:40	11:49	38°10.150	17°37.330	38°13.280	17°37.450	143936	144529

7026	07.07.2017	12:32	13:22	38°12.982	17°35.741	38°10.009	17°35.641	144910	145312
7027	07.07.2017	14:06	15:09	38°10.210	17°37.280	38°13.290	17°37.410	145697	146241
7028	07.07.2017	15:46	16:40	38°13.290	17°35.700	38°10.140	17°35.600	146545	147015
7029	07.07.2017	17:21	18:16	38°10.510	17°37.210	38°13.307	17°37.361	147368	147838
7030	07.07.2017	18:52	19:53	38°13.284	17°35.666	38°10.155	17°35.565	148148	148665
7031	07.07.2017	20:31	21:22	38°10.169	17°37.206	38°13.303	17°37.324	148997	149430
7032	07.07.2017	21:58	23:01	38°13.870	17°37.560	38°10.150	17°36.520	149787	150290
7033	07.07.2017	23:38	00:35	38°10.150	17°37.160	38°13.622	17°37.185	150603	151110
7034	08.07.2017	01:14	02:07	38°13.144	17°35.609	38°10.130	17°35.480	151400	151877
7035	08.07.2017	02:43	03:44	38°10.150	17°37.130	38°13.300	17°37.240	152186	152707
7036	08.07.2017	04:24	05:19	38°13.310	17°35.550	38°10.150	17°35.440	153049	153528
7037	08.07.2017	05:59	07:06	38°10.165	17°37.095	38°13.311	17°37.200	153864	154434
7038	08.07.2017	7:49	08:40	38°13.285	17°35.512	38°10.164	17°35.397	154780	155242
7039	08.07.2017	09:22	10:40	38°10.177	17°37.038	38°13.710	17°35.361	155608	156250
7040	08.07.2017	11:00	11:54	38°13.013	17°35.432	38°10.077	17°35.361	156450	156899
7041	08.07.2017	12,34	13:37	38°10.230	17°36.990	38°13.885	17°36.877	157260	157770
7042	08.07.2017	14:00	15:05	38°13.310	17°35.410	38°10.170	17°35.320	157992	158547
7043	08.07.2017	15:45	16:36	38°10.198	17°36.995	38°13.290	17°37.070	158884	159342
7044	08.07.2017	17:18	18:23	38°13.310	17°35.390	38°10.172	17°35.282	159689	160243
7045	08.07.2017	19:10	19:52	38°10.174	17°36.928	38°13.270	17°37.040	160560	161010
7046	08.07.2017	20:33	21:30	38°13.297	17°35.365	38°10.093	17°35.251	161363	161842
7047	08.07.2017	22:08	23:06	38°10.250	17°36.910	38°13.330	17°36.990	162180	162687
7048	08.07.2017	23:46	00:39	38°13.310	17°35.300	38°10.150	17°35.20	163013	163476
7049	09.07.2017	01:14	02:23	38°10.060	17°36.820	38°13.300	17°36.950	163779	164366
7050	09.07.2017	03:04	04:07	38°13.300	17°35.270	38°09.730	17°35.310	164720	165255
7051	09.07.2017	04:42	05:50	38°10.150	17°36.800	38°13.290	17°36.910	165557	166136
7052	09.07.2017	06:26	07:22	38°13.294	17°35.213	38°10.156	17°35.113	166444	166921
7053	09.07.2017	08:45	09:00	38°10.178	17°36.752	38°13.322	17°36.874	167290	167773
7054	09.07.2017	09:40	10:41	38°13.296	17°35.175	38°10.160	17°35.070	168107	168635

7055	09.07.2017	11:19	12:09	38°10.180	17°36.710	38°13.420	17°36.820	168962	169387
7056	09.07.2017	12:48	13:49	38°13.209	17°35.138	38°10.160	17°35.030	169706	170241
7057	09.07.2017	14:25	15:22	38°10.120	17°36.670	38°13.300	17°36.780	170556	171046
7058	09.07.2017	16:10	17:14	38°13.290	17°35.140	38°10.170	17°34.990	171300	171711
7059	09.07.2017	17:45	18:47	38°10.160	17°36.660	38°13.414	17°36.755	172014	172515
7060	09.07.2017	18:29	20:21	38°13.288	17°35.075	38°10.169	17°34.949	172873	173308
7061	09.07.2017	20:59	22:05	38°10.230	17°36.604	38°13.315	17°36.699	173630	174208
7062	09.07.2017	22:45	23:30	38°13.211	17°35.011	38°10.150	17°34.902	174540	174949
7063	10.07.2017	0:09	1:16	38°10.157	17°36.552	38°13.398	17°36.661	175272	175820
7064	10.07.2017	01:52	02:43	38°13.190	17°34.940	38°10.180	17°34.860	176156	176594
7065	10.07.2017	03:24	04:24	38°10.180	17°36.500	38°13.610	17°36.340	176945	177458
7066	10.07.2017	05:01	06:01	38°13.320	17°34.890	38°10.166	17°34.382	177772	178292
7067	10.07.2017	06:40	07:30	38°10.198	17°36.471	38°13.334	17°36.580	178616	179050
7068	10.07.2017	08:07	09:12	38°13.325	17°34.902	38°10.184	17°34.785	179374	179922
7069	10.07.2017	9:46	10:38	38°10.217	17°36.198	38°13.414	17°36.305	180213	180645
7070	10.07.2017	11:04	11:57	38°12.787	17°37.387	38°10.123	17°37.311	180910	181341
7071	10.07.2017	12:24	13:20	38°10.181	17°36.229	38°13.328	17°36.334	181573	182051
7072	10.07.2017	13:44	14:38	38°13.223	17°37.453	38°10.310	17°37.360	182263	182725
7073	10.07.2017	15:06	16:05	38°19.820	17°36.290	38°13.300	17°36.380	182959	183469
7074	10.07.2017	16:37	17:30	38°13.290	17°35.080	38°10.170	17°34.930	183731	184229
7075	10.07.2017	18:02	19:02	38°10.195	17°36.317	38°13.321	17°36.415	184505	185016
7076	10.07.2017	19:30	20:20	38°13.291	17°35.270	38°10.072	17°35.156	185259	185657
7077	10.07.2017	20,49	21:47	38°10.190	17°36.350	38°13.331	17°36.451	185993	186478
7078	10.07.2017	22:20	23:10	38°12.743	17°35.279	38°10.287	17°35.186	186761	187171
7079	10.07.2017	23:48	0:34	38°11.357	17°36.440	38°13.307	17°36.503	187365	187883
7080	11.07.2017	1:02	1:57	38°13.315	17°35.550	38°10.160	17°35.420	188113	188557
7081	11.07.2017	2:29	3:24	38°10.160	17°36.820	38°13.310	17°36.930	188842	189311
7082	11.07.2017	04:05	4:37	38°13.340	17°35.000	38°11.530	17°34.930	189665	189934
7083	11.07.2017	5:00	5:30	38°11.550	17°35.880	38°13.320	17°35.920	190125	190380

7084	11.07.2017	05:56	6,52	38°13.280	17°37.180	38°10.134	17°37.066	190607	191088
7085	11.07.2017	07:21	08:19	38°10.209	17°35.882	38°13.328	17°35.987	191331	191821
7086	11.07.2017	09:10	10:03	38°13.260	17°36.339	38°10.131	17°36.433	192239	192692
7087	11.07.2017	10:29	not recorded	38°10.245	17°37.567	not recorded		192913	not recorded
7088	11.07.2017	not recorded	11:22	not recorded		38°13.325	17°37.563	not recorded	193381
7089	11.07.2017	11:44	12:34	38°13.266	17°36.540	38°10.146	17°36.429	193560	193992
7090	11.07.2017	13:16	13:54	38°11.042	17°36.150	38°13.369	17°36.252	194350	194666

Table B.6: 2D Survey lines across Cetus mud volcano

Profile No.	Date	Time Start	Time End	Latitude Start	Longitude Start	Latitude End	Longitude End	Shot-No. Start	Shot-No. End
2D Survey P8000									
8001	11.07.2017	18:41	19:11	37°53.525	17°27.707	37°51.577	17°27.708	195142	195363
8002	11.07.2017	19:25	19:54	37°51.657	17°27.225	37°53.583	17°27.166	195468	195685
8003	11.07.2017	20:12	20:40	37°53.493	17°27.981	37°51.565	17°27.948	195826	196033
8004	11.07.2017	20:57	21:16	37°51.660	17°27.482	37°53.064	17°27.488	196157	196307
8005	11.07.2017	22:14	22:41	37°53.507	17°28.217	37°51.594	17°28.200	196499	196701
8006	11.07.2017	23:26	00:18	37°52.715	17°26.371	37°52.769	17°30.910	197026	197426
8007	11.07.2017	00:29	not recorded	37°52.383	17°30.816	37°52.263	17°26.457	197513	197877
8008	11.07.2017	not recorded	02:19	not recorded		37°52.890	17°30.890	197948	198331
8009	11.07.2017	02:44	03:43	37°52.640	17°30.800	37°52.580	17°26.510	198515	199085
8010	11.07.2017	3:46	4:00	37°53.070	17°26.560	37°53.060	17°27.750	198979	199085

8. References

Bialas, J. and Flueh, E. (1999) A new Ocean Bottom Seismometer (with a new type of data logger), Sea Technol., 40, 41-46

Bohrmann, G. and cruise participants (2015) Report and preliminary results of R/V METEOR cruiseM112, Dynamic of Mud Volcanoes and Seeps in the Calabrian Accretionary Prism, Ionian Sea,Catania (Italy) – Catania (Italy), November 6 – December 15, 2014. Berichte, MARUM – Zentrumfür Marine Umweltwissenschaften, Fachbereich Geowissenschaften, Universität Bremen.urn:nbn:de:gbv:46-00104282-14.

Bohrmann, G., Bachmann, K., Buchheister, S., Candoni, O., Ceramicola, S., Loher, M., Meinecke, G., Renken, J., Spiesecke, U., von Wahl, T. and Wintersteller, P. (2016) Report and preliminary results of R/V POSEIDON cruise POS499, Calabrian Mud Volcanoes, Catania (Italy) – Catania (Italy), 04 May – 22 May, 2016. Berichte, MARUM – Zentrum für Marine Umweltwissenschaften, Fachbereich Geowissenschaften, Universität Bremen, 311, Bremen, 76 pp.

Ceramicola, S., Praeg, D., and the OGS Explora Scientific Party (2006) Mud volcanoes discovered on the Calabrian Arc: preliminary results from the HERMES-HYDRAMED IONIO 2005 campaign. CIESM Workshop Monographs 29: 35–39.

Ceramicola, S., Praeg, D., Cova, A., Accetella, D. and Zecchin, M. (2014) Seafloor distribution and last glacial to postglacial activity of mud volcanoes on the Calabrian accretionary prism, Ionian Sea. Geo-Marine Letters 34: 111-129.

Chamot-Rooke, N., Rangin, C., Le Pichon, X. and DOTMED Working Group (2005) DOTMED: A Synthesis of Deep Marine Data in the Eastern Mediterranean. Mémoires de la Société Géologique de France, n.s., no. 177, 64 pp.

Cita, M.B., Wright, R.C., Ryan, W.B.F., and Longinelli, A. (1978) Messinian Paleoenvironments. In Hsü, K.J., Montadert, L. et al. Initial Reports DSDP, 42A: Washington (U.S. Govt. Printing Office), 1003-1035.

Cita, M.B., Ryan, W.B.F., and Paggi, L. (1981) Prometheus Mud Breccia. An example of shale diaprism in the western Mediterranean Ridge. Annales géologiques des Pays Hélléniques 30(2): 543–570.

Faccenna, C., Piromallo, C., Crespo-Blanc, A., Jolivet, L., and Rossetti, F. (2004) Lateral slab deformation and the origin of the western Mediterranean arcs. Tectonics 23, TC1012, doi:10.1029/2002TC001488.

Faccenna, C., Molin, P., Orecchio, B., Olivetti, V., Bellier, O., Funiciello, F., Minelli, L., Piromallo, C., and Billi, A. (2011) Topography of the Calabria subduction zone (southern Italy): clues for the origin of Mt. Etna. Tectonics 30, TC1003.doi:10.1029/2010TC002694.

Flueh, E. R., and Bialas, J. (1996) A digital, high data capacity ocean bottom recorder for seismic investigations, Int. Underwater Syst. Design, 18(3), 18–20.

Fusi, N., and Kenyon, N.H. (1996) Distribution of mud diapirism and other geological structures from long-range sidescan sonar (GLORIA) data, Eastern Mediterranean Sea. Marine Geology 132: 21–38.

Goes, S., Giardini, D., Jenny, S., Hollenstein, C., Kahle, H.-G., and Geiger, A. (2004) A recent tectonic reorganization in the south-central Mediterranean. Earth and Planetary Science Letters 226:335–345. doi:10.1016/j.epsl.2004.07.038.

Gutscher, M.-A., Kopp, H., Krastel, S., Bohrmann, G., Garlan, T., Zaragosi, S., Klaucke, I., Wintersteller, P., Loubrieu, B., Faou, Y.L., San Pedro, L., Dominguez, S., Rovere, M., de Lepinay, B.M., Ranero, C., and Sallares, V. (2017) Active tectonics of the Calabrian subduction revealed by new multi-beam bathymetric data and high-resolution seismic profiles in the Ionian Sea (Central Mediterranean), Earth and Planetary Science Letters 461, 61-72, http://dx.doi.org/10.1016/j.epsl.2016.12.020

Kopp, H., Gutscher, M.-A., Crozon, J., Dellong, D., Graindorge, D., Klaeschen, D., Klaucke, I., Klingelhofer, F., Krabbenhoeft, A., Kurzawski, R., Matthiessen, T., Mögeltönder, J., Papenberg, C.A., Peyronnet, C., Prunier, C., Rovere, M., Schröder, H., Steffen, K.-P., Wehner, D., Wieprich, M., and Wollatz-Vogt, M. (2015) Deep Structure of the Ionian Sea and Sicily: Dionysus - Cruise No. M111 – October 10 – November 1, 2014 – Catania (Italy – Catania (Italy), Meteor cruise report, 44p, doi: 10.2312/cr_m111.

Malinverno, A., and Ryan, W.B.F. (1986) Extension in the Tyrrhenian Sea and shortening in the Apennines as result of arc migration driven by sinking of the lithosphere. Tectonics 5 (2): 227–245.

Mascle, J., Mary, F., Praeg, D., Brosolo, L., Camera, L., Ceramicola, S., and Dupré, S. (2014) Distribution and geological control of mud volcanoes and other fluid/free gas seepage features in the Mediterranean Sea and nearby Gulf of Cadiz, Geo-Marine Letters, doi 10.1007/s00367-014-0356-4.

Minelli, L., and Faccenna, C. (2010) Evolution of the Calabrian accretionary wedge (central Mediterranean). Tectonics 29, TC4004; doi:10.1029/2009TC002562.

Morlotti, E., Sartori, R., Torelli, L., Barbieri, F., and Raffi, I. (1982) Chaotic deposits from the external Calabrian Arc (Ionian Sea, eastern Mediterranean). Memorie della Società Geologica Italiana 24: 261–275.

Polonia, A., Torelli, L., Mussoni, P., Gasperini, L., Artoni, A., and Klaeschen, D. (2011) The Calabrian Arc subduction complex in the Ionian Sea: regional architecture, active deformation and seismic hazard. Tectonics 30, TC5018.

Praeg, D., Ceramicola, S., Barbieri, R., Unnithan, V., and Wardell, N. (2009) Tectonically-driven mud volcanism since the late Pliocene on the Calabrian accretionary prism, central Mediterranean Sea, J. of Marine and Petroleum Geology 26: 1849–1865.

Praeg, D., Ceramicola, S., Pierre, C., Mascle, J., Dupré, S., Andersen, A., Camera, L., Cova, A., De Lange, G., Ducassou, E., Freiwald, A., Harmegnies, F., Hebbeln, D., Loncke, L., Mastalerz, V., Migeon, S., and Taviani, M. (2012) Active mud volcanism and seabed seepage on the Calabrian accretionary prism, Ionian Sea. Congresso Nazionale della Società Geologica Italiana (SGI), 18-20 September, Arcavacata di Rende (CS) ITALY; Rend. Online Soc. Geol. It., v. 21, pp. 973-974.

Rabaute, A., and Chamot-Rooke, N. (2007) Quantitative mapping of active mud volcanism at the western Mediterranean Ridge-backstop contact. Marine Geophysical Researches 28: 271-293.

Robertson, A.H.F., and the Ocean Drilling Program Leg 160 Shipboard Scientific Party (1996) Mud volcanism on the Mediterranean Ridge; Initial Results of Ocean Drilling Program Leg 160. Geology 24 (3): 239–242.

Rossi, S., and Sartori, R. (1981) A seismic reflection study of the external Calabrian Arc in the northern Ionian Sea (eastern Mediterranean). Marine Geophysical Researches 4: 403–426.

Somoza, L., Medialdea, T., Leon, R., Ercilla, G., Vazquez, J.T., Farran, M., Hernandez-Molina, F.J., Gonzales, J., Juan, C., and Fernandez-Puga, M.C. (2012) Structure of mud volcano system and pockmarks in the region of the Ceuta Contourite Depositional System (Western Alboran Sea). Mar Geol 332-334: 4-26.

Zecchin, M., Caffau, M., Civile, D., Critelli, S., Di Stefano, A., Maniscalco, R., Muto, F., Sturiale, G., and Roda, C. (2012) The Plio-Pleistocene evolution of the Crotone Basin (southern Italy): Interplay between sedimentation, tectonics and eustasy in the frame of Calabrian Arc migration. Earth-Science Reviews 115: 273-303.